

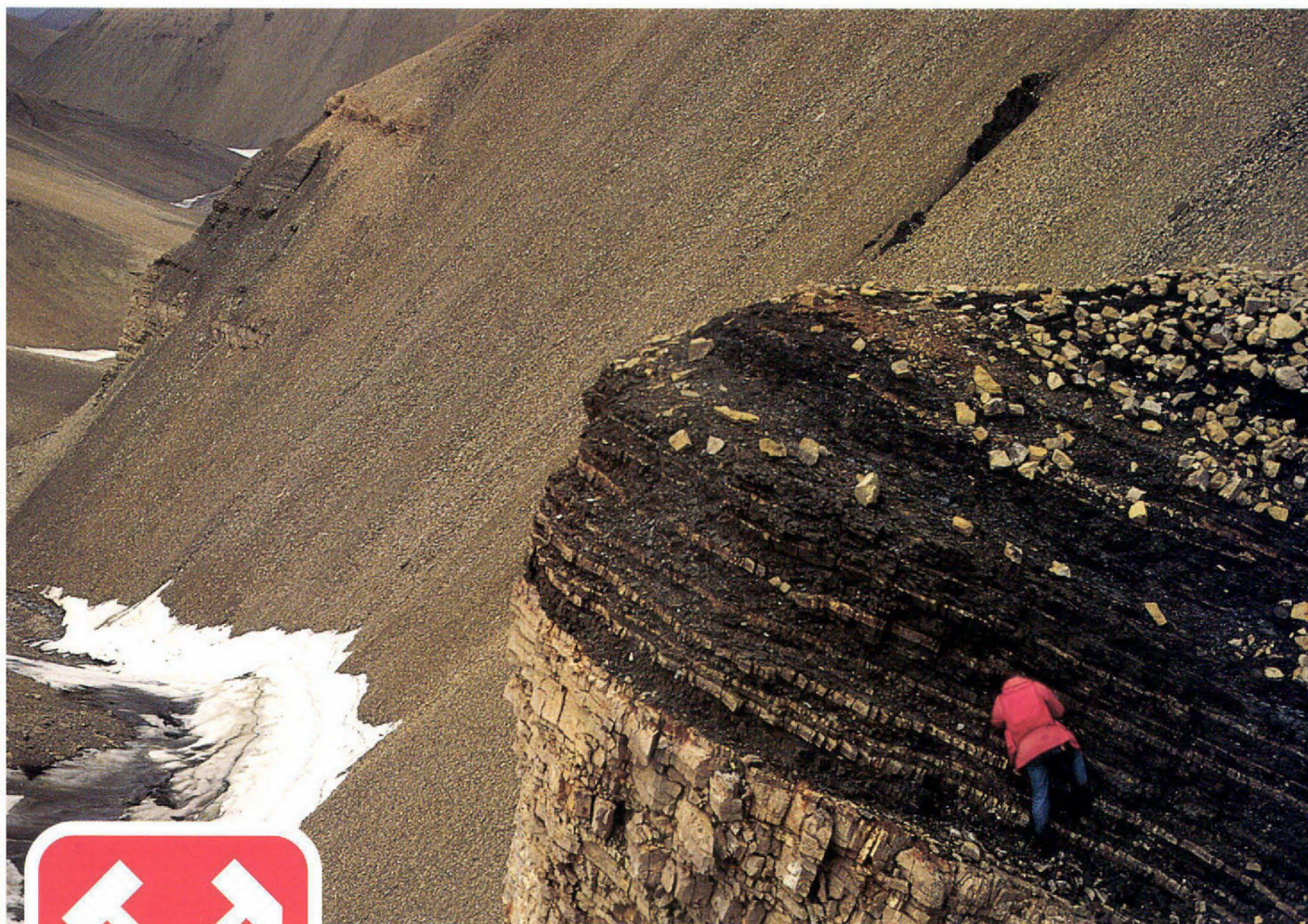
Research papers

GEUS

Report file no.

22323

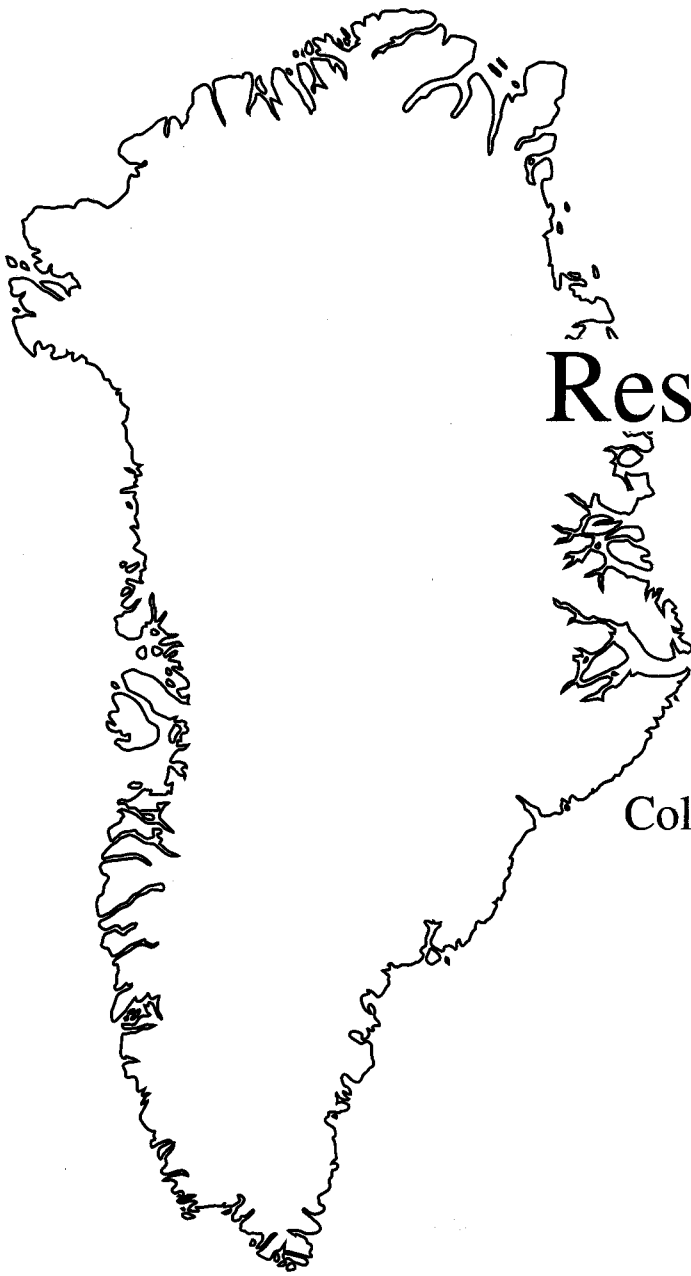
Collection of scientific articles



GRØNLANDS GEOLOGISKE UNDERSØGELSE

Bulletin 171

1996



Research papers

Collection of scientific articles

Preface

This volume consists of four research articles – two concerned with Tertiary basalts from West and East Greenland, one concerned with the Upper Palaeozoic succession in the Wandel Sea Basin in eastern North Greenland and one with Upper Permian foraminifers in East Greenland.

The first article describes the filling of a marine embayment with volcanic rocks forming hyaloclastites and breccias. The history of the filling and subsequent erosion is illustrated by photogrammetrically measured sections. A new member of the volcanic Vaigat Formation is defined, and chemical analyses are given.

The second article is a description of the dykes and sills in East Greenland from the sediment areas that lie between the plateau lava areas of Hold with Hope in the

north and Scoresby Sund in the south. Their chemistry suggests a genetic relationship with the lavas to the north rather than the plateau lavas to the south.

The third article describes the Upper Palaeozoic sedimentary succession from eastern Peary Land with new biostratigraphic data on fusulinids, conodonts, palynomorphs and small foraminifera. The lithostratigraphy of these deposits has been revised based on new biostratigraphic data and the appearance of a major Lower Permian hiatus.

The final article is a description of Upper Permian foraminiferal assemblages from East Greenland which suggests a broad correlation of the Wagener Halvø Formation with Zechstein 1 and younger strata in the Zechstein basin of North-West Europe.

Cover picture

Bedded chert-rich carbonates abruptly overlain by black laminated shales reflecting a major Late Permian drowning event in the Wandel Sea Basin, eastern North Greenland. (Photo: L. Stemmerik.)

Contents

Filling and plugging of a marine basin by volcanic rocks: the Tunoqqu Member of the Lower Tertiary Vaigat Formation on Nuussuaq, central West Greenland	<i>A. K. Pedersen, L. M. Larsen, G. K. Pedersen & K. S. Dueholm</i>	5
Early Tertiary lavas and sills on Traill Ø and Geographical Society Ø, northern East Greenland: petrography and geochemistry	<i>N. Hald</i>	29
Stratigraphy and depositional evolution of the Upper Palaeozoic sedimentary succession in eastern Peary Land, North Greenland	<i>L. Stemmerik, E. Håkansson, L. Madsen, I. Nilsson, S. Piasecki & J. A. Rasmussen</i>	45
Upper Permian foraminifera from East Greenland	<i>J. Pattison & L. Stemmerik</i>	73



Filling and plugging of a marine basin by volcanic rocks: the Tunoqqu Member of the Lower Tertiary Vaigat Formation on Nuussuaq, central West Greenland

Asger Ken Pedersen, Lotte Melchior Larsen, Gunver Krarup Pedersen and Keld S. Dueholm

The volcanic Tunoqqu Member formed at the end of the second of three volcanic cycles in the Paleocene Vaigat Formation. The Tunoqqu Member consists of brown aphyric and feldspar-phyric basalts and forms a marker horizon within the grey picritic rocks of the Vaigat Formation. Most of the basalts are siliceous and were produced by contamination with crustal rocks of magmas ranging in composition from picrite to evolved basalt.

Some of the basalts were erupted from local volcanic centres of which four have been identified, whereas other basalts form more regional flows. The four identified eruption centres are located along fault lines and zones of uplift and subsidence, indicating tectonic control. Tectonic control is also inferred to be important in terminating the volcanic cycle and causing the development of high-level magma chambers where the magmas stagnated, fractionated, and became contaminated.

The basalts of the Tunoqqu Member form subaerial lava flows in western Nuussuaq. Central Nuussuaq constituted a marine embayment in which the volcanics were deposited as eastward prograding foreset-bedded hyaloclastite breccia fans which indicate water depths of up to 160 m. Eastern Nuussuaq was a gneiss highland with a more than 700 m high NW–SE-elongated gneiss promontory stretching into the sea. During Tunoqqu Member time the volcanic rocks reached the gneiss promontory and blocked the outlet from the south to the sea in the north. This resulted in increased water levels in the enclosed embayment and transformation of the outlet into a torrential river. This river eroded the concomitantly forming Tunoqqu Member volcanics and the gneiss promontory and deposited the material in up to more than 250 m thick foreset-bedded boulder conglomerates in the sea where the north coast of Nuussuaq is now situated.

A. K. P., Geological Museum, Øster Voldgade 5–7, DK-1350 Copenhagen K, Denmark.

L. M. L., Geological Survey of Denmark and Greenland, Thoravej 8, DK-2400 Copenhagen NV, Denmark.

G. K. P., Geological Institute, University of Copenhagen, Øster Voldgade 10, DK-1350 Copenhagen K, Denmark.

K. S. D., Institute of Surveying and Photogrammetry, Technical University of Denmark, Landmålervej 7, DK-2800 Lyngby, Denmark.

The early phases of the Tertiary volcanism in the West Greenland Basin are represented by the Vaigat Formation. This formation records a complicated interplay between the concomitantly developing volcanic pile and sedimentary basin through more than 3 million years (Clarke & Pedersen, 1976; Henderson *et al.*, 1981; Pedersen, 1985a; Pedersen, 1989; Piasecki *et al.*, 1992; Larsen *et al.*, 1992).

On Disko and Nuussuaq (Fig.1) an area of more than 10 000 km² is well exposed and only weakly affected by post-volcanic faulting, tilting, and subsidence. In this area the evolution of the volcanic rocks in space and time and their relation to the coeval sediments can be studied in considerable detail. Until recently, such studies have been impeded by the rugged topography and the complex geology. However, the recent development of multi-model

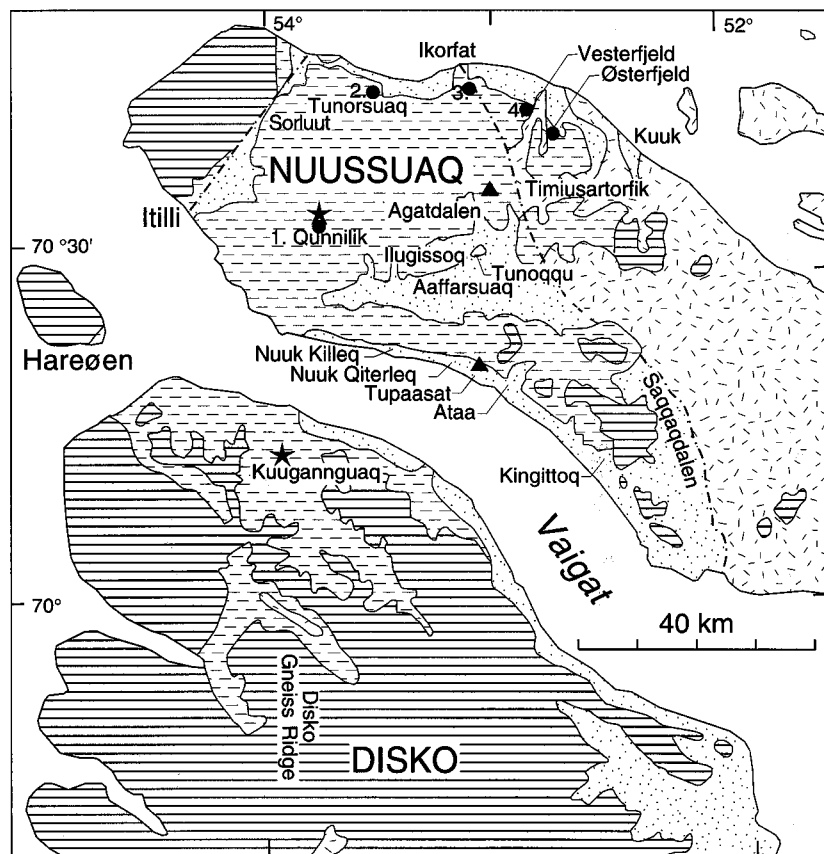


Fig. 1. Geological map of Nuussuaq and central and northern Disko. Kuugannuaq is new spelling of Kûgánguaq.



photogrammetry, based on colour stereo-photography from a helicopter (Dueholm & Pedersen, 1992; Pedersen & Dueholm, 1992) has provided the basis for new progress through quantitative studies of inaccessible mountain walls.

Koch (1959) studied the Tertiary non-marine sediments on Nuussuaq. He concluded that parts of the sedimentary succession in the east were contemporaneous with volcanic rocks in the west, and that progradation of volcanic hyaloclastite breccias into a water-covered basin affected the sedimentary facies evolution. Pedersen (1989) likewise suggested that the advancing hyaloclastite fronts caused rapid increases in water depths and changed fluvial plains into deep lakes.

Pedersen *et al.* (1993) presented a photogrammetrically measured 80 km long vertical section along the south

coast of Nuussuaq. The section documents the eastward younging of the volcanic rocks with time, the eastward progradation of hyaloclastite breccia fans into the water-covered basin, and the variations in water depth with time.

The lithostratigraphy of the Vaigat Formation on Disko (Pedersen, 1985a) and Nuussuaq (Pedersen *et al.*, 1993) is based on a number of lithologically and chemically distinct marker units of contaminated volcanic rocks. These are mostly brown aphyric or feldspar-phyric basalts and andesites which occur as minor horizons within the succession of lithologically uniform grey picritic volcanics. The most widespread of these brown marker horizons is present over large areas of Nuussuaq and is formalised in this paper as the Tunoqqu Member.

Heim (1910) discovered thick conglomerates of basalt

and gneiss blocks at the base of the volcanic succession at Vesterfjeld in north-eastern Nuussuaq. S. Munck and A. Noe-Nygaard visited the same area in 1939 and discovered that the conglomerates are associated with hyaloclastite breccias (unpublished field notes). The geological map sheet 1:100 000 Agatdal shows the conglomerate as a 200 m thick body which covers *c.* 1 km² at the ridge at point 1230 m named Mellemfjeld by Heim (1910). The conglomerate occurrences were visited in the field in 1992. The conglomerates were found to be part of the Tunoqqu Member and to have a geometry quite different from that shown on the geological map.

This paper combines volcanology, geochemistry, sedimentology, and multi-model photogrammetry in a presentation of a geological analysis of the West Greenland Basin within the narrow time-window represented by the Tunoqqu Member. It demonstrates that this member with its huge conglomerates formed at a critical stage of the development during which a large marine embayment was cut off by the advancing volcanic front and subsequently developed into a fresh-water lake.

Geological setting

The West Greenland Basin is underlain and bordered to the east by Precambrian gneisses and metasediments of Archaean to Mid-Proterozoic age (Henderson & Pulvertaft, 1987; Garde & Steenfelt, in press). The dominant lithologies are quartzo-feldspathic gneisses.

The oldest known sediments in the basin, both onshore and offshore, are of Cretaceous age. On Disko and in southern and central Nuussuaq the Cretaceous sediments include fluvial, deltaic, and marine deposits of the Atane Formation (Pedersen & Pulvertaft, 1992). The Atane Formation is dated as Albian?–Cenomanian to latest Santonian on the basis of palynomorphs and rare marine invertebrates (Croxtton, 1978; Koppelhus & Pedersen, 1993; Nøhr-Hansen, in press). In central Nuussuaq the Atane Formation is erosively overlain by marine shales of late Cretaceous age (Nøhr-Hansen, 1994).

The basin was affected by considerable tectonic movements in the latest Cretaceous to earliest Tertiary (Rosenkrantz & Pulvertaft, 1969; Henderson, 1973; Pulvertaft, 1979, 1989). Block faulting and tilting due to extension led to a general deepening of the basin in western and north-western Nuussuaq, and to uplift and rejuvenation in the eastern, bounding gneiss terrain which became a mountainous area with considerable relief. The tectonism and onset of volcanism in the Tertiary were caused by large scale plate tectonic processes in connection with incipient break-up of the Laurasian continent.

Paleocene pre- to syn-volcanic sediments are exposed in eastern Nuussuaq and northern and eastern Disko. The

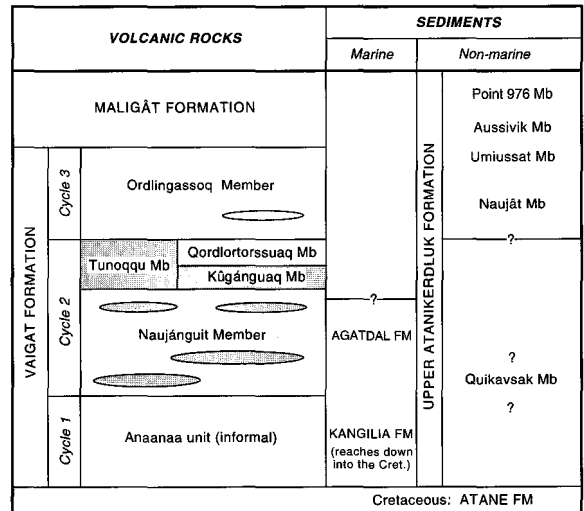


Fig. 2. Summary stratigraphy of the Tertiary volcanic rocks and sediments on Nuussuaq and Disko. The Vaigat Formation comprises three cycles of volcanic activity; various minor members within the formation are shown schematically. Stipple denotes crustally contaminated members.

non-marine sediments on Nuussuaq were described as the Upper Atanikerdluk Formation by Koch (1959), whereas the marine sediments on Nuussuaq are referred to the Kangilia and Agatdal Formations (Rosenkrantz, 1970). The main stratigraphic relationships are illustrated in Fig. 2.

None of the established sediment formations and members are known to be coeval with the volcanic rocks of Tunoqqu Member described here. The marine Kangilia and Agatdal Formations are definitely older (Fig. 2). The dominantly non-marine Quikavsak Member is overlain by the Tunoqqu Member but is rather unconstrained in time (question marks in Fig. 2). The Quikavsak Member is interpreted as a fault-controlled incised valley system filled with fluvial and estuarine deposits. The valleys were eventually drowned during a phase of rapid rise in relative sea level (Dam & Sønnerholm, in press). The overlying Naujât Member consists of dark grey to black shales which were deposited in relatively deep water. The shales overlie an erosion surface which truncates either the Atane Formation or the Quikavsak Member. The non-marine (lacustrine) origin of the Naujât Member is inferred from the lack of dinoflagellate cysts and the scarcity or absence of pyrite in the sediment (Piasecki *et al.*, 1992). These authors suggested that the Naujât Member might be partly coeval with the Tunoqqu Member, but later studies (unpublished data) indicate that the Naujât Member post-dates the Tunoqqu Member and is coeval with the Ordlingassoq Member volcanic rocks (Fig. 2). The shales of the Naujât Member and the younger Aussivik-

Table 1. Lithostratigraphy of the Tunoqqu Member

New member. Forms part of the Lower Tertiary Vaigat Formation (Hald & Pedersen, 1975). Correlated with Kûgánguaq Member (Pedersen, 1985a).

Name. After the mountain top Tunoqqu on the north side of Aaffarsuaq valley, central Nuussuaq (Fig. 1).

Type section. The south side of Tunoqqu mountain (Fig. 7).

Reference sections. See Figs 1 and 3: Qunnilik (Fig. 3,1), Tunorsuaq (Fig. 3,2), Ikorfat (Fig. 3,3), Vesterfjeld (Fig. 3,4), and Tupaasat (Larsen & Pedersen, 1988, fig. 2, section c).

Thickness. From less than 50 m to about 300 m.

Lithology. Brown mostly aphyric and plagioclase-phyric basalts forming subaerial lavas, subaqueous lavas, hyaloclastite breccias, and boulder conglomerates dominated by volcanic clasts.

Boundaries. The Tunoqqu Member rests on grey picritic lava flows and hyaloclastite breccias from the Naujánguit Member, on marine or non-marine Cretaceous sediments, or on Precambrian gneiss. In parts of southern Nuussuaq the lower boundary is not exposed. The Tunoqqu Member is overlain by grey picritic lava flows and hyaloclastite breccias of the Ordlingassoq Member.

Distribution. Tunoqqu Member covers more than 2000 km² on Nuussuaq (Fig. 5). The extent towards the north and south are delimited by the present coastline, whereas the western extent is delimited by erosion.

vik Member are referred to pollen zones P4 and P5 by Hjortkjær (1991) and are tentatively correlated with marine nannoplankton zones NP6 and NP7 (Piasecki *et al.*, 1992; B. Hjortkjær, personal communication, 1994).

The volcanic rocks on Disko and Nuussuaq are divided into two formations. The older Vaigat Formation consists mainly of primitive, olivine-rich rocks (see below), whereas the younger Maligât Formation consists mainly of feldspar-phyric plateau basalts (Hald & Pedersen, 1975; Hald, 1977; Larsen & Pedersen, 1992). Only the Vaigat Formation is considered in the present context.

The Vaigat Formation is subdivided into three main units which are, successively, Anaanaa unit (informal), Naujánguit Member, and Ordlingassoq Member (Pedersen, 1985a; Pedersen *et al.*, 1993, and unpublished data). These units may enclose, or be separated by, a few minor members with distinctive lithology and composition (Fig. 2). Whereas the three main units are dominated by grey, olivine-rich, primitive rocks, most of the minor members consist of brownish-weathering aphyric or feldspar-phyric rocks which are enriched in silica and may contain more or less digested sediment xenoliths. These rocks are interpreted as resulting from reaction between mafic magmas and crustal rocks, and in many cases the reactions occurred in high-level magma chambers within Cretaceous to early Tertiary sediments. Distinctive negative Ni and Cu anomalies in some of the sediment-contaminated rocks show that they have been affected by sulphide and iron fractionation (e.g. Pedersen, 1979, 1985b).

Three volcanic cycles of the Vaigat Formation

The volcanism of the Vaigat Formation started from eruption centres in western Nuussuaq. Subaqueous mounds of pillow breccia and hyaloclastite and sequences of thin subaerial lava flows were deposited. The lavas flowed eastwards and into a deep water-filled basin, presumably of tectonic origin, where they formed huge eastwards-prograding hyaloclastite fans. With time, the active eruption centres also migrated eastwards, and eventually the water-filled basin was filled up. The volcanism occurred in three separate cycles each of which started with olivine-rich primitive magmas and ended with more evolved, often contaminated magmas. These three cycles are represented by the three main units, as follows.

1st cycle: the Anaanaa unit comprises the oldest known Tertiary volcanic rocks in West Greenland. It is only known from a limited area in western Nuussuaq. The rocks comprise picrites, olivine-rich basalts, feldspar-phyric basalts, and siliceous contaminated basalts. The unit is considered to be contemporaneous with parts of the marine sedimentary Kangilia Formation to the east and north-east.

2nd cycle: the Naujánguit Member comprises picrites and olivine-rich basalts, whereas the *associated minor members* mainly consist of siliceous contaminated basalts and andesites with subordinate feldspar-phyric basalts. During the Naujánguit Member cycle the volcanic rocks prograded considerably towards the east on both Disko and Nuussuaq and filled in the marine basin. The *Tunoqqu Member*, which is the subject of the present paper,

formed at the end of this volcanic cycle. The 2nd cycle is considered contemporaneous with the uppermost part of the marine sedimentary Kangilia Formation, with the uppermost part of the marine sedimentary Agatdal Formation, and with parts of the Quikavsuaq Member of the Upper Atanikerdluk Formation (Fig. 2).

3rd cycle: the Ordlingassoq Member is the most widespread of the three main units. The rocks comprise almost exclusively picrites and olivine-rich basalts. During the third cycle the volcanic migration eastwards continued, and large parts of the gneiss terrain were overlapped by volcanic rocks. The member is probably contemporaneous with parts of the sedimentary Naujât and Umiussat Members (Fig. 2).

Tunoqqu Member

The formal lithostratigraphy of the Tunoqqu Member is given in Table 1 and in descriptions and sections presented below.

The basalts of the Tunoqqu Member cover an area of more than 2000 km² on Nuussuaq. The rocks are contemporaneous with the volcanic rocks of the Kûgânguaq Member on Disko (Pedersen, 1985a, b). Type and reference sections through the Tunoqqu Member are shown in Figs 3 and 7. A crude estimate of the minimum volume of erupted rocks is in the order of 50 km³.

The Tunoqqu Member volcanic rocks show a substantial compositional diversity and form a number of compositional groups (Fig. 4, Tables 2 and 3). Rocks from some of these groups have a limited areal distribution and were erupted from local volcanic centres, whereas rocks from other groups occur widely dispersed and without apparent relations to specific volcanic centres. Four local volcanic centres, including the contemporaneous Kûgânguaq centre (new spelling: Kuugannguaq), are shown in Fig. 1.

1. *Kûgânguaq Member* on Disko was erupted from vents situated in the eastern side of Kuugannguaq valley in northern Disko (Pedersen, 1985b).

2. Around *Tupaasat* on the south coast of Nuussuaq a distinct series of brown pahoehoe lavas and hyaloclastites occur (Pedersen *et al.*, 1993). No eruption sites have been located. A section is presented in Larsen & Pedersen (1988, fig. 2 section C).

3. In *Qunnilik* valley on Nuussuaq a large compound lava composed of numerous individual pahoehoe flows forms a rusty brown marker horizon, and a neck-shaped feeder body is located in the northern side valley. The flow attains a maximum thickness of c. 30 m and a volume of at least 0.6 km³. The eruption site is situated near to a later N–S trending hinge zone which was probably also active in Tunoqqu Member time.

4. In the inner part of *Agatdalen* Tunoqqu Member

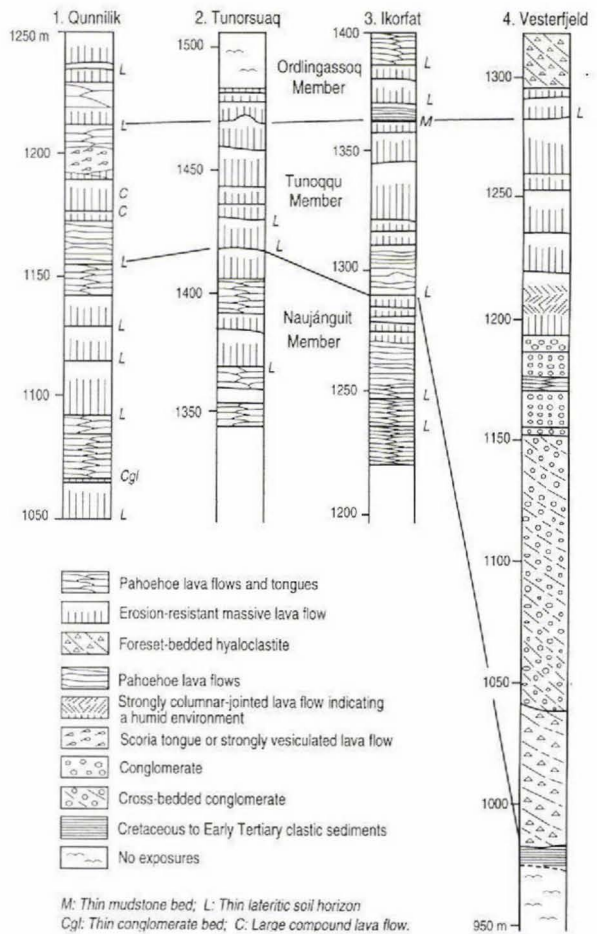


Fig. 3. Reference sections for the Tunoqqu Member. Location of the sections is shown in Fig. 1. Detailed locations are as follows. Section 1: western side of unnamed side valley to Qunnilik valley, 70°33'46''N, 53°45'10''W. Section 2: northern side of Tunorsuaq valley, 70°42'54''N, 53°27'04''W. Section 3: eastern side of glacier south of Ikorfat, 70°44'04''N, 53°03'45''W. Section 4: eastern side of Vesterfeld, 70°42'57''N, 52°51'41''W.

contains some strongly silica-enriched lavas which are probably derived from a local but as yet unidentified volcanic centre in this region.

In addition to these local centres, a number of Tunoqqu Member lava flows are widely distributed between the Aaffarsuaq valley and the north coast of Nuussuaq. Some individual lava flows have been followed for more than 25 km between Tunorsuaq and Vesterfeld in northern Nuussuaq.

Chemical variation

The chemical variation within the Tunoqqu Member is illustrated in Fig. 4. Representative analyses of rocks

Table 2. Chemical analyses of rocks from the volcanic centres and dispersed lavas from the Tunoqqu Member, Nuussuaq

GGU	400208	400238	400239	400307	400204	340711	362020	332703	400129	362039
SiO ₂	46.15	51.44	54.14	52.65	51.59	49.89	51.39	49.25	50.31	47.60
TiO ₂	1.22	1.55	1.82	1.38	1.34	0.97	1.30	1.44	1.57	1.88
Al ₂ O ₃	11.45	15.03	14.73	14.83	14.80	12.33	14.57	14.82	15.23	13.46
Fe ₂ O ₃	3.68	5.24	1.68	2.41	3.65	1.06	0.85	2.77	2.47	4.80
FeO	7.56	5.12	7.82	6.84	6.13	8.66	8.52	8.19	7.64	5.74
MnO	0.17	0.18	0.16	0.15	0.16	0.16	0.19	0.17	0.16	0.15
MgO	17.39	5.73	5.13	8.16	8.23	14.90	11.19	7.69	8.18	9.37
CaO	9.4	10.17	8.93	9.77	10.39	8.02	8.58	12.80	10.76	10.69
Na ₂ O	1.45	2.65	2.61	1.92	1.79	1.38	1.59	1.96	2.02	1.94
K ₂ O	0.090	0.910	0.740	0.454	0.257	0.287	0.432	0.136	0.328	0.920
P ₂ O ₅	0.109	0.160	0.225	0.156	0.150	0.140	0.169	0.125	0.199	0.221
Vol	1.19	1.31	1.36	1.13	1.54	1.82	1.51	0.90	1.04	3.18
	99.86	99.48	99.34	99.85	100.03	99.62	100.29	100.26	99.92	99.94
Cr	1350	192	387	645	624	1186	1048	484	762	502
Ni	705	49	19	121	131	81	23	72	56	203
Sc	34	36	36	33	34	26	32	42	36	31
V	263	269	199	256	258	216	238	345	256	289
Cu	125	42	21	34	38	18	13	98	44	107
Zn	87	83	93	85	85	84	87	92	90	88
Ba	17	809	401	200	142	81	129	65	277	175
Sr	136	313	241	211	209	133	180	218	247	274
Rb	0.8	17	31	16	10	11	7.5	2.9	9.9	31
Y	19	27	34	23	22	20	22	23	27	24
Zr	58	119	187	111	113	93	129	82	113	113
Nb	2.0	17	17	7.9	8.8	4.9	8.2	7.5	12	20
Ga	17	19	22	20	20	15	17	19	21	20
Pb	<2	3	6	5	<2	4	4	<2	<2	4
Th	<1	2	8	6	4	2	3	2	5	3

Major elements: GGU's chemical laboratory. XRF except for Na₂O (AAS) and FeO (titration).

Trace elements: XRF, John Bailey, Geological Institute, University of Copenhagen.

400208: Uncontaminated picrite lava from Naujánguit Member, representing a possible parent magma for the magmas of Tunoqqu Member. West side of side valley to Qunnilik valley, 40 m below Tunoqqu Mb. 70°33'46"N, 53°45'10"W, alt. 1114 m.

400238: Aphyric basalt lava from the Agatdal volcanic centre. Mountain ridge in northern part of Agatdalen, 70°35'45"N, 53°07'30"W, alt. 705 m.

400239: As 400238, alt. 610 m.

400307: Plagioclase-orthopyroxene-olivine-phyric basalt, volcanic neck (feeder) from the Qunnilik volcanic centre. West side of side valley to Qunnilik valley, 70°34'24"N, 53°45'10"W, alt. 1150 m.

400204: Orthopyroxene-olivine-phyric basalt lava flow from the Qunnilik volcanic centre. West side of side valley to Qunnilik valley, 70°33'46"N, 53°45'10"W, alt. 1185 m.

340711: Olivine-phyric basalt hyaloclastite breccia from the Tupaasat volcanic centre. Tupaasat, south coast of Nuussuaq, 70°21'11"N, 53°05'12"W, alt. 750 m.

362020: Aphyric basalt, thin pahoehoe lava flow from the Tupaasat volcanic centre. South coast of Nuussuaq between Tupaasat and Nuuk Qiterleq, 70°21'33"N, 53°10'58"W, alt. 825 m.

332703: Plagioclase-olivine-phyric basalt, subaqueous lava flow. Tunoqqu type section, central Nuussuaq, 70°30'26"N, 53°04'20"W, alt. c. 906 m.

400129: Olivine-plagioclase-phyric basalt lava flow. Tunorsuaq valley, NW Nuussuaq, 70°42'54"N, 53°27'04"W, alt. 1508 m.

362039: Olivine-phyric basalt lava flow with slightly enriched chemistry. South coast of Nuussuaq 7.5 km west of Nuuk Killeq. 70°23'50"N, 53°38'37"W, alt. 1110 m.

Table 3. Chemical analyses of volcanic rocks from the Tunoqqu Member in the profile at Vesterfjeld, north-eastern Nuussuaq

GGU	400333	400332	400330	400335	400338	400339	400340	400341	400342
SiO ₂	53.89	53.04	52.08	51.38	50.36	50.30	48.76	52.90	51.69
TiO ₂	1.64	1.73	1.39	1.38	1.59	1.59	1.36	1.37	1.53
Al ₂ O ₃	14.93	14.77	14.97	15.08	14.33	14.35	13.91	15.77	15.24
Fe ₂ O ₃	1.28	3.02	2.15	3.74	2.51	2.78	2.69	2.26	2.25
FeO	7.97	6.59	7.50	6.06	7.75	7.54	7.65	6.98	7.88
MnO	0.16	0.17	0.16	0.19	0.18	0.17	0.18	0.16	0.17
MgO	5.99	5.51	7.57	7.30	8.60	8.52	10.84	6.50	6.70
CaO	8.88	9.86	9.57	9.75	10.85	10.93	10.57	10.24	10.81
Na ₂ O	2.41	2.12	2.21	1.98	2.13	2.09	1.73	1.92	2.07
K ₂ O	0.602	0.429	0.308	0.279	0.295	0.339	0.333	0.390	0.645
P ₂ O ₅	0.200	0.214	0.155	0.150	0.161	0.164	0.155	0.144	0.161
Vol	1.58	2.22	1.37	2.02	0.86	0.68	1.40	0.86	0.44
	99.52	99.67	99.44	99.31	99.62	99.46	99.58	99.49	99.59
Cr	459	431	666	736	481	505	1020	744	765
Ni	24	20	31	33	177	166	107	15	28
Sc	37	36	35	33	37	38	35	36	39
V	212	213	248	245	307	312	277	243	273
Cu	26	27	27	29	87	80	48	18	37
Zn	91	91	89	96	87	92	90	86	88
Ba	370	262	239	158	157	177	221	197	172
Sr	236	281	235	231	226	232	234	232	219
Rb	30	13	18	11	7.3	5.0	5.5	14	18
Y	30	32	24	24	25	25	22	24	25
Zr	167	174	124	125	107	105	92	121	115
Nb	15	16	11	11	9	8.7	10	7.3	8.8
Ga	20	23	19	21	21	21	19	20	21
Pb	4	6	7	9	5	4	<2	<2	2
Th	6	7	5	5	1	2	1	1	2

Major elements: GGU's chemical laboratory. XRF except for Na₂O (AAS) and FeO (titration).

Trace elements: XRF, John Bailey, Geological Institute, University of Copenhagen.

400333: Aphyric basalt, clast in conglomerate, alt. 1150 m.

400332: Aphyric basalt, clast in conglomerate, alt. 1150 m.

400330: Aphyric basalt, pillow in hyaloclastite breccia, alt. 1150 m.

400335: Aphyric basalt, 2 m thick pahoehoe lava flow, alt. 1180 m.

400338: Olivine-microphyric basalt, 25 m thick lava flow, no. 1 above conglomerates, alt. 1193 m.

400339: Olivine-microphyric basalt, 10 m thick lava flow, no. 2 above conglomerates, alt. 1220 m.

400340: Olivine-phyric basalt, 15 m thick lava flow, no. 3 above conglomerates, alt. 1234 m.

400341: Plagioclase-augite-phyric basalt, 5 m thick lava flow, no. 4 above conglomerates, alt. 1255 m.

400342: Plagioclase-augite-olivine-phyric basalt, min. 25 m thick lava flow, no. 5 above conglomerates, alt. 1260 m.

The Vesterfjeld profile is shown in Fig. 3 and its location is given there.

typical of the various centres and of the more dispersed flows are given in Table 2, and analyses showing the variation within one profile (Vesterfjeld) are given in Table 3.

The rocks of the Tunoqqu and Kûgánguaq Members span a large range of MgO contents (5–16%), but the different compositional groups present cannot be related by ordinary crystal fractionation processes because this

would require that they followed evolutionary trends as those shown in Fig. 4 for uncontaminated rocks. Instead, crustal contamination is the major controlling factor, as has been shown for the Kûgánguaq Member by Pedersen (1985b).

Many rocks of the Tunoqqu Member are distinctly silica-enriched and clearly contaminated, whereas other rocks, including those from the profile at Tunoqqu, with 49–50% SiO₂ are not clearly contaminated although their

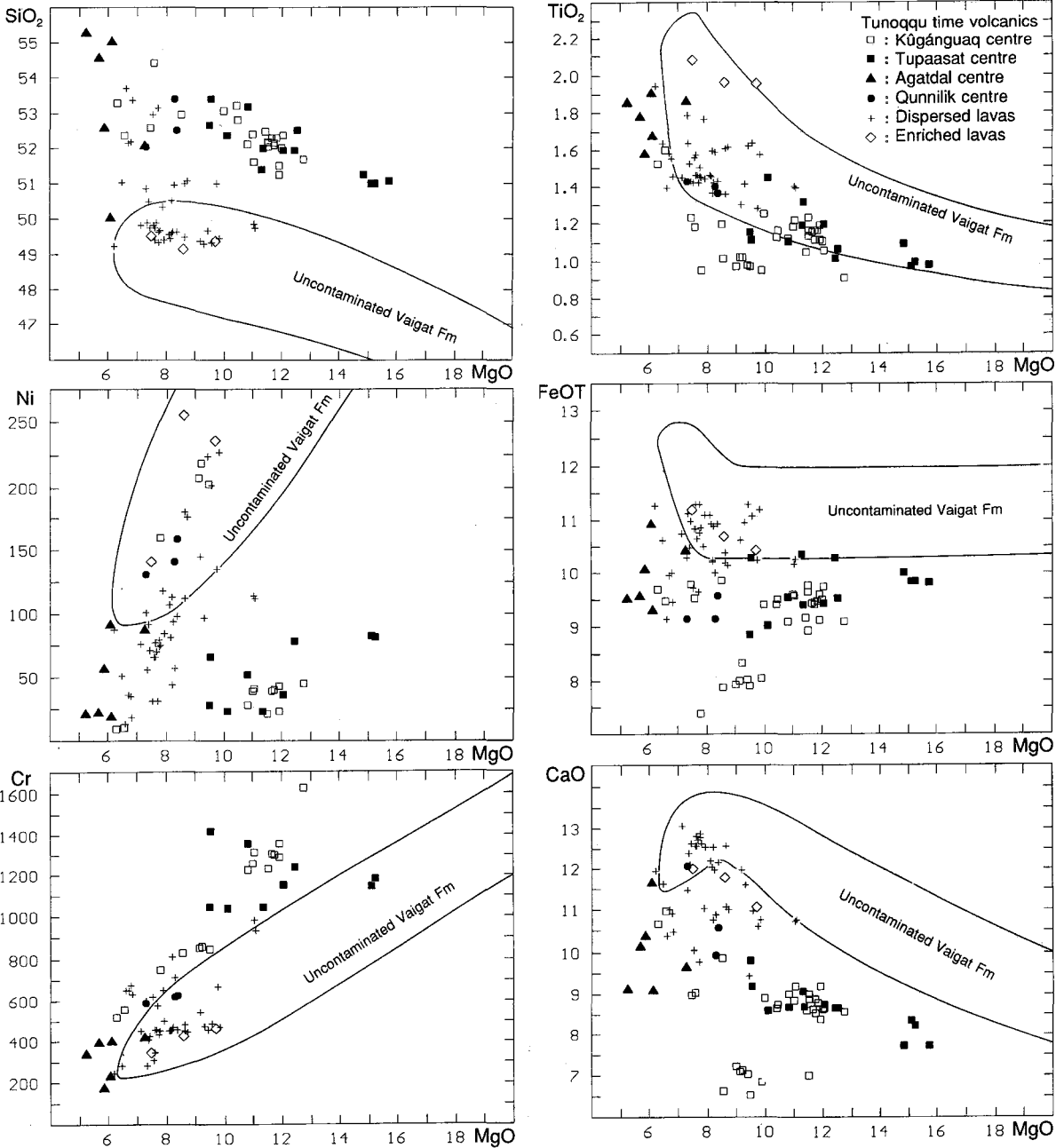


Fig. 4. Diagrams of the variation of TiO_2 , FeOT (total iron as FeO), CaO, SiO_2 , Ni and Cr v. MgO for volcanic rocks of the Tunoqqu Member and the coeval Kùgànguaq Member. Rocks from the four identified volcanic centres are indicated. The variation trends for uncontaminated rocks from the Vaigat Formation (mainly unpublished data) are shown for reference.

slight displacement within the 'normal' ranges for the Vaigat Formation towards high SiO_2 and low FeOT, CaO and Ni show that they may be just slightly contaminated. The group of lavas with 49–50% SiO_2 and 6–10% MgO represents essentially normal, evolved, feldspar-phyric and aphyric basalts.

A group of lavas with 50–51% SiO_2 have low FeOT

and low CaO outside the normal range and are probably contaminated evolved rocks.

All four local eruption centres have produced highly silicic, strongly contaminated rocks. The *Kùgànguaq* and *Tupaasat* centres both produced silicic high-Mg basalts with 9–13% MgO (Tupaasat centre up to 16% MgO) and distinctly low FeOT, CaO and TiO_2 . The

uncontaminated parents for these rocks must have been picrites with at least 18% MgO, estimated from the high Cr contents in the resultant rocks. The low Ni contents in most of these rocks are indicative of sulphide fractionation (Pedersen, 1985b). The Kûgánguaq centre in addition produced magnesian andesites with 8–10% MgO and 56–59% SiO₂ (not shown in the SiO₂ diagram), and silicic feldspar-phyric basalts.

The *Agatdalen* centre produced low-Mg basalts and andesites with 50–55% SiO₂. They have relatively high TiO₂ contents, low Cr, and very low Ni contents in continuation of the uncontaminated evolution trend for Ni. This indicates that the parent magma for this centre was evolved basalt similar to or more evolved than the almost uncontaminated dispersed lavas from the Tunoqqu Member.

The *Qunnilik* centre produced silicic basalts with around 8% MgO, fairly similar to the silicic feldspar-phyric basalts from the Kûgánguaq centre. According to the Cr contents the parent magma for this centre would have had at least 12% MgO. There are no signs in the Ni contents of sulphide fractionation.

Some dispersed lavas show the same silica enrichment as the lavas of the centres. Such lavas occur in several profiles but correlation between them is equivocal.

A lava with *c.* 11% MgO (Table 3, 400340) occurs in two neighbouring profiles and is sufficiently characteristic to be unequivocally correlatable. It is slightly contaminated from a parent with at least 14% MgO (Cr diagram), and it is sulphide fractionated (Ni diagram).

A few lavas enriched in TiO₂ and P₂O₅ (Table 2, 362039) occur at the top of the Tunoqqu Member in two neighbouring profiles and are probably from the same, late eruption centre.

In conclusion, the Tunoqqu Member is characterised by a range of dominantly silicic basalts produced contemporaneously in a number of independent volcanic reservoirs by contamination of magmas ranging in composition from picrite to evolved basalt.

Geographical distribution of the Tunoqqu Member

The areal extent of the Tunoqqu Member is shown in Fig. 5. In the following description of the terrains and the volcanic products, the area in which the Tunoqqu Member has been identified is subdivided into five: the western subaerial lava plain; the eastern gneiss highland; the marine embayment in between; the western volcanic shore zone; and the conglomerate-dominated areas at the north coast of Nuussuaq.

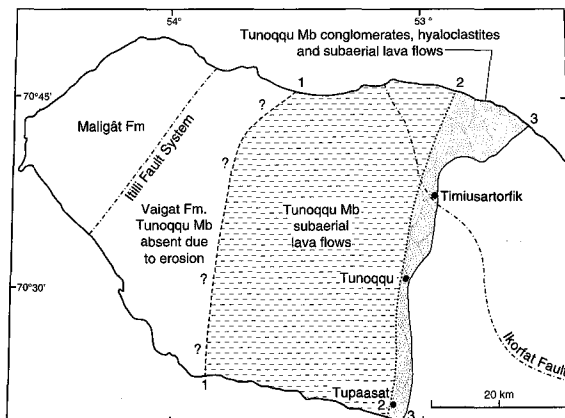


Fig. 5. Geographical distribution of the Tunoqqu Member.

Line 1 – 1: Approximate western limit of exposures of the Tunoqqu Member, controlled by the present topography.

Line 2 – 2: Earliest shoreline, where the oldest Tunoqqu Member lavas entered the marine embayment.

Line 3 – 3: The eastern limit of progradation of Tunoqqu Member volcanic rocks.

The three named localities are described later in the text.

Western subaerial lava plain

Just prior to the formation of the Tunoqqu Member, central and western Nuussuaq and northern Disko were covered by a lava plain of picritic pahoehoe lavas. This lava plain extended east to a shore zone shown on Fig. 5. In central Nuussuaq an older, partly buried crater cone of graphite andesite tuffs at Ilugissoq (Fig. 1) rose about 30 m above the lava plain. Other irregularities were associated with zones of local synvolcanic tectonic movements. Two such zones have been documented through detailed photogrammetric work: a zone of uplift north of Nuuk Killeq associated with extension (Fig. 1; Pedersen & Dueholm, 1992, fig. 10; Pedersen *et al.*, 1993), and a zone of gentle subsidence on the western fringe of the Ikkorfat fault system (Fig. 1).

Eastern gneiss highland

Fig. 6 shows a simplified contour map of parts of the gneiss highland on Nuussuaq east of the Ikkorfat fault system and north of the Aaffarsuaq valley at the end of Tunoqqu Member time. The gneiss highland shows local topographic relief of several hundred metres. Many details of the relief have been preserved under the cover of later lavas which has been stripped off only in comparatively recent time.

The essential feature of the gneiss highland is a NW-trending ridge extending from eastern Nuussuaq to just east of Agatdalen. It had the form of a promontory

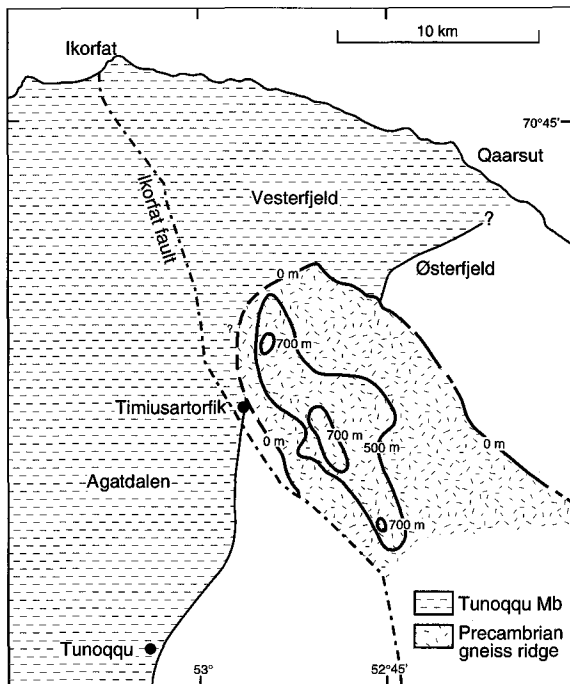


Fig. 6. Detailed palaeogeographical map of parts of the eastern gneiss highland and its surroundings at the end of Tunoqqu Member time. The contours on the gneiss ridge were compiled from the contours on the 1:100 000 map sheet Agatdal, with the top of the Tunoqqu Member taken as reference (zero) level, and assuming no later tilting in the area. The eastern boundary of the Tunoqqu Member is drawn at its maximum eastern extent. The localities Tunoqqu and Timiusartorfik are described later in the text and shown in Figs 7–9.

extending into the sea and rising to more than 500 m, locally more than 700 m above the surroundings, with no documented cross-cutting channels. The NW end of the promontory is now buried beneath volcanic rocks and may have been affected by post Vaigat Formation downthrow to the west along the Ikorfat fault system. The shape of the gneiss ridge is probably tectonically controlled: its NW trend is sub-parallel to the Ikorfat fault system, and also to a prominent direction of dyke intrusion on both Disko and Nuussuaq (e.g. Pedersen, 1977), indicating tension in a SW–NE direction.

At the time just prior to the formation of the Tunoqqu Member the progressively eastwards advancing subaerial lava plain turned the marine embayment in south central Nuussuaq into an enclosed water body connected to the sea in the north only through a comparatively narrow strait between the volcanic front and the gneiss promontory.

The marine embayment

The geological section along the south coast of Nuussuaq (Pedersen *et al.*, 1993) shows that the hyaloclastite breccias of the Naujánguit Member decrease in thickness eastwards. The height of the foresets in the hyaloclastite fans from the Tunoqqu Member shows water depths of *c.* 160 m at that time. The coeval eastern clastic shoreline is tentatively positioned in the vicinity of Kingittoq (Fig. 13). This was done by backstripping to an extensive plateau lava flow from the Maligât Formation (Pedersen *et al.*, 1993, unit mM; and Pedersen & Dueholm, 1992, fig. 14).

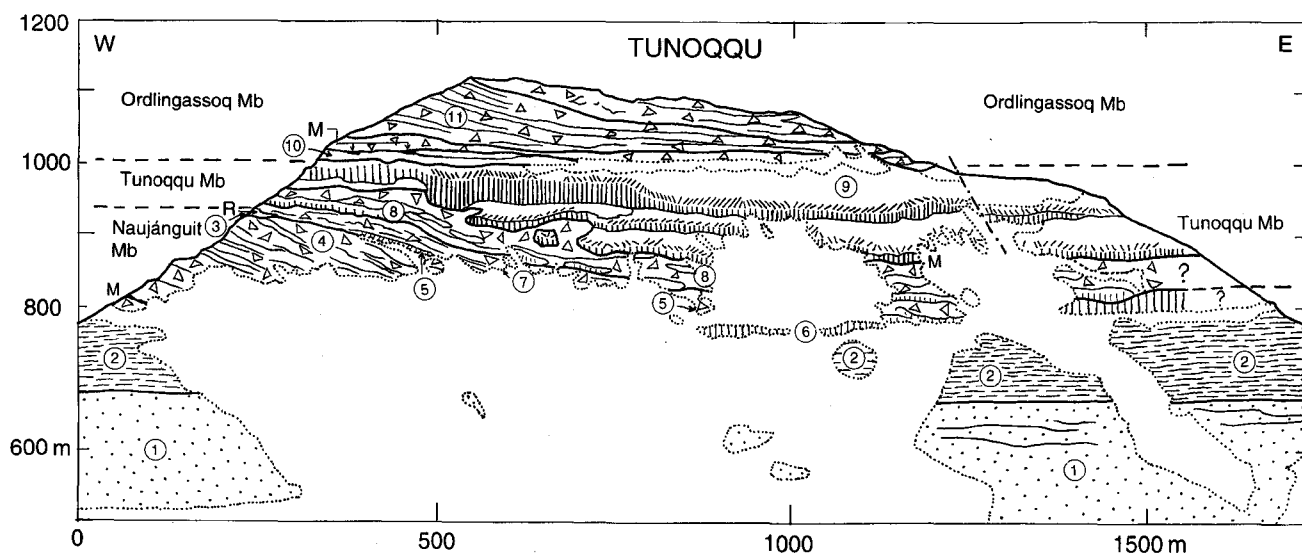
Further north, in the inner part of Saqqaq dalen, Pulvertaft (1989) noted a marked relief on the boundary between the Atane Formation and the overlying Naujánguit Member, whereas no traces of Quikavsak Member were found. This may indicate that erosion of the Atane Formation continued into Tunoqqu Member time. The clastic shoreline thus lay to the west of inner Saqqaq dalen.

The palaeogeographic reconstruction in Fig. 13 shows the inferred extension of the marine embayment and proposes the existence of a low-energy shoreline to the east. Very little clastic sediment accumulated during the time of hyaloclastite breccia progradation.

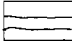

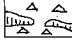
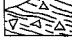

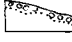
Western volcanic shore zone

The volcanic rocks of the Tunoqqu Member entered the marine embayment from the west, along a shoreline running roughly N–S from southern to central Nuussuaq. Here the line turned slightly to the NE towards the present north coast of Nuussuaq (Fig. 5). The shore is characterised below by means of detailed descriptions of three localities shown on Fig. 5.

Tupaasat. A section through the shore zone where Tunoqqu Member lavas entered the sea is exposed at Tupaasat and also shown by Larsen & Pedersen (1988, fig. 2, loc. C) and Pedersen *et al.* (1993, at about 32 km, the easternmost contaminated basalts grouped with the Asuk Member). The sediments of the sea floor are not exposed but are supposed to be clastic sediments from the Quikavsak Member, possibly covered by mudstone. A series of foreset-bedded Tunoqqu Member hyaloclastite breccias indicate infilling from the south-west and a minimum water depth of 160 m. These are covered by *c.* 50 m of thin subaerial pahoehoe flows of silicic magnesian basalt (Table 2) which successively go into hyaloclastite facies over a horizontal distance of 800 m. At the eastern end of the exposure the last lava has entered the water. The Tunoqqu Member volcanic rocks are covered by thin lenses of mudstone that were deformed when the overlying

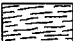


Vaigat Formation, (Paleocene)

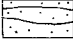
-  Picritic subaerial lava flow
-  Strongly columnar-jointed basalt lava indicating a humid environment
-  Subaqueous-basalt lava flows interbedded with hyaloclastite
-  Foreset-bedded hyaloclastite
-  Invasive basalt lava flow
-  Conglomerate with volcanic clasts

- M Thin mudstone bed
- R Rocky shore

Upper Cretaceous marine clastic sediments

-  Shale, locally with intraformational conglomerates at base

Atane Formation

-  Fluvial and deltaic sediments

--- Fault

Ordlingassoq Member: ⑩ ⑪

Tunoqu Member: ⑥ ⑦ ⑧ ⑨

Naujánguit Member: ③ ④ ⑤

Fig. 7. The south side of Tunoquq mountain. The section was compiled from colour diapositives by multi-model photogrammetry. The projection plane is vertical, west–east orientated, looking north. At this locality the Tunoquq Member lavas flowed from the west into the marine basin. A shore zone in the older Naujánguit Member rocks is defined by a rocky coast of eroded lavas (R) and local conglomerates (5) derived by erosion of lavas and hyaloclastites. The Tunoquq Member rocks are a lava invasive into sediments (6), and hyaloclastite breccias and subaqueous lava tongues (7 and 8) overlain by strongly columnar-jointed partly subaqueous lavas (9). One lava flow has bulldozed into the underlying hyaloclastites and thickened to form an 80 m deep lava pond that just surfaced above the water level.

hyaloclastites of the Ordlingassoq Member were deposited. One dinoflagellate cyst was found in a sample of these mudstones (Piasecki *et al.*, 1992, loc. 9).

Tunoquq. The south side of the small mountain Tunoquq in central Nuussuaq displays an excellent east–west section approximately perpendicular to the Tunoquq Member shore zone (Figs 7 and 8). The Atane Formation is here overlain by grey ammonite-bearing marine shales which are generally poorly exposed. These shales may

perhaps belong to the Kangilia Formation but formally they have not been referred to any formation. The pre-Tunoquq Member shore consists of foreset-bedded picrite lava flows from the Naujánguit Member. Both hyaloclastites and particularly the lavas have been eroded by wave action under conditions of relatively rising water level. The lavas are sculpted as a rocky, boulder-strewn coast, and conglomerate and gravel of rounded picrite lava cobbles and re-worked hyaloclastite are deposited

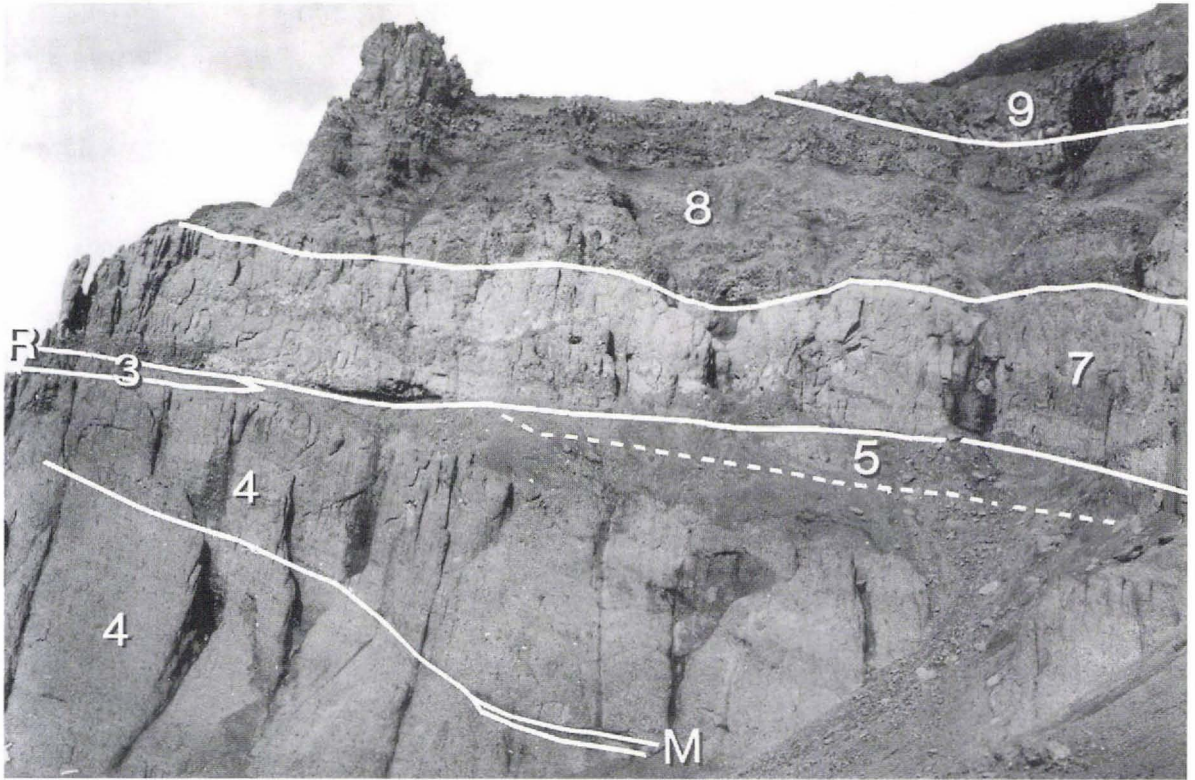


Fig. 8. Photographs from the south side of Tunoqu mountain. *Top*: The western part of the section shown in Fig. 7. The Naujánguit Member here includes hyaloclastite breccias (4) with a local mudstone (M), overlain by eroded picrite lavas (3) defining a rocky shore (R) and locally derived conglomerates (5). The Tunoqu Member includes foreset-bedded hyaloclastite breccias (7), subaqueous lava tongues and hyaloclastite (8), and a large lava flow (9) which in this part of the section is in subaerial facies. *Bottom*: Detail of the beach conglomerate (5), showing well rounded clasts of lava and hyaloclastite in a matrix of volcanic fragments.

along a sloping, slightly eroded hyaloclastite shelf up to 120 m deep. The lowest unit of the Tunoqu Member is a foreset-bedded hyaloclastite breccia with pillow lava

tongues. It is covered by a series of small subaqueous lava tongues embedded in hyaloclastite and with local patches of mudstone on the top. The upper part of the

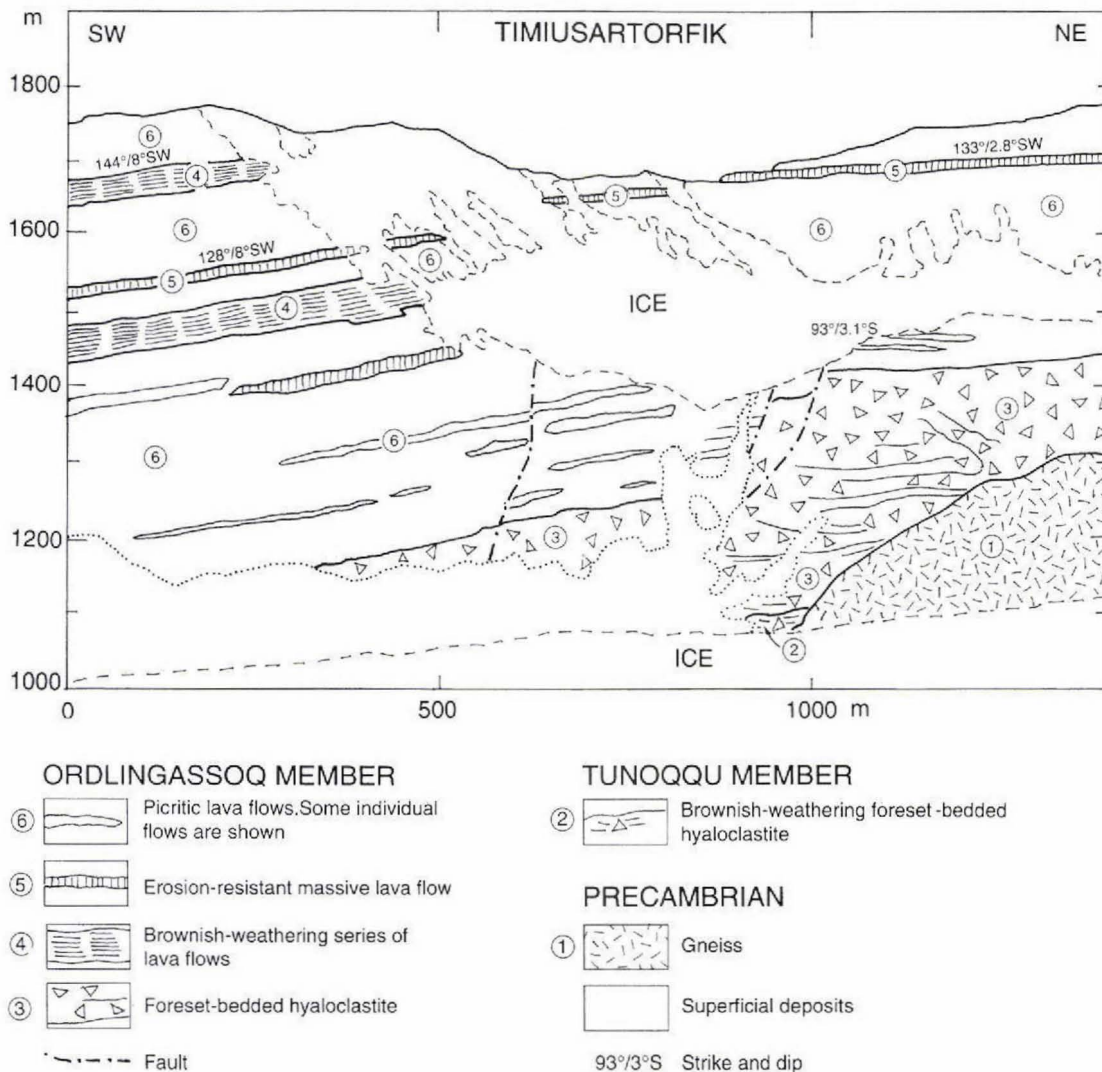


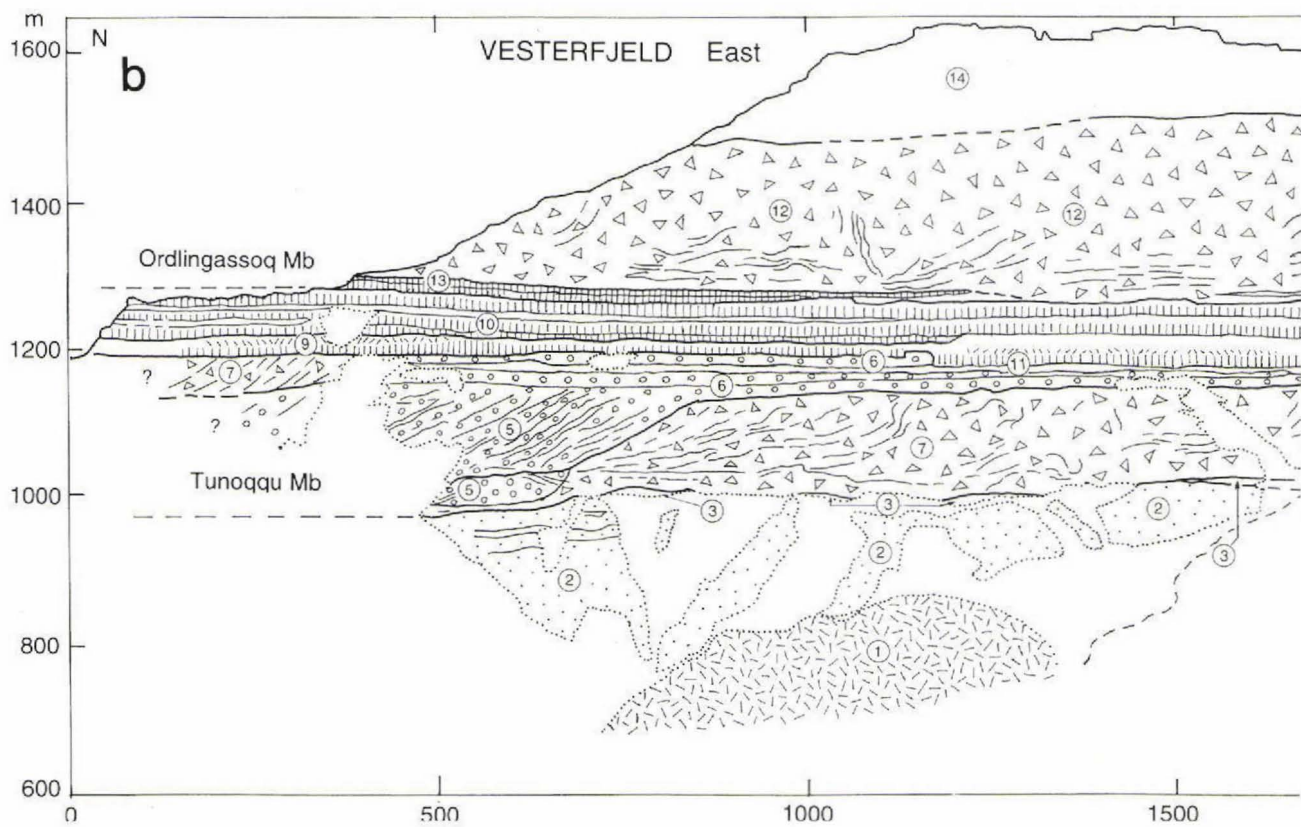
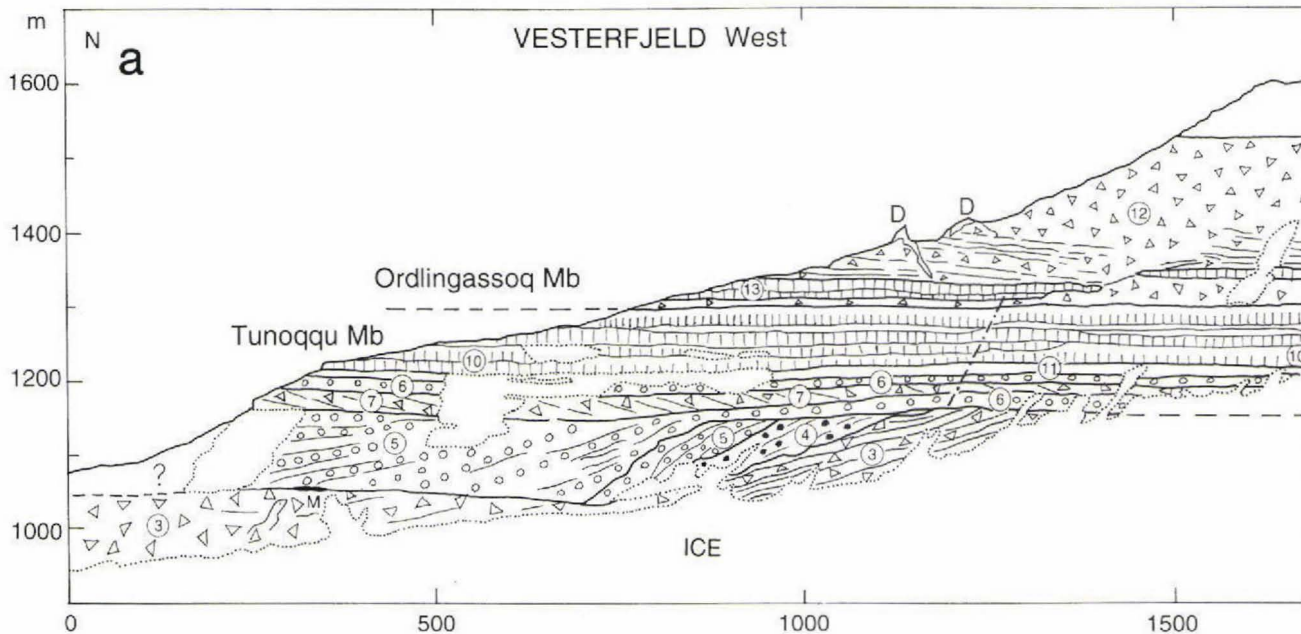
Fig. 9. Timusartorfik. The section was compiled from colour diapositives by multi-model photogrammetry. The projection plane is vertical, SW-NE orientated, looking NW. The Ikorfat fault system runs through the section and is approximately perpendicular to it. The lowermost volcanic unit (2) is brown hyaloclastite or conglomerate from the Tunoqqu Member, onlapping Precambrian gneiss (1). The Tunoqqu Member is covered by several hundred metres of hyaloclastite breccia from the Ordlingassoq Member (3). The lavas south-west of the fault zone dip about 8° SW and define a shallow syncline along the margin of the Ikorfat fault.

Tunoqqu Member consists of distinctly columnar-jointed basalt lavas. The uppermost of these lavas shows a very well developed transition from subaerial to subaqueous facies. In the western part of the section it is a 25 m thick aa lava with the top showing high-temperature subaerial oxidation. Where the lava reached the shore zone it bulldozed into the underlying brecciated units which caused a local thickening of the flow to 60 m. Farther into the basin it formed a 80 m thick ponded lava that built up right to the surface of the basin. The top zone of the subaerial part of the lava is reworked into a minor basalt

conglomerate with rounded oxidised clasts and fining-upwards structure. A relative rise in the water level of 35 m during the interval pre- to end-Tunoqqu Member time is indicated. The Tunoqqu Member is covered by a c. 10 m thick picrite lava flow from the Ordlingassoq Member. This flow is in places covered by up to 40 cm of mudstone deposited in local depressions, and this is again covered by more than 100 m of Ordlingassoq Member picrite hyaloclastites.

Timusartorfik. About 14 km NNE of Tunoqqu 25 m

18



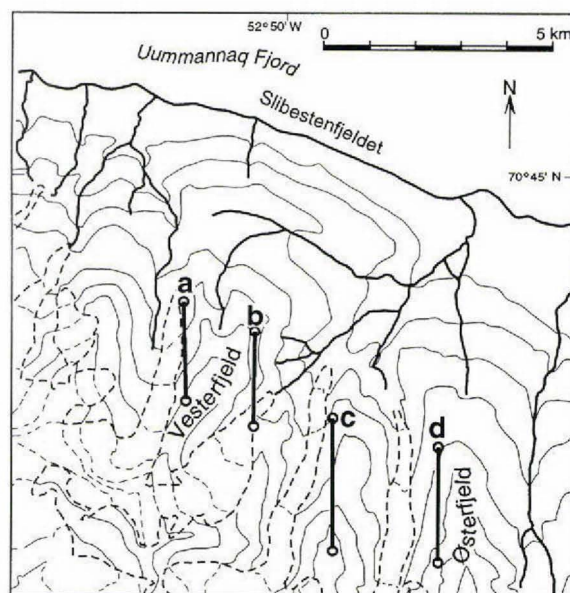
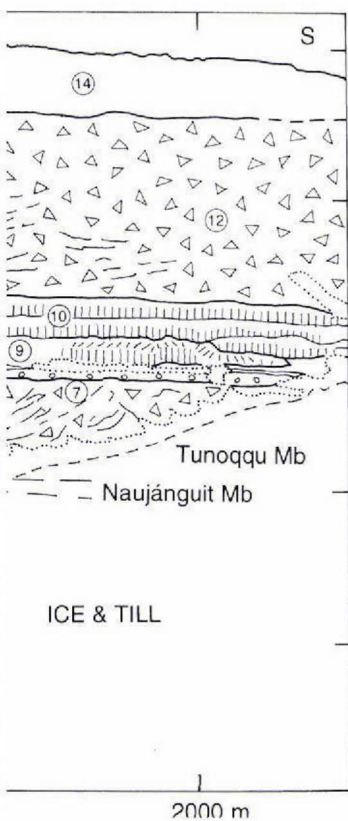
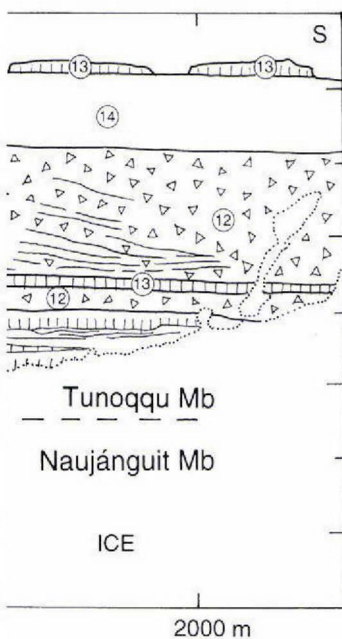


Fig. 10. Four sections through the Tunoquq Member between Vesterfjeld and Østerfjeld at the north coast of Nuussuaq (index map). The sections were compiled from colour diapositives by multi-model photogrammetry. The projection planes are vertical, north-south orientated, looking east.

a. West side of Vesterfjeld. Hyaloclastite breccias from the Naujánquit Member (3) are overlain by several units of cross-bedded boulder conglomerates from the Tunoquq Member (4, 5, 6) which prograded northwards into the sea. The conglomerates are interbedded with a hyaloclastite horizon (7), and overlain by subaerial lava flows (10, 11). The Tunoquq Member is overlain by hyaloclastite breccias (12) and lavas (13, 14) from the Ordlingassoq Member.

b. East side of Vesterfjeld. Precambrian gneiss (1) and Cretaceous to lower Tertiary clastic sediments (2) are overlain by thin discontinuous deposits of hyaloclastite from the Naujánquit Member (3). These are followed by thick deposits of Tunoquq Member hyaloclastite breccias (7) and cross-bedded boulder conglomerates (5, 6) which prograded north and north-eastwards into the sea. The clastic rocks are covered by Tunoquq Member subaerial lava flows (9, 10, 11). Flow 9 flowed over humid ground, as indicated by its structure with a thick entablature zone. These lavas are covered by hyaloclastite breccias (12) and lava flows (13, 14) from the Ordlingassoq Member.

c. West side of Mellemfjeld (Heim, 1910, p. 178). Precambrian gneiss (1) and Cretaceous to lower Tertiary clastic sediments (2) are overlain by more than 200 m of conglomerates from the Tunoquq Member. Six conglomerate units are distinguished; they show transport directions towards the east and south-east. An invasive lava (8) is seen in the lower part of the conglomerates. An irregular lava flow (9) with a thick entablature zone has filled a humid erosional? depression in the conglomerates. The Tunoquq Member ends with subaerial lavas (10) and is overlain by hyaloclastite breccias from the Ordlingassoq Member (12).

d. West side of Østerfjeld. Precambrian gneiss (1) and Cretaceous to lower Tertiary clastic sediments (2) are overlain by foreset-bedded hyaloclastite breccias from the Tunoquq Member (7). A Tunoquq Member lava (8) has invaded the lower part of the hyaloclastites. The hyaloclastites are covered by subaerial lavas (11). The Tunoquq Member is overlain by hyaloclastite breccias (12) and lavas (13) from the Ordlingassoq Member.

Continued next page

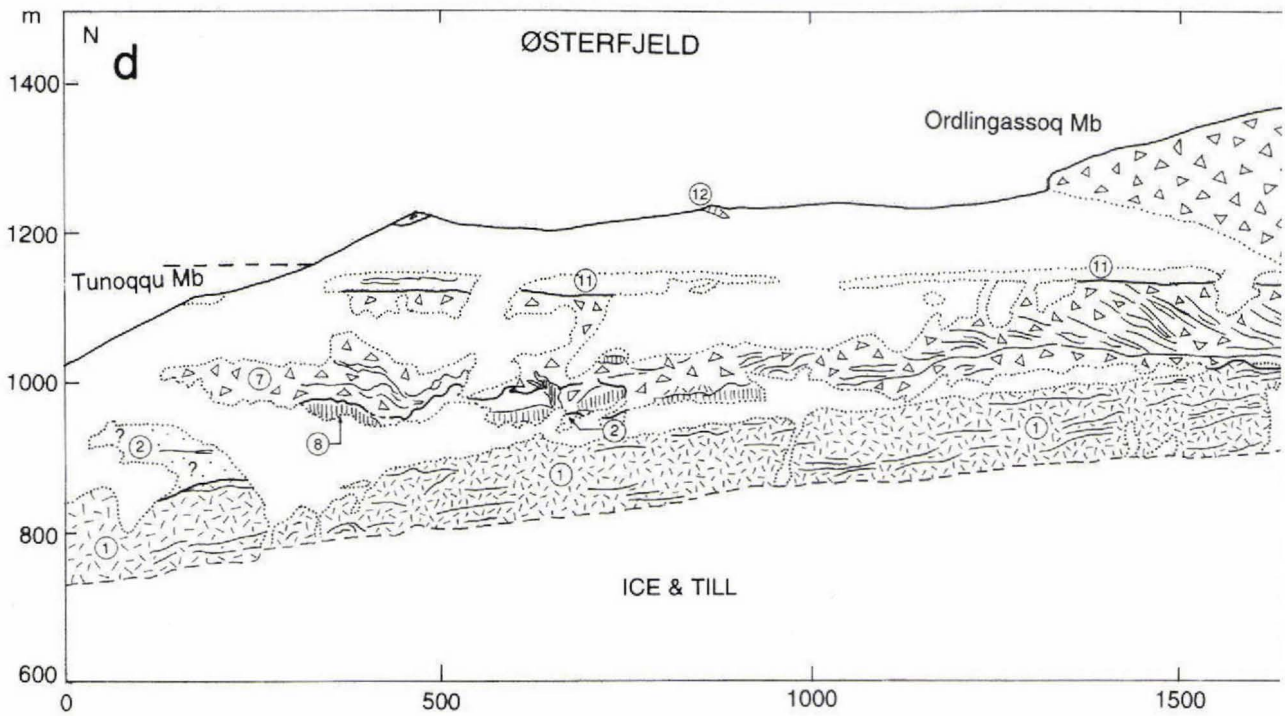
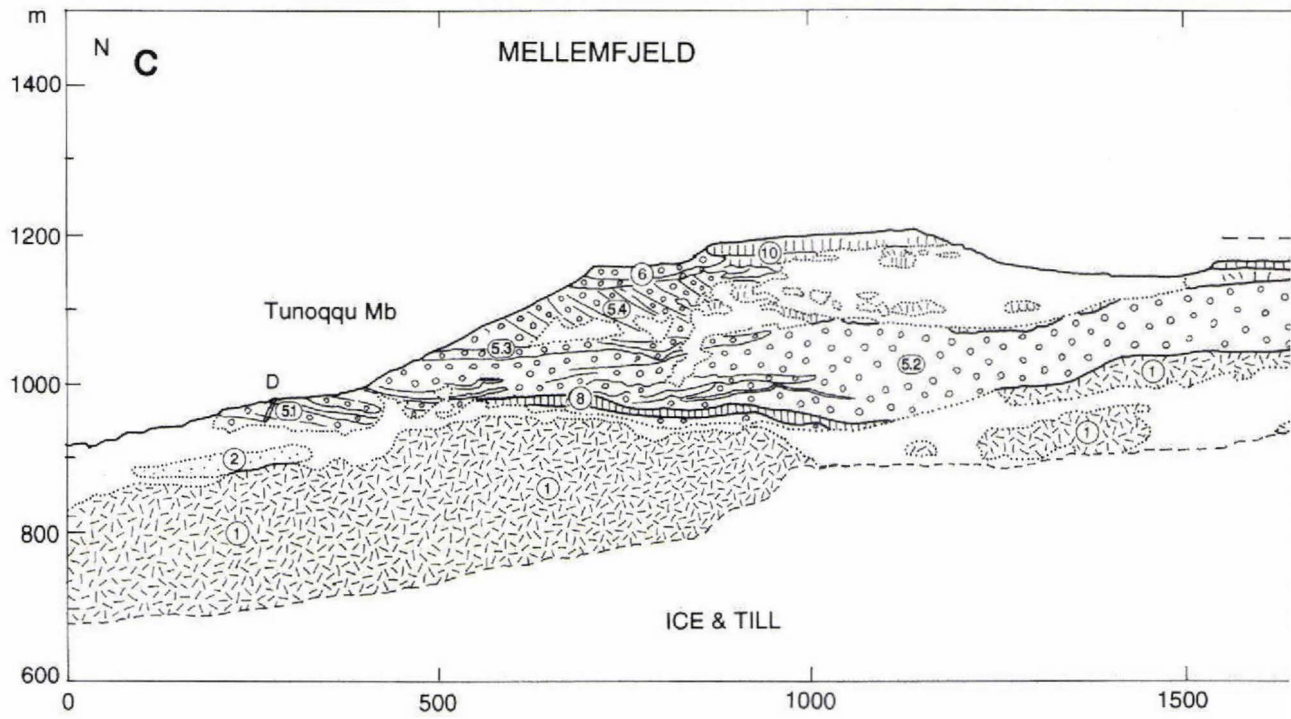
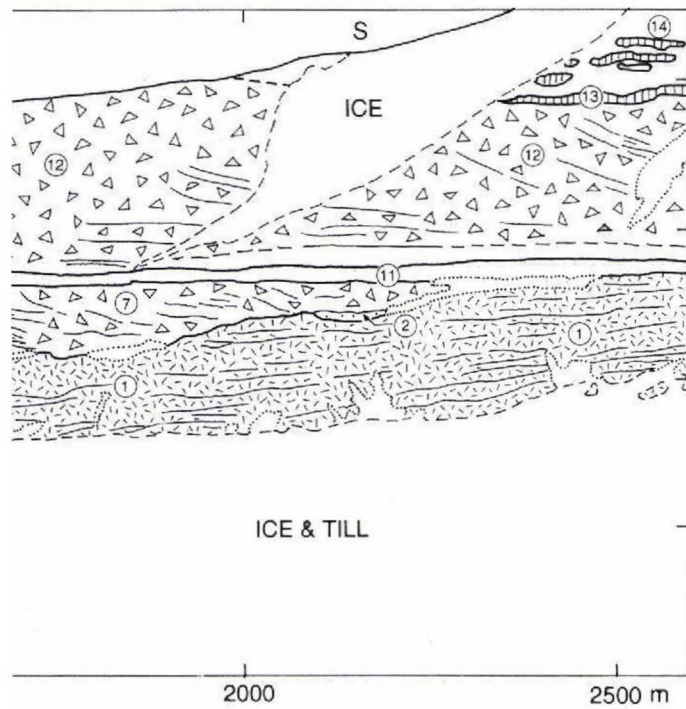
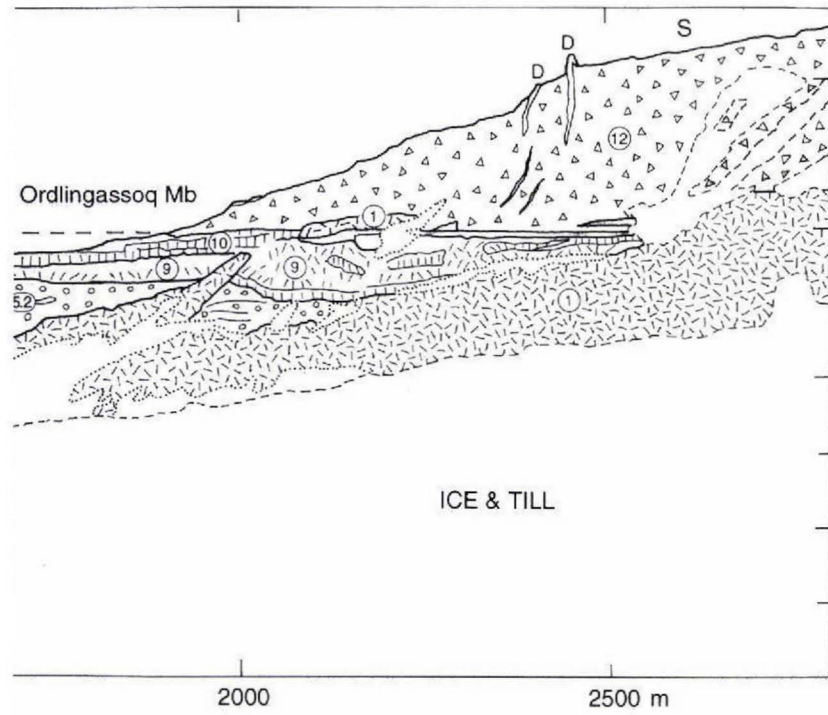


Fig. 10 cont.



Ordlingassoq Member

- ⑭ Pahoehoe lava flows and tongues
- ⑬ Erosion-resistant massive lava flows
- ⑫ Foreset-bedded hyaloclastite

Tunoqqu Member

- ⑪ Pahoehoe lava flows and tongues
- ⑩ Erosion-resistant massive lava flows
- ⑨ Strongly columnar-jointed lava flow indicating a humid environment
- ⑧ Invasive lava flow
- ⑦ Foreset-bedded hyaloclastite
- ⑥ Conglomerate with Tunoqqu Member lava blocks
- ⑤ Cross-bedded conglomerate with Tunoqqu Member lava blocks
- ④ Cross-bedded conglomerate with olivine-rich lava blocks

Naujanguit Member

- ③ Foreset-bedded hyaloclastite

Cretaceous to Early Tertiary

- ② Clastic sediments sand- and mudstone

Precambrian

- ① Gneiss and amphibolite

M Thin mudstone bed

D Dyke Fault

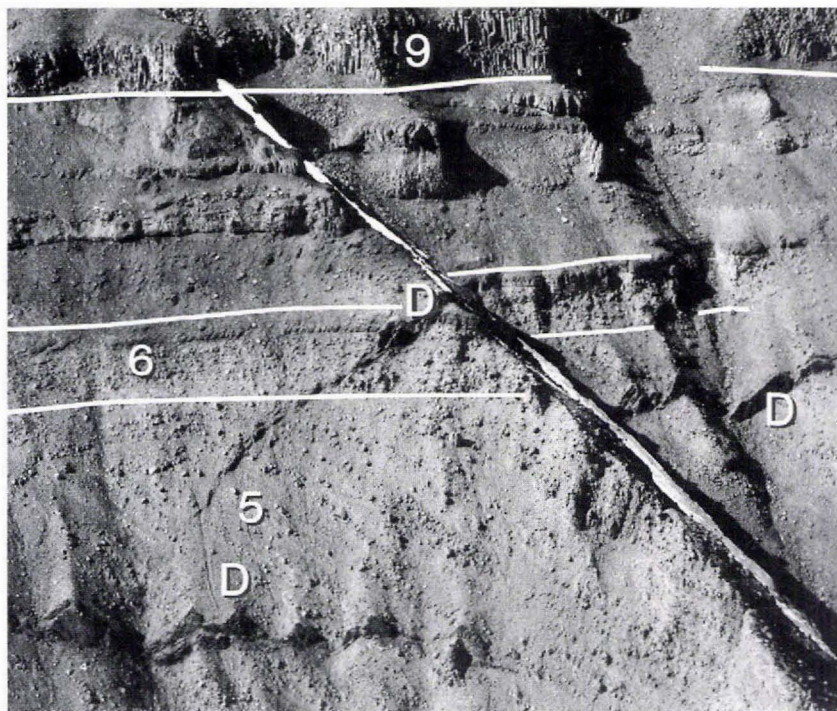


Fig. 11. Tunoqu Member boulder conglomerates. *Top*: Thick, cross-bedded conglomerates (5) overlain by horizontally bedded conglomerates (6), overlain by subaerial lavas. Basaltic dykes (D) cut the conglomerates. East side of Vesterfjeld; numbers are the same as in Fig. 10. *Bottom*: Conglomerate with large rounded blocks of vesicular lava and numerous small rounded pebbles of hyaloclastite. The matrix is hyaloclastite sand.



North coast of Nuussuaq from Vesterfjeld to Østerfjeld

In this area, the Tunoqu Member possesses a complicated geological structure and large lithological variations. A prominent feature is the occurrence of thick, foreset-bedded boulder conglomerates. The rocks have been studied in four parallel N–S orientated valley sections 2.5–3.5 km in length, and covering an E–W distance of 7 km (Fig. 10).

The *substrate* for the Tunoqu Member varies from section a to section d in Fig. 11. In section a, the substrate consists of foreset-bedded picritic hyaloclastite breccias from the Naujánguit Member. These are more than 100 m thick and were filled in from the south-west. Thin inter-layered mudstones with a few Tertiary dinoflagellate cysts (S. Piasecki, personal communication, 1994) show that the hyaloclastites were deposited in a marine environment. On the eroded top of these hyaloclastites is deposited an up to 50 m thick very coarse, cross-bedded grey conglomerate with lava boulders up to 2.5 m in size consisting of olivine basalt and subordinate aphyric basalt and gneiss blocks. In section b, only a very thin layer of picritic hyaloclastite separates sediments and Tunoqu Member rocks. In sections c and d the north-sloping surface of the gneiss promontory is well exposed and rises high to the south. Poorly exposed Cretaceous sediments cover the northern tip of the gneiss in section c. In section d, coarse sandstone and mudstone deposited on

of light brown Tunoqu Member hyaloclastites or conglomerates are exposed, banked up against a sloping gneiss surface which rose 200 m above them (Fig. 9). The Tunoqu Member rocks are covered by 325 m of Ordlingassoq Member picritic hyaloclastites which are also banked up against the gneiss. The locality marks the point where the advancing Tunoqu Member volcanic rocks reached the gneiss promontory. However, the thick Ordlingassoq Member hyaloclastites show that a permanent land bridge between the lava plateau and the gneiss was not established.

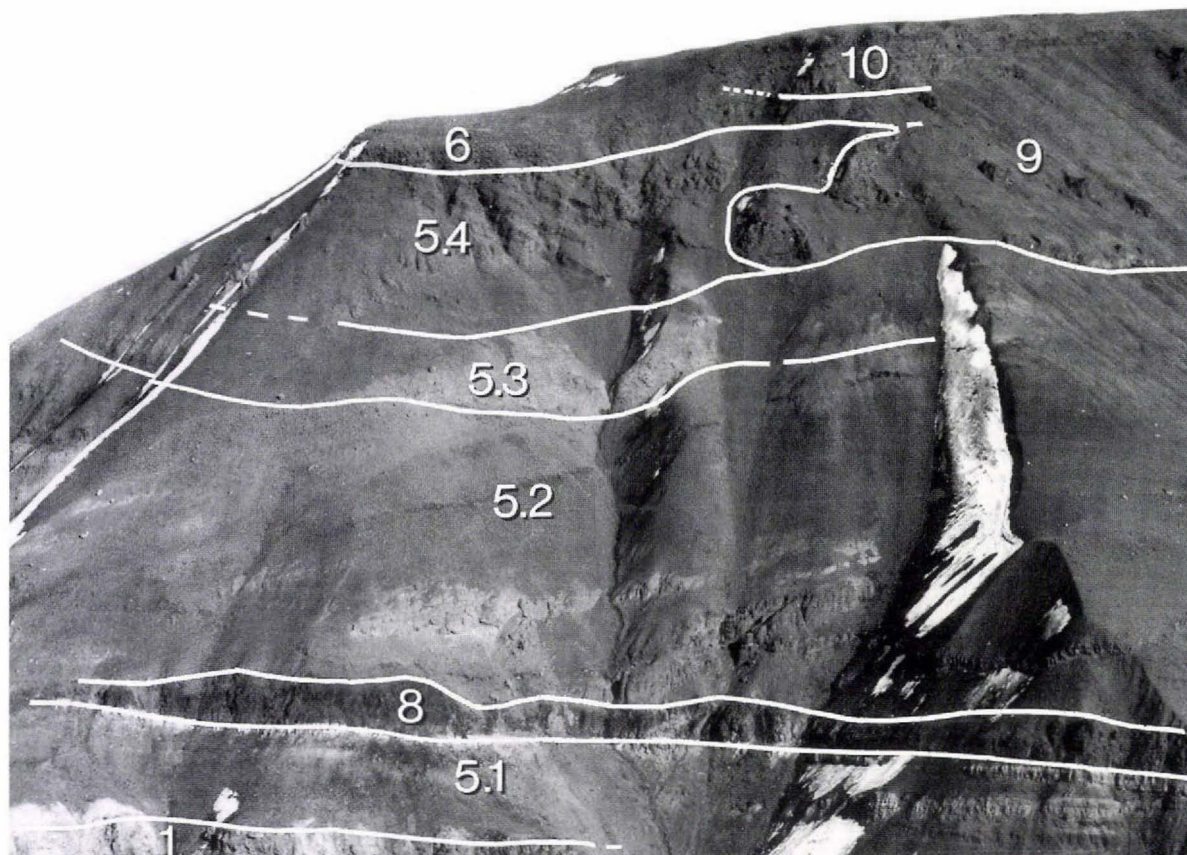


Fig. 12. The west side of Mellemfjeld (Fig. 10 c). Numbers are the same as in Fig. 10. Five different conglomerate units (5.1 to 5.4 and 6) from the Tunoqqu Member overlie Precambrian gneiss (1). An invasive lava (8), a strongly columnar-jointed lava indicating a humid environment (9), and normal subaerial lavas (10) also belong to the Tunoqqu Member. Note that the deposition of the strongly cross-bedded conglomerate unit 5.4 was contemporaneous with the emplacement of the lava 9.

the weathered gneiss surface are exposed locally. Over most of sections c and d, Tunoqqu Member rocks rest directly on the gneiss.

Sections a and b (Vesterfjeld west and east). In section b, the Tunoqqu Member starts with orange-brown fore-set-bedded hyaloclastites which entered from the SW into a 130–150 m deep water-filled basin where they prograded more than 1.3 km towards the NE. The lavas probably entered the basin near to this locality. The pre-Tunoqqu Member units in section a and the hyaloclastite unit in section b are eroded on the top and covered by a 20 m thick conglomerate bed which continued the progressive infilling of the basin. The conglomerate forms a cross-bedded orange-brown deposit which is almost indistinguishable from hyaloclastite when seen from a distance. It consists of up to 0.7 m large lava blocks of silicic low-Mg basalt with subordinate olivine-phyric basalt and gneiss blocks (Fig. 11). In addition, rounded

pillow fragments with glassy margins are found, and the conglomerate matrix is rich in glass gravel derived from reworked Tunoqqu Member hyaloclastite.

The conglomerate unit is covered by pahoehoe lavas which pass into shallow hyaloclastite facies with transport directions from the south, seen in the northern part of section b. In section a, a single 10–30 m thick hyaloclastite bed shows infill from the north and north-west.

This unit is covered by an up to 15 m thick conglomerate bed (sections a and b) showing transport directions from the south. It contains blocks of Tunoqqu Member lavas and hyaloclastites, and subordinate gneiss blocks.

In sections a and b five subaerial Tunoqqu Member lava flows follow next, of which the lowest has a very regular and prominent colonnade indicating that it flowed over humid ground. In section b, this flow is seen to invade and disrupt the underlying conglomerate.

Between sections b and c a marked change in lithology

takes place and sections c and d are described separately.

In section c (*Mellemfjeld*) there is a remarkable development of conglomerates. These are up to 250 m thick and consist of at least five separate units described below.

Conglomerate 1 (Fig. 10, section c, unit 5.1) is up to 30 m thick and consists of a number of distinct, flat-lying beds with blocks of Tunoqqu Member lavas, reworked hyaloclastite, and subordinate gneiss. It also contains scattered fragments of petrified wood.

An intrusive sheet of basalt (Fig. 10, section c, unit 8) separates conglomerates 1 and 2. Because of its distinctive chemical composition the sheet is correlated with subaerial lava 3 on Vesterfjeld, and it is probably an invasive tongue of that lava.

Conglomerate 2 (Fig. 10, section c, unit 5.2) is up to 120 m thick and may be a continuation of conglomerate 1. It contains beds of glassy hyaloclastite gravel. A shallow trough is eroded into its top.

Conglomerate 3 (Fig. 10, section c, unit 5.3) is a distinctive, 5–10 m thick light-coloured bed.

Conglomerate 4 (Fig. 10, section c, unit 5.4) is an up to 70 m thick, brown, regularly cross-bedded conglomerate or hyaloclastite filled in from the north or north-west. It has not been visited in the field. To the south, the foresets interfinger steeply with a number of columnar-jointed, subaqueous or at least humid-facies-type lava tongues which have also filled the shallow trough in the top of conglomerate 2. These lavas can be correlated with subaerial lavas 4 and 5 on Vesterfjeld, indicating that at least some of the conglomerates in section c are younger than any of those in sections a and b.

Conglomerate 5 (Fig. 10, section c, unit 6) is up to 25 m thick and consists of a number of very coarse beds with well-rounded basalt boulders up to 1 m in size. To the south, it interfingers with subaerial lava flows (unit 10), and it must have been deposited in a shallow river bed with torrential water flow. This river existed at least during the time interval covered by the eruption of two successive lavas, probably the last ones in the Tunoqqu Member.

A photo of the Mellemfjeld section is shown in Fig. 12.

In section d (*Østerfjeld*) the lithology is much simpler and no conglomerates are present. The Tunoqqu Member is banked up against the gneiss and varies in thickness from 0 to more than 250 m. Three volcanic units are present.

The lowest unit (Fig. 10, section d, unit 8) is up to 120 m thick and composed of strongly columnar-jointed, irregular basalt overlain by pillow lava and hyaloclastite (S. Munck & A. Noe-Nygaard, unpublished field notes), probably subaqueous lava tongues. These are veined and intruded by irregular, approximately N–S trending dyke-like bodies.

The middle unit (no 7) is an up to 100 m thick, regularly foreset-bedded, orange-brown hyaloclastite deposited from the north.

The upper unit (no 11) is up to 25 m thick and composed of brown subaerial lavas.

Ordlingassoq Member. In the western area (sections a and b) a few subaerial picrite lavas overlie the Tunoqqu Member, followed by subaqueous lavas and hyaloclastite. In the eastern area (sections c and d) Ordlingassoq Member hyaloclastites directly overlie the Tunoqqu Member, and in section d they show infilling from the north.

Summary of events in the north coast area (Fig. 13)

1. At the start of Tunoqqu Member time the western shoreline was marked by an earlier hyaloclastite deposited towards the NE. Seawards of this, a conglomerate with metre-sized boulders of olivine basalt and gneiss was deposited towards the north and NE, indicating the start of local erosion (Fig. 11, section a).

2. A Tunoqqu Member foreset-bedded hyaloclastite advanced farther towards the NE (Fig. 10, sections a and b).

3. Over a several kilometres broad area, blocks of Tunoqqu Member lavas and hyaloclastites, and gneiss, were transported towards the NE and deposited in a 150 m thick conglomerate fan (Fig. 10, sections a and b).

4. Further advance of Tunoqqu Member subaerial lavas and equivalent hyaloclastites (Fig. 10, sections a and b).

5. Further erosion and deposition of conglomerates (Fig. 10, sections a-c). High-energy torrential flows started to transport the conglomerates towards the east (section c).

6. The volcanic front advanced from the west; sections a-b were then on dry land. The water flow was increasingly constrained between the gneiss promontory and the lava plain and deflected towards the east, still depositing conglomerates, the youngest from the north. Concomitantly, lavas repeatedly flowed into the river bed and threatened to block it completely (Fig. 10, section c).

7. The volcanic front engulfed the gneiss promontory, swung eastwards, and deposited hyaloclastites towards the SE and south (Fig. 10, section d). Finally, the river ceased to flow and the emergent hyaloclastites and conglomerates were covered by subaerial Tunoqqu Member lava flows which formed a horizontal plain around the gneiss 'promontory' which still rose to more than 700 m above the lavas.

8. In Ordlingassoq Member time, the plain was again inundated by a several hundred metres deep water-filled basin.

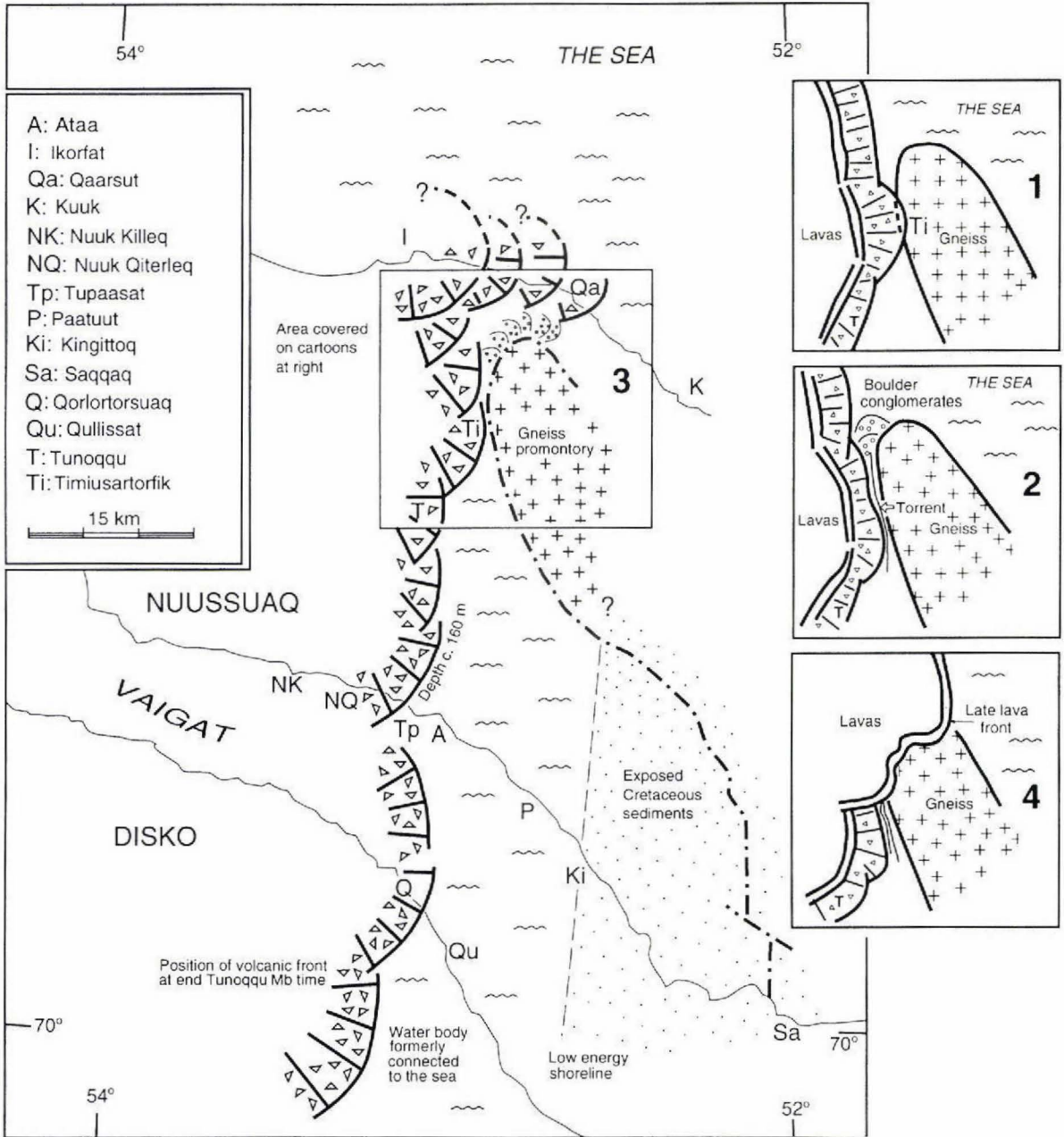


Fig. 13. Sketch of the palaeogeography of central Nuussuaq and north-eastern Disko at Tunoqu Member time. A water body with a depth of c. 160 m was confined between a high gneiss promontory in the north-east, a low-energy clastic shoreline in the east, and the advancing volcanic front in the west, leaving only a narrow connection to the sea in the north. Three stages in the development are illustrated on separate maps. 1. Progradation of Tunoqu Member hyaloclastites towards the east. At a single locality (Timiusartorfik) the hyaloclastite onlaps the gneiss surface. 2. Fluvial erosion occurs between the easily erodible Tunoqu Member volcanic rocks and the gneiss promontory. A boulder conglomerate is deposited in front of the torrent. 3. Continued volcanic activity produces additional hyaloclastites and lavas in the north, which force the conglomerates eastwards. 4. Finally, both volcanics and conglomerates are covered by subaerial lava flows onlapping the gneiss.

Interpretations and conclusions

Fractionation and contamination at the end of a magmatic cycle

The volcanic rocks of the Tunoqqu Member on Nuussuaq and the contemporary Kûgánguaq Member on Disko show an unusually large compositional diversity which can not all be explained by crystal fractionation processes. Many of the compositional groups were formed by various degrees of crustal contamination of various parent magmas which ranged in composition from picrite with around 18% MgO to evolved feldspar-phyric basalts with around 7% MgO. The rocks of the Tunoqqu and Kûgánguaq Members are the most widespread and voluminous products of the crustal contamination that took place during the deposition of the Vaigat Formation.

Contamination of the magmas took place in a number of separate magma chambers situated high in the crust, probably in the sediments of the West Greenland Basin. Pedersen (1985b) showed that the dominant contaminant of the Kûgánguaq Member rocks is most likely a sulphur-bearing sandstone; the contaminants for the rocks of the Tunoqqu Member are poorly constrained.

Contamination usually induces crystallisation and decrease of MgO in the contaminated magmas. However, some of the low-MgO basalts of the Tunoqqu Member are not noticeably contaminated and must mainly have formed by normal fractional crystallisation of more Mg-rich, probably picritic parent magmas. This evolution must also have taken place in magma chambers which could have been more deep-seated than the chambers where the contamination took place.

Dwindling magma supply rates at the end of a magmatic cycle may explain the preponderance of evolved and contaminated basalts in the Tunoqqu and Kûgánguaq Members. Dwindling magma supply rates would lead to longer residence times in magma chambers and formation of evolved basalts. Likewise, the likelihood that the magmas would stagnate and react with their surroundings at higher levels on their way to the surface would be increased.

The occurrence of slightly enriched lavas at the top of the Tunoqqu Member may herald the start of the third volcanic cycle in the region, which produced picrites that were slightly enriched relative to those of the preceding cycle.

Tectonic control

Detailed structural analysis by photogrammetry in well-exposed areas has shown that there is a connection between the position of the eruption centres, the config-

uration of fault blocks, and the location of zones with subtle synvolcanic movements.

The Kûgánguaq centre is located along an old palaeo-escarpment related to the Disko Gneiss Ridge (Fig. 1). The Qunnilik centre is situated due north of this and may be related to a northern prolongation of this gneiss ridge. The Tupaasat centre formed within an area which at that time was affected by repeated small vertical movements. Finally, the Agatdal centre is situated somewhere along the south-western margin of the Ikorfat fault system which was affected by semi-continuous, probably tension-related, sagging in Naujánguit Member time.

The more regionally dispersed and less contaminated lavas could have been erupted from fissures outside the centres. Dykes with fairly similar chemistry occur at various places, but they are not sufficiently characteristic to be related unequivocally to the Tunoqqu Member because the much younger Maligât Formation contains very similar basalts.

In conclusion, all the known eruption sites were situated in tectonically active zones, and it is probable that magmas were channelled towards the surface and developed magma chambers along pre-existing, deep faults.

The ultimate cause for the magmatic stagnation at the end of the Naujánguit Member cycle is not known. Based on the observations above, it may be speculated that the stagnation was tectonically controlled, e.g. caused by a slight shift in the direction and magnitude of the tectonic forces driving the plates in the Baffin Bay region.

Conglomerates and basin development

The spectacular Tunoqqu Member conglomerates at the north coast of Nuussuaq were deposited by torrents along the gneiss promontory. The cause of the development of the conglomerates could be either 1. a relative sea-level rise, 2. a relative sea-level fall, 3. local tectonic movements, or 4. non-tectonic damming of a large water body.

1. A relative sea-level rise may be caused by the loading effect of the heavy volcanic rocks. It would lead to formation of coastal cliffs of eroded lavas and deposition of local conglomerates at the foot of the cliffs, as described for the Tunoqqu type locality. But transport of metre-sized gneiss blocks over several kilometres would not be possible, and a relative sea-level rise cannot explain the north coast conglomerates.

2. A relative sea-level fall leading to rejuvenation of water courses may lead to deposition of conglomerates. It should also be expressed as falling palaeoshore levels. The palaeoshore levels are recorded very precisely in the volcanic facies, where falling sea-level should give rise to a lowering of the top of the hyaloclastite level. Such a feature has not been observed.

3. Localised syn-volcanic movements may also lead to rejuvenation of water courses. Syn-volcanic uplift has been observed along the south coast of Nuussuaq (Pedersen *et al.*, 1993), and sagging has been observed along the south-western margin of the Ikorfat fault system. None of these movements would be likely to trigger high-energy flows across the Ikorfat fault system from the Agatdal region towards the north-east.

4. From the discussion above we conclude that relative sea-level changes cannot explain the observations. We therefore interpret the conglomerates as caused by a simple damming effect. The eastward-prograding volcanic rocks gradually obliterated the marine embayment in central Nuussuaq, but north-flowing water courses in the eastern Disko Bugt region would still exist. Because of the damming the water table rose, and the increased gradient between the enclosed basin and the sea to the north generated an outlet torrent between the volcanic front and the gneiss promontory.

Acknowledgements. The field work was carried out during GGU expeditions led by F. Kalsbeek and F. G. Christiansen. Field support was also provided by the Arctic Station in Godhavn. AKP and GKP were supported by the Danish Natural Science Research Council (grant no. 11-8949-1).

References

- Clarke, D. B. & Pedersen, A. K. 1976: Tertiary volcanic province of West Greenland. In Escher, A. & Watt, W. S. (ed.) *Geology of Greenland*, 364-385. Copenhagen: Geol. Surv. Greenland.
- Croxton, C. A. 1978: Report on field work undertaken between 69° and 72°N, central West Greenland in 1975 with preliminary palynological results. *Open File Report Grønlands geol. Unders.* **78-1**, 88 pp.
- Dam, G. & Sønderholm, M. (in press). Sedimentological evolution of a fault-controlled Early Paleocene incised valley system, Nuussuaq Basin, West Greenland. In Shanley, K. W. & McCabe, P. J. (ed.) *Relative role of eustasy, climate, and tectonism in continental rocks. Spec. Publ. Soc. Econ. Palaeont. Miner.*
- Dueholm, K. S. & Pedersen, A. K. (ed.) 1992: Geological analysis and mapping using multi-model photogrammetry. *Rapp. Grønlands geol. Unders.* **156**, 72 pp.
- Garde, A. A. & Steenfelt, A. (in press): Precambrian geology of Nuussuaq and the area north-east of Disko Bugt, West Greenland. *Rapp. Grønlands geol. Unders.*
- Hald, N. 1977: Lithostratigraphy of the Maligât and Hareøen Formations, West Greenland basalt group, on Hareøen and western Nûgssuaq. *Rapp. Grønlands geol. Unders.* **79**, 9-16.
- Hald, N. & Pedersen, A. K. 1975: Lithostratigraphy of the early Tertiary volcanic rocks of central West Greenland. *Rapp. Grønlands geol. Unders.* **69**, 17-24.
- Heim, A. 1910: Über die Petrographie und Geologie der Umgebungen von Karsuarsuk, Nordseite der Halbinsel Nugsuaq, W. Grönland. *Meddr Grønland* **47**, 173-228.
- Henderson, G. 1973: The geological setting of the West Greenland basin in the Baffin Bay region. *Pap. Geol. Surv. Canada* **71-23**, 521-544.
- Henderson, G. & Pulvertaft, T. C. R. 1987: Geological map of Greenland 1:100 000. Descriptive text. Mårmorilik 71V 2 Syd, Nûgâtsiaq 71 V 2 Nord, Pangnertôq 72 V 2 Syd. Lithostratigraphy and structure of a Lower Proterozoic dome and nappe complex. Copenhagen: Grønlands Geologiske Undersøgelse, 72 pp.
- Henderson, G., Schiener, E. J., Risum, J. B., Croxton, C. A. & Andersen, B. B. 1981: The West Greenland Basin. In Kerr, J. W. (ed.) *Geology of the North Atlantic Borderlands. Mem. Can. Soc. Petrol. Geol.* **7**, 399-428.
- Hjortkjær, B. F. 1991: Palynologisk undersøgelse af tertiære skifre fra Disko og Nûgssuaq, Vestgrønland. Unpublished thesis, University of Copenhagen, 94 pp. & plates.
- Koch, B. E. 1959: Contribution to the stratigraphy of the non-marine Tertiary deposits on the south coast of the Nûgssuaq Peninsula, northwest Greenland. *Bull. Grønlands geol. Unders.* **22**, 100 pp. (Also *Meddr Grønland* **162**, 1).
- Koppelhus, E. B. & Pedersen, G. K. 1993: A palynological and sedimentological study of Cretaceous floodplain deposits of the Atane Formation at Skansen and Illunnguaq, Disko, West Greenland. *Cretaceous Res.* **14**, 707-734.
- Larsen, L. M. & Pedersen, A. K. 1988: Investigations of Tertiary volcanic rocks along the south coast of Nûgssuaq and in eastern Disko, 1987. *Rapp. Grønlands geol. Unders.* **140**, 28-32.
- Larsen, L. M. & Pedersen, A. K. 1992: Volcanic marker horizons in the upper part of the Maligât Formation on eastern Disko and Nuussuaq, Tertiary of West Greenland: syn- to post-volcanic basin movements. *Rapp. Grønlands geol. Unders.* **155**, 85-93.
- Larsen, L. M., Pedersen, A. K., Pedersen, B. K. & Piasecki, S. 1992: Timing and duration of Early Tertiary volcanism in the North Atlantic: new evidence from West Greenland. In Storey, B. C. Alabaster, T. & Pankhurst, R. J. (ed.) *Magmatism and the causes of continental break-up. Spec. Publ. Geol. Soc., London* **68**, 321-333.
- Nøhr-Hansen, H. 1994: Dinoflagellate cyst biostratigraphy of the Upper Cretaceous black mudstones in central Nuussuaq, West Greenland. *Open File Ser. Grønlands geol. Unders.* **94-12**, 26 pp.
- Nøhr-Hansen, H. (in press): Upper Cretaceous dinoflagellate cyst stratigraphy, onshore West Greenland. *Bull. Grønlands geol. Unders.* **170**.
- Pedersen, A. K. 1977: Dyke intrusions along the south coast of Disko. *Rapp. Grønlands geol. Unders.* **81**, 57-67.
- Pedersen, A. K. 1979: Basaltic glass with high-temperature equilibrated immiscible sulphide bodies with native iron from Disko, central West Greenland. *Contrib. Miner. Petrol.* **96**, 397-407.
- Pedersen, A. K. 1985a: Lithostratigraphy of the Tertiary Vaigat Formation on Disko, central West Greenland. *Rapp. Grønlands geol. Unders.* **124**, 30 pp.
- Pedersen, A. K. 1985b: Reaction between picrite magma and continental crust: early Tertiary silicic basalts and magnesian andesites from Disko, West Greenland. *Bull. Grønlands geol. Unders.* **152**, 126 pp.

- Pedersen, A. K. & Dueholm, K. S. 1992: New methods for the geological analysis of Tertiary volcanic formations on Nuussuaq and Disko, central West Greenland, using multi-model photogrammetry. *Rapp. Grønlands geol. Unders.* **156**, 19–34.
- Pedersen, A. K., Larsen, L. M. & Dueholm, K. S. 1993: Geological section along the south coast of Nuussuaq, central West Greenland. 1:20 000 coloured geological sheet. Copenhagen: Geol. Surv. Greenland.
- Pedersen, G. K. 1989: A fluvial-dominated lacustrine delta in a volcanic province, W Greenland. In Whateley, M. K. G. & Pickering, K. T. (ed.) *Deltas: sites and traps for fossil fuels. Spec. Publ. Geol. Soc., London* **41**, 139–146.
- Pedersen, G. K. & Pulvertaft, T. C. R. 1992: The nonmarine Cretaceous of The West Greenland Basin, onshore West Greenland. *Cretaceous Res.* **13**, 263–272.
- Piasecki, S., Larsen, L. M., Pedersen, A. K. & Pedersen, G. K. 1992: Palynostratigraphy of the Lower Tertiary volcanics and marine clastic sediments in the southern part of the West Greenland Basin: implications for the timing and duration of the volcanism. *Rapp. Grønlands geol. Unders.* **154**, 13–31.
- Pulvertaft, T. C. R. 1979: Lower Cretaceous fluvial-deltaic sediments at Kûk, Nûgssuaq, West Greenland. *Bull. Geol. Soc. Denmark* **28**, 57–72.
- Pulvertaft, T. C. R. 1989: Reinvestigation of the Cretaceous boundary fault in Sarqaqdaalen, Nûgssuaq, central West Greenland. *Rapp. Grønlands geol. Unders.* **145**, 28–32.
- Rosenkrantz, A. 1970: Marine Upper Cretaceous and lowermost Tertiary deposits in West Greenland. *Bull. Geol. Soc. Denmark* **19**, 406–453.
- Rosenkrantz, A. & Pulvertaft, T. C. R. 1969: Cretaceous–Tertiary stratigraphy and tectonics in northern West Greenland. *Mem. Amer. Ass. Petrol. Geol.* **12**, 883–898.



Early Tertiary lavas and sills on Traill Ø and Geographical Society Ø, northern East Greenland: petrography and geochemistry

Niels Hald

The Early Tertiary extrusion of flood basalts in East Greenland was accompanied by intrusion of numerous sills in the Upper Palaeozoic and Mesozoic sediments of the N–S trending East Greenland rift zone. With a few exceptions the lavas and sills have low contents of Ti and other incompatible elements, indicating a genetic relationship with the lavas and sills north of Kejser Franz Joseph Fjord rather than with the lavas in the Scoresby Sund area. Two sills are described in greater detail. The first, from Geographical Society Ø, is 60 m thick and homogeneous throughout. The second, from southern Traill Ø, is more than 150 m thick and atypical as it ranges in composition from low-Ti tholeiite to diorite.

N. H., Geological Museum, Øster Voldgade 5–7, DK-1350 Copenhagen K, Denmark.

The Early Tertiary opening of the NE Atlantic was accompanied by intense magmatic activity along 1000 km of the East Greenland coast (Fig. 1). Basaltic lavas with an estimated maximum stratigraphic thickness of 7 km were erupted between Kangerlussuaq and Scoresby Sund (Brooks & Nielsen, 1982; Watt *et al.*, 1986; Larsen *et al.*, 1989), whereas the remnants of a much thinner (less than 1.5 km) northern lava plateau are found between Kejser Franz Joseph Fjord and Shannon (Noe-Nygaard, 1976; Upton *et al.*, 1980; Upton, 1988). Apart from a few nunatak exposures (Anwar, 1955; Fawcett *et al.*, 1982) the plateau south of Scoresby Sund consists entirely of tholeiitic flows (Brooks *et al.*, 1976; Nielsen *et al.*, 1981; Larsen & Watt, 1985; Larsen *et al.*, 1989). These are apparently all reversely magnetised, and were most likely formed during chron C24R (Tarling *et al.*, 1988). Only the lavas of the Igtertivå Formation exposed at Kap Dalton may have formed during the subsequent period of normal polarity (C24N) (Larsen *et al.*, 1989). In the plateau north of Kejser Franz Joseph Fjord most of the flows are also tholeiitic, while mainly transitional to mildly alkaline basalts enriched in incompatible elements form the upper part of the lava sequence on Gauss Halvø, Hold with Hope and Bontekoe Ø (Hald, 1976; Noe-Nygaard & Pedersen, 1983; Upton *et al.*, 1984a). The change in chemical composition almost coincides with a change in the magnetic polarity from reverse to normal, possibly C24R and C24N (cf. Eldholm *et al.*, 1989).

The lavas of the northern plateau spilled across a thick succession of Upper Palaeozoic and Mesozoic sediments which were deposited in a rift system with an overall N–S trend and bounded to the west by the Post-Devonian Main Fault of Vischer (1943). These sediments are intruded by numerous dolerite sills. Nearly all are tholeiites and compositionally related to the overlying tholeiitic lavas (Hald, 1976; Upton *et al.*, 1984a). While the Tertiary lavas are only found in a single small outcrop south of Kejser Franz Joseph Fjord (Donovan, 1955) the sills are widely distributed from Shannon in the north to Jameson Land in the south, and thus they bridge the gap between the lavas south of Scoresby Sund and those north of Kejser Franz Joseph Fjord (Fig. 1).

The main object of this paper is to give a petrographical and chemical description of the lavas in the outcrop and of the central part of the sill complex. Published analyses of lavas from the Scoresby Sund region and northwards from Kejser Franz Joseph Fjord display some regional variation (Upton *et al.*, 1984a; Larsen *et al.*, 1989); a purpose of the investigations is, therefore, to place the basalts and dolerites from the intervening area in this context. The paper also describes some scattered dykes, some of which are observed to cut the sills. No attention is paid to the major intrusive complexes, Kap Parry and Kap Simpson, which form the two eastern promontories of Traill Ø. Dominated by quartz syenites and quartz diorites (Rheinhard *in* Schaub, 1942; Engell,

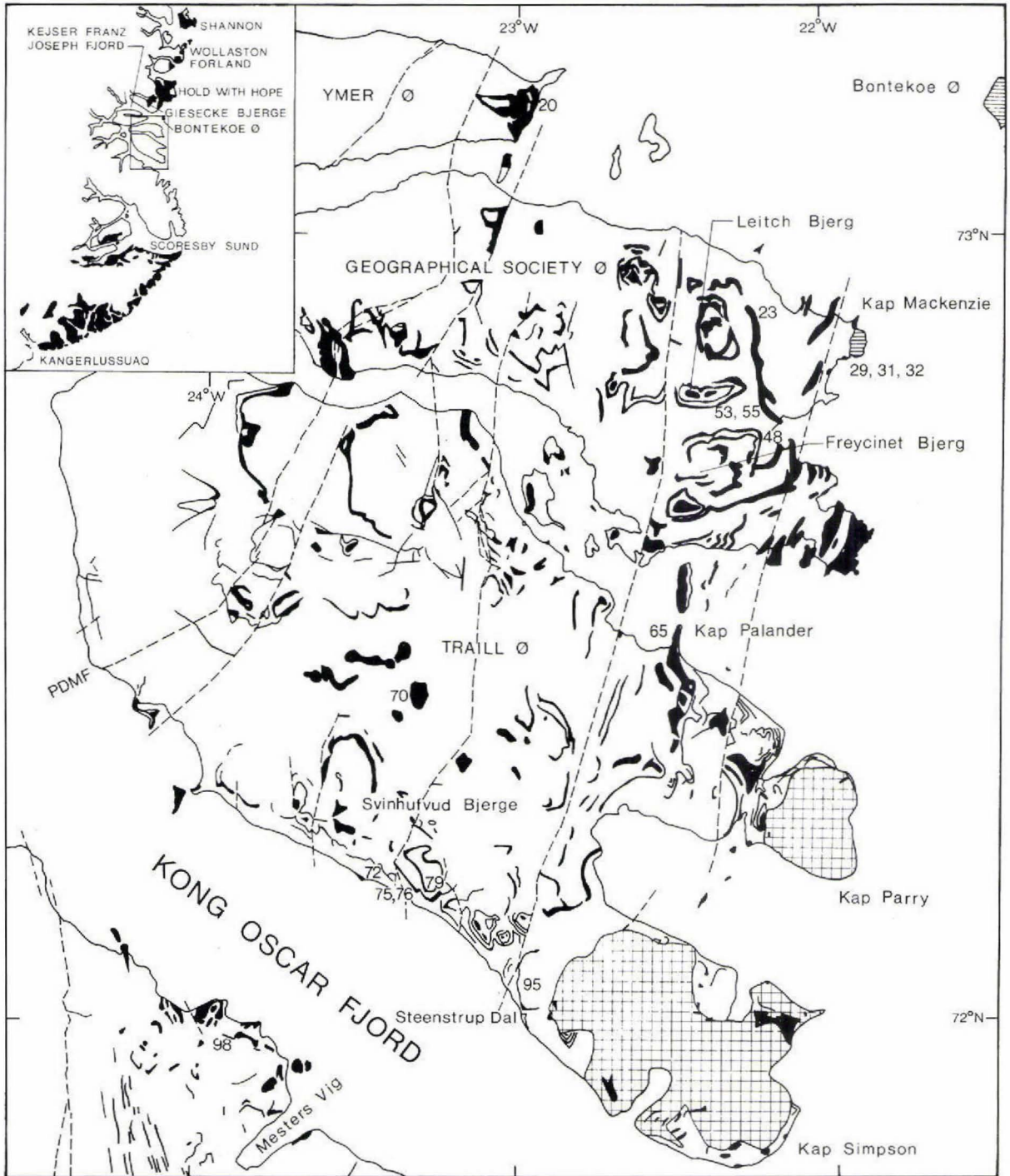


Fig. 1. Tertiary volcanic and intrusive rocks in central East Greenland. Redrawn from Koch & Haller (1971). Horizontal lines: lavas, black: sills and dykes, cross-hatched: larger intrusions. PDMF = Post-Devonian Main Fault (Vischer, 1943). Two-digit numbers refer to analysed samples in Table 1 and have the prefix GGU 2395xx.

1975) they are but two of several high-level intrusions formed along the East Greenland coast subsequent to the continental break-up.

Geological setting

Geographical Society Ø and Traill Ø are cut obliquely (from NNE to SSW) by the Post-Devonian Main Fault which separates Devonian sediments in the west from Carboniferous and younger sediments in the east (Fig. 1). The Devonian succession is dominated by sandstones, formed during denudation of the East Greenland Caledonides (Olsen, 1993), while the Carboniferous is dominated by interbedded sandstones and shales deposited during initial rifting in the North Atlantic (Stemmerik *et al.*, 1991, 1992). Further to the east, Mesozoic sediments formed in association with renewed tectonic activity within the rift system: generally sand and conglomerates were deposited along the shorelines and muds in the deeper parts of the basins (Surlyk *et al.*, 1981; Surlyk, 1990).

The major structural elements within the Mesozoic rift are tilted blocks bounded by faults trending NNE. Dips of the sediments are low, generally to the west (Donovan, 1953, 1955).

Lavas at Kap Mackenzie. The lavas at Kap Mackenzie were first described by Donovan (1955). They form an outcrop with an area of 2 to 3 km². To the west the lavas are bounded by low-lying ground with no exposures of pre-Quaternary rocks. The sequence dips 15–25° to the west, and it is cut by a few N–S trending normal faults with minor displacements. The total exposed thickness is about 150 m.

Investigations along the southern side of the outcrop (Fig. 2) show that the sequence is dominated by compound flows consisting of thin (1–5 m), vesicular feldspar-phyric or aphyric flow units, usually of the pahoehoe type. Weathered surfaces have a vivid yellowish-brown or reddish-brown colouration, while flow interiors appear to be relatively fresh. A few thin tuffaceous layers have been observed.

The original landward extent of the lavas is unknown. No intercalated sediments have been found to indicate the presence of nearby elevated ground at the time of eruption. Seawards, on the shelf, buried volcanic rocks appear to be widespread (Larsen, 1990), and through these the outlier at Kap Mackenzie is linked with the lavas north of Kejser Franz Joseph Fjord.

Sills and dykes. Large sills characterise the terrain of major parts of Geographical Society Ø and Traill Ø. They are most abundant in the eastern region where they often show strongly transgressive relationships to the sediments. Intruded in the soft Cretaceous sediments they stand out

as irregular ridges or are seen to sandwich the sediments in Freycinet Bjerg and other steep-sided hills, which may also be capped by sills. Frebold & Noe-Nygaard (1938) record thicknesses of 55 m and 150 m for two sills in the Svinhufvud Bjerge on the south coast of Traill Ø, whereas three sills on Freycinet Bjerg are each around 100 m thick (Donovan, 1955). The combined thickness of 300 m at this locality appears to be the maximum value at any place for exposed sills on the two islands. No geophysical investigations exist to evaluate the distribution and size of sills below the present surface.

In the pre-Cretaceous sediments sills are more wide-spaced and only a few are found west of the Main Fault (cf. Koch & Haller, 1971). The westward decrease in number may depend on the nature of the sediments, the distance to the magmatic source or the present level of erosion.

Only seven dykes were seen during the present field work despite many excellent exposures. A few other dykes are shown on the geological map of Koch & Haller (1971). The seven dykes are all less than 8 m across, and most are less than 2 m. They strike either N–NE, parallel to the major faults, or W–NW. Three are seen to cut through sills, while the opposite relationship has not been observed. A strong and pervasive hydrothermal alteration of two dykes sampled in Steenstrup Dal at the south coast of Traill Ø suggests that at least these dykes predate the Kap Simpson Complex.

Palaeomagnetism. In the field all samples were marked

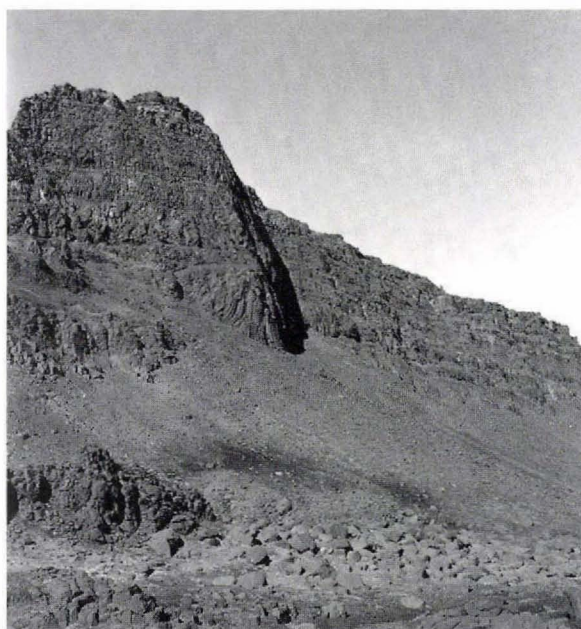


Fig. 2. The lavas along the south side of the outcrop at Kap Mackenzie, Geographical Society Ø.

'up-down'. Preliminary examination in the laboratory indicates that the lavas and the 'main type' sills (see later) are reversely magnetised, while the 'enriched' sills – except for GGU 239548 – are normally magnetised. Cores from selected specimens were demagnetised stepwise in an alternating field of up to 30 mT. Measurements on the cores support this distribution of polarities. Among the dykès both normal and reverse polarities were found during the preliminary investigations.

Petrography

Lavas. The lava flows are composed of basalt, mainly with intergranular texture, and range from almost aphyric to strongly porphyritic. Lath-shaped plagioclase phenocrysts vary in amount from < 1 to 20 %. They have maximum lengths of 1 to 6 mm and occur as single crystals or in aggregates of several grains together with a few grains of olivine ± augite. The olivines are stout and have regular subhedral to euhedral outlines. In most flows they are small (less than 0.3 mm) and rather inconspicuous as they are mostly replaced by clay minerals. A

few of the flows contain equant augite phenocrysts up to 1 mm in size. The groundmasses are fine-grained with plagioclase, clinopyroxene, Fe-Ti oxides (titanomagnetite and ilmenite) and olivine pseudomorphs. Interstices are occupied mainly by green clayey material including recrystallised glass.

Microprobe analyses were carried out on the lava GGU 239529. It has phenocrysts of bytownite (An_{85-73}) and microphenocrysts of olivine (Fo_{77-71}). Groundmass plagioclases range from An_{70} to An_{60} . Augites form a well defined trend of decreasing Ca with increasing Fe/Mg ratio (Fig. 3). Pigeonite is absent.

Sills. The sills are dolerites consisting of plagioclase, olivine, clinopyroxene and Fe-Ti oxides. Quartz and alkali feldspar, often found in granophyric intergrowth, apatite and clay minerals occur interstitially. Samples GGU 239548 and 239570, which are both enriched in potassium, contain small grains of biotite.

In general, superficial deposits prevent sampling of individual sills from the lower to the upper contact. A 55 m thick sill exposed on Leitch Bjerg on eastern

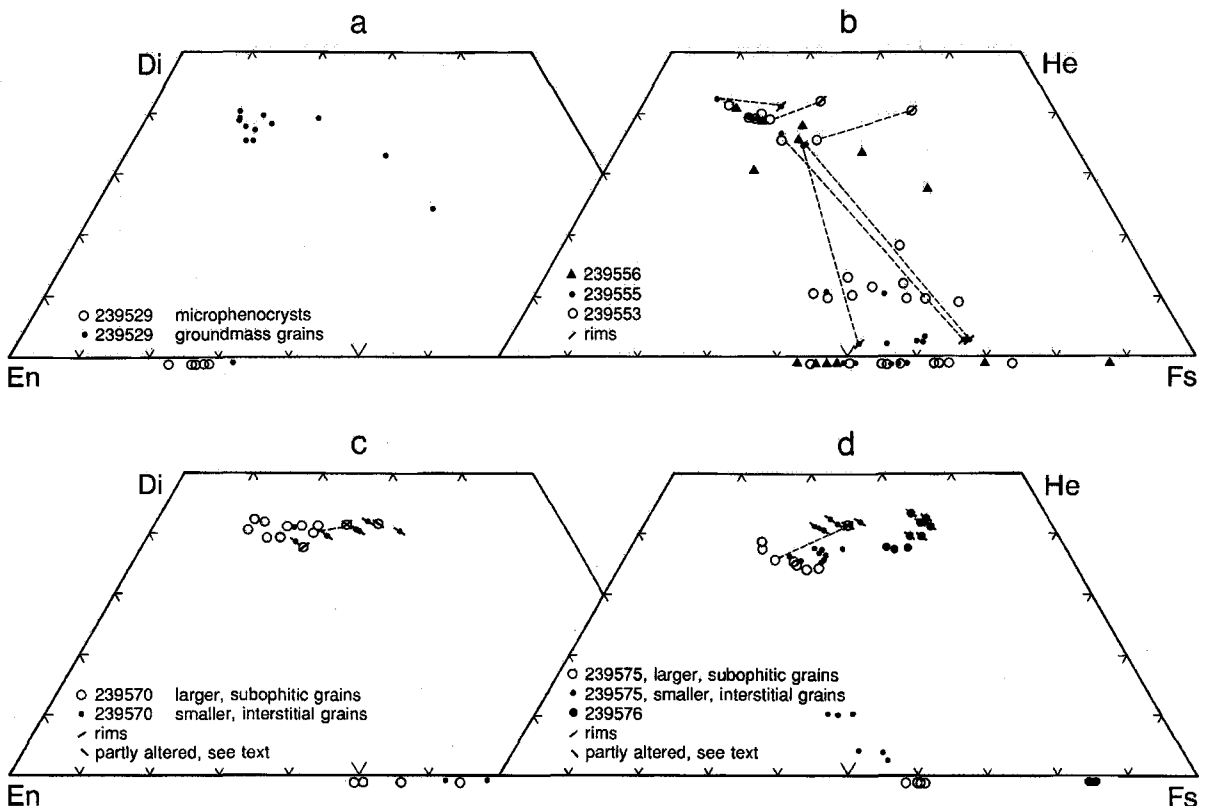


Fig. 3. Composition of pyroxenes and olivines. a. Lava from Kap Mackenzie (GGU 239529). b. Sill on Leitch Bjerg (GGU 239556, 75 cm above lower contact; GGU 239555, 3 m above lower contact, and GGU 239553, 40 m above lower contact). c. Enriched sill on southern Traill Ø (GGU 239570). d. Strongly fractionated sill on Svinhufvud Bjerge (GGU 239575, lower basaltic part, and GGU 239576, upper dioritic part).

Geographical Society Ø forms an exception to this rule, and it is therefore described in some detail.

The lower chilled margin is porphyritic with in total 1% phenocrysts of olivine (replaced by clay minerals) and clinopyroxene, both up to 0.5 mm in size, and 4% plagioclase phenocrysts. These are 0.5–1 mm in size and form clusters 5 mm across.

At 0.75 m above the lower contact the dolerite is still fine grained. Only a few plagioclase clusters are present at this level. Olivines (5%) are partly fresh. Smaller crystals have euhedral to subhedral outlines, but the larger grains may be pierced by plagioclase laths. Fe-Ti oxides mainly occur as skeletal crystals confined to interstices together with clay minerals.

The grain size gradually increases upwards. From the 3 m level the oxides form millimetre-sized irregular grains which partly enclose slender plagioclase laths. Interstitial alkali feldspar and quartz become significant constituents. At 40 m the sill reaches its coarsest grain size. Plagioclase and clinopyroxene in subophitic intergrowth, olivine partly replaced by clay minerals, and Fe-Ti oxides, all 2 to 3 mm in size, enclose fine-grained interstitial domains of strongly zoned plagioclase laths with minor pyroxenes, Fe-Ti oxides, alkali feldspar, quartz, apatite and clay minerals. Two metres below the upper contact the grain size is reduced to 1 mm.

In its upper half the sill contains scattered and discontinuous pegmatitic (gabbroic) veins. Most are only a few centimetres wide and parallel to the contacts of the sill.

The compositions of the main silicate minerals have been analysed by microprobe in samples from 75 cm, 3 m and 40 m above the lower contact (samples GGU 239556, -55 and -53). The plagioclase phenocrysts in the lowermost sample are bytownites (An_{82-72}). Major plagioclase laths in the three samples range from An_{70} to An_{50} , and the average An/Ab ratio tends to decrease upwards. Small interstitial grains in the two upper samples range from An_{50} to An_{15} . Olivine range from Fo_{55} to Fo_{35} and major grains of pyroxene (all augite) from $Ca_{42}Mg_{49}Fe_9$ to $Ca_{35}Mg_{35}Fe_{30}$ (Fig. 3). Ferropigeonite and ferrohypersthene are found as tiny interstitial grains in sample GGU 239555, whereas the leucocratic domains of sample GGU 239553 carry ferropigeonite and ferroaugite. In both samples the ferropigeonite shows very fine-scale exsolution structures and have apparently recrystallised to orthopyroxene and high-Ca clinopyroxene.

As detailed later the Leitch Bjerg sill only shows small chemical variations from base to top. Throughout the sill mg' lies in the range 56.9 to 53.6. A more pronounced fractionation has occurred in the thick sill on Svinhufvud Bjerge. The lowermost sample, GGU 239575, from 125 m below the upper contact (and an estimated 50 m

above the lower contact), has a basaltic composition ($mg' = 51.7$) with olivine (Fo_{42-38}), plagioclase (An_{66-38}), pyroxene, Fe-Ti oxides, interstitial clay minerals and quartz feldspar micropegmatite. Larger pyroxene grains in subophitic intergrowth with the plagioclase laths are augites ($Ca_{34-39}Mg_{44-37}Fe_{18-29}$). Augite also occurs in intergranular aggregates together with pigeonite and hypersthene (Fig. 3).

In the upper part of the sill the composition is dioritic (Fig. 3). In sample GGU 239576 from 90 m below the upper contact ($mg' = 19.0$) andesine (An_{41-35}) is intergrown with a pale brown ferroaugite ($Ca_{38}Mg_{44-37}Fe_{18-29}$). Olivine (Fo_{20-14}) and Fe-Ti oxides are other major constituents. Interstices are occupied by quartz-feldspar micropegmatite.

Both samples also carry colourless to pale green clinopyroxene, which is low in Ti and Al and displaced towards the He-corner (Fig. 3). This variety, which in the dolerite usually contains small patches of a sheet silicate, and in the diorite a ferroedenitic amphibole, is considered to be deuterically altered brownish augite or ferroaugite rather than a primary phase (cf. Smith, 1970, Walker *et al.*, 1973). Larger amphibole grains in optical continuity with the inclusions are often adjacent to the pale green pyroxene grains in the diorite sample.

Dykes. Among the seven sampled dykes five have basaltic composition and carry phenocrysts of olivine + plagioclase \pm augite.

Two non-basaltic dykes were found on Traill Ø. One dyke strikes NNW and cuts a dolerite sill at Kap Palander. It is a fine grained basanite (as defined by Le Bas *et al.*, 1986) and consists of plagioclase, augite, brown amphibole, Fe-Ti oxides, slender needles of apatite and interstitial clay minerals and small amounts of carbonate. It contains scattered phenocrysts of augite and plagioclase up to 2 mm in size, and microphenocrysts of olivine, plagioclase and augite. The second dyke strikes NNE and cuts through Mesozoic sediments west of Steenstrup Dal. It is a hydrothermally altered plagioclase-phyric rock, apparently a basaltic trachyandesite, and may be related to the nearby Kap Simpson Complex.

Major and trace element chemistry

Fifty nine samples of lavas, sills and dykes have been analysed for major and trace elements. Selected analyses are shown in Table 1 together with analytical details. The full data set is available on request.

The lavas and sills (apart from the fractionated upper part of the Svinhufvud Bjerge sill) are marginally olivine or quartz normative tholeiites. Their tholeiitic affinity is confirmed by a plot of alkalis versus SiO_2 (not shown)

Table 1. Chemical analyses of lavas and sills in central East Greenland

GGU no.	Lavas, Kap Mackenzie			Sills, main type and fractionated					
	239529	239531	239532	239520	239523	239553	239555	239575	239576
SiO ₂	49.34	47.57	47.58	49.26	49.08	48.55	49.07	49.83	47.57
TiO ₂	1.73	3.39	2.49	2.10	1.60	1.95	1.76	2.26	3.44
Al ₂ O ₃	14.68	15.04	13.74	13.75	14.35	14.22	14.33	13.58	10.53
Fe ₂ O ₃	3.01	5.93	5.31	2.14	2.29	3.26	2.87	1.76	4.25
FeO	7.86	7.28	8.01	10.56	8.61	8.58	8.81	10.17	16.77
MnO	0.17	0.19	0.20	0.20	0.18	0.18	0.19	0.20	0.30
MgO	7.09	4.66	6.43	6.52	7.62	6.67	7.01	6.21	2.39
CaO	11.75	10.30	10.92	10.98	12.16	11.96	11.80	11.26	8.07
Na ₂ O	2.18	2.70	2.40	2.63	2.26	2.35	2.21	2.42	2.68
K ₂ O	0.14	0.59	0.19	0.29	0.21	0.23	0.24	0.35	0.98
P ₂ O ₅	0.17	0.46	0.27	0.21	0.16	0.17	0.17	0.23	1.75
LOI	2.03	2.08	2.40	1.47	1.43	1.81	1.57	1.14	1.53
Total	100.14	100.19	99.94	100.11	99.94	99.93	100.02	99.40	100.25
mg'	57.6	42.8	50.4	51.4	59.1	54.0	55.4	51.7	19.0
Trace elements in ppm									
Cr	330	122	206	144	328	166	253	107	<3
Co	46	43	47	54	48	52	51	47	57
Ni	68	77	73	74	100	82	90	62	2
Cu	116	412	85	244	179	220	208	224	664
Zn	99	126	115	113	90	98	99	101	201
Rb	4.7	14	0.7	6.7	5.5	5.4	6.0	6.7	23
La	13	27	15	13	7	10	8	13	50
Ce	24	53	31	21	20	19	20	29	105
Nd	14	39	21	16	15	16	16	18	80
Sr	227	251	222	207	184	187	182	243	251
Y	25	53	37	36	29	28	29	35	111
Zr	126	277	175	146	110	114	118	143	425
Nb	10	23	15	10	6.9	7.8	7.5	10	32
Ba	38	92	62	43	83	49	58	73	247
V	300	310	364	374	319	359	346	382	67
Sc	37	32	40	40	38	38	39	39	22
⁸⁷ Sr/ ⁸⁶ Sr							0.70355	0.70355	0.70384

Sample locations are shown on Fig. 1. Chemical analyses by XRF. Major elements: GGU, trace elements: Geol. Inst., Univ. of Copenhagen. Sr-isotopes: Geol. Inst., Univ. of Copenhagen. For ⁸⁷Sr/⁸⁶Sr ratios the within run precision was better than ± 0.00001 (1 S.D.), and standard material NB 987 gave ⁸⁷Sr/⁸⁶Sr = 0.710268 ± 0.000009 (1 S.D., N=36) in the period of analysis. mg' = atomic 100 Mg/(Mg+Fe²⁺) with Fe₂O₃/FeO adjusted to 0.15.

where they all plot well below the Hawaiian dividing line of MacDonald & Katsura (1964). The mg' ratios range from 59.1 to 42.8 which indicates that the magmas were fractionated before they were emplaced. The five basaltic dykes are also tholeiites. The alkaline affinities of the basanite and the basaltic trachyandesite are supported by low Zr/Nb ratios (4.2 and 5.4).

The tholeiitic basalts and dolerites have volatile contents between 1 and 3 wt.% and Fe₂O₃/FeO ratios between 0.14 and 0.81 (lavas: 0.33–0.81; sills: 0.14–0.43).

The tholeiitic sills and dykes show good correlation between K₂O and immobile Nb (Fig. 4), indicating that remobilisation in most of the samples is of minor importance. A more severe alteration including redistribution of Ca has only been observed in dyke GGU 239589 from the vicinity of the Kap Simpson Complex.

The lavas plot slightly more scattered in the K₂O–Nb diagram and may have suffered some post-emplacement alteration.

Table 1 continued

239579	239598	Sills, enriched		239572	Dykes, alkaline	
		239548	239570		239565	239595
49.22	49.25	51.08	48.77	49.03	41.21	50.12
2.20	1.98	2.48	2.86	2.64	3.06	1.89
13.29	14.05	13.87	13.52	13.06	14.17	16.28
2.63	2.97	3.56	3.28	2.93	4.12	1.84
10.41	9.32	8.54	9.56	10.18	8.17	6.68
0.20	0.20	0.18	0.20	0.20	0.19	0.15
6.45	6.63	5.55	5.57	5.90	5.69	2.66
10.82	11.25	9.38	9.90	10.30	11.88	6.43
2.43	2.47	2.71	2.84	2.52	2.28	3.75
0.32	0.28	1.10	1.06	0.76	0.77	2.53
0.21	0.19	0.32	0.37	0.31	0.65	0.64
1.47	1.46	1.37	1.54	1.61	7.13	6.67
99.66	100.03	100.14	99.47	99.46	99.32	99.65
50.5	52.8	48.9	47.4	48.2	49.2	39.2
108	164	38	105	100	21	8
58	51	45	48	50	46	21
69	78	20	67	72	31	10
204	234	18	143	171	34	8
109	106	105	111	110	89	100
7.5	6.3	32	26	18	16	128
15	13	36	31	28	39	63
26	24	56	51	43	72	119
20	17	34	30	26	41	58
228	200	345	328	337	674	589
34	34	34	39	36	27	34
145	135	230	217	195	176	315
12	8.4	31	34	27	42	58
80	51	390	374	260	425	768
355	345	324	375	360	367	165
36	40	29	27	28	23	13
	0.70395		0.70471			

Lavas. Eight lavas have been analysed. In the plot of TiO_2 versus mg' (Fig. 5), seven of the lavas define a narrow elongated field with mg' decreasing from 57.6 to 44.5, accompanied by an increase in TiO_2 from 1.8 to 2.6 wt.%. These 'main type' lavas also form a coherent group in most other variation diagrams: decreasing mg' values correlate with increasing concentrations of total iron, Na_2O , K_2O , P_2O_5 and incompatible trace elements, and decreasing contents of Al_2O_3 , MgO , CaO , Ni and Cr . SiO_2 , Co and Sc remain constant (Table 1 and Fig. 5).

The lava GGU 239531 ($\text{mg}' = 42.8$) has significantly

higher concentrations of the incompatible minor and trace elements than the other lavas. The content of TiO_2 is 3.5 wt.% as compared to 2.6 wt.% TiO_2 in the most fractionated lavas of the 'main type', and the relative enrichment of Nb is even higher: 23 ppm versus 14 ppm in the 'main type' lavas. The lava contains 20 % plagioclase phenocrysts which were probably accumulated, judging from the high whole-rock concentration of Al_2O_3 (Table 1, Fig. 5).

No regular up-section variations have been found in the chemical composition of the lavas.

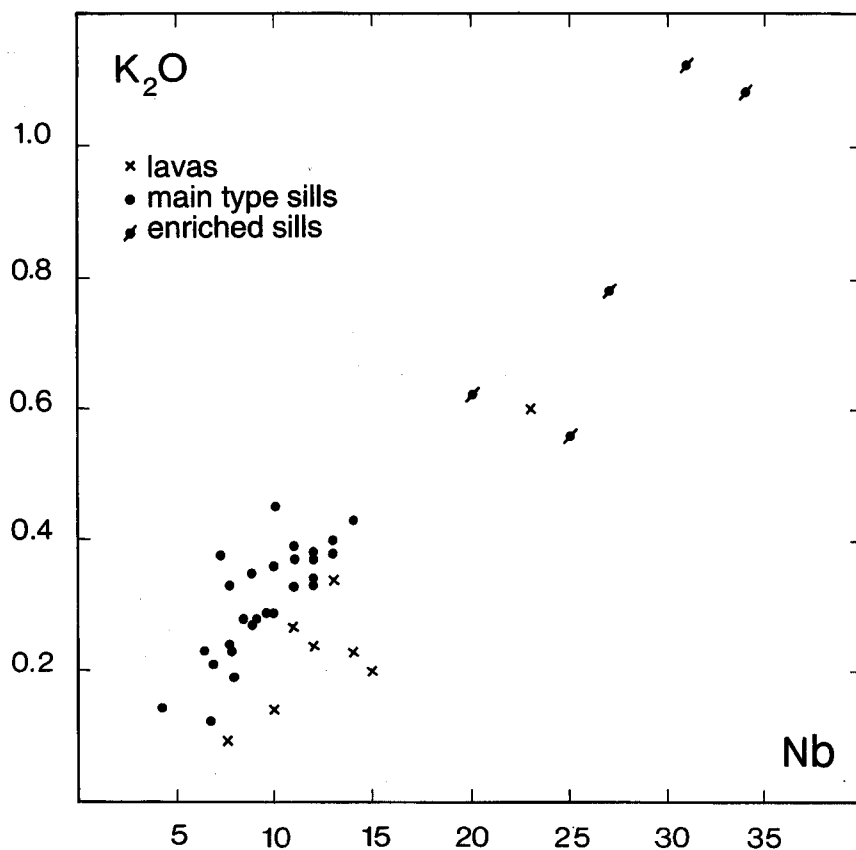


Fig. 4. Correlation between K_2O and Nb.

Sills and dykes. Sills may display systematic compositional variations from base to top due to flow differentiation or differentiation during solidification. Investigations of doleritic sills from Antarctica (Hergt *et al.*, 1989) and South Africa (Le Roex & Reid, 1978) similar in thickness to those of East Greenland suggest that the variations are mainly restricted to the middle and upper parts of the individual sills, and that samples from the lower parts in most cases provide good estimates on the average compositions. Samples of the East Greenland sills were, therefore, collected 3 to 5 m above the estimated lower contact.

The oxides and trace elements versus mg' diagrams demonstrate that most of the sills (the 'main type' sills) and a few of the dykes fit the 'main type' lavas rather closely. The sample GGU 239521 ($mg' = 52.3$), which otherwise plots within the field defined by the 'main type' lavas, has a higher-than-usual content of Al_2O_3 and a low total-iron, whereas the opposite relationship is found in GGU 239543 ($mg' = 57.3$). The two analysed samples are high in plagioclase and clinopyroxene, respectively, and may reflect local enrichment of these two minerals.

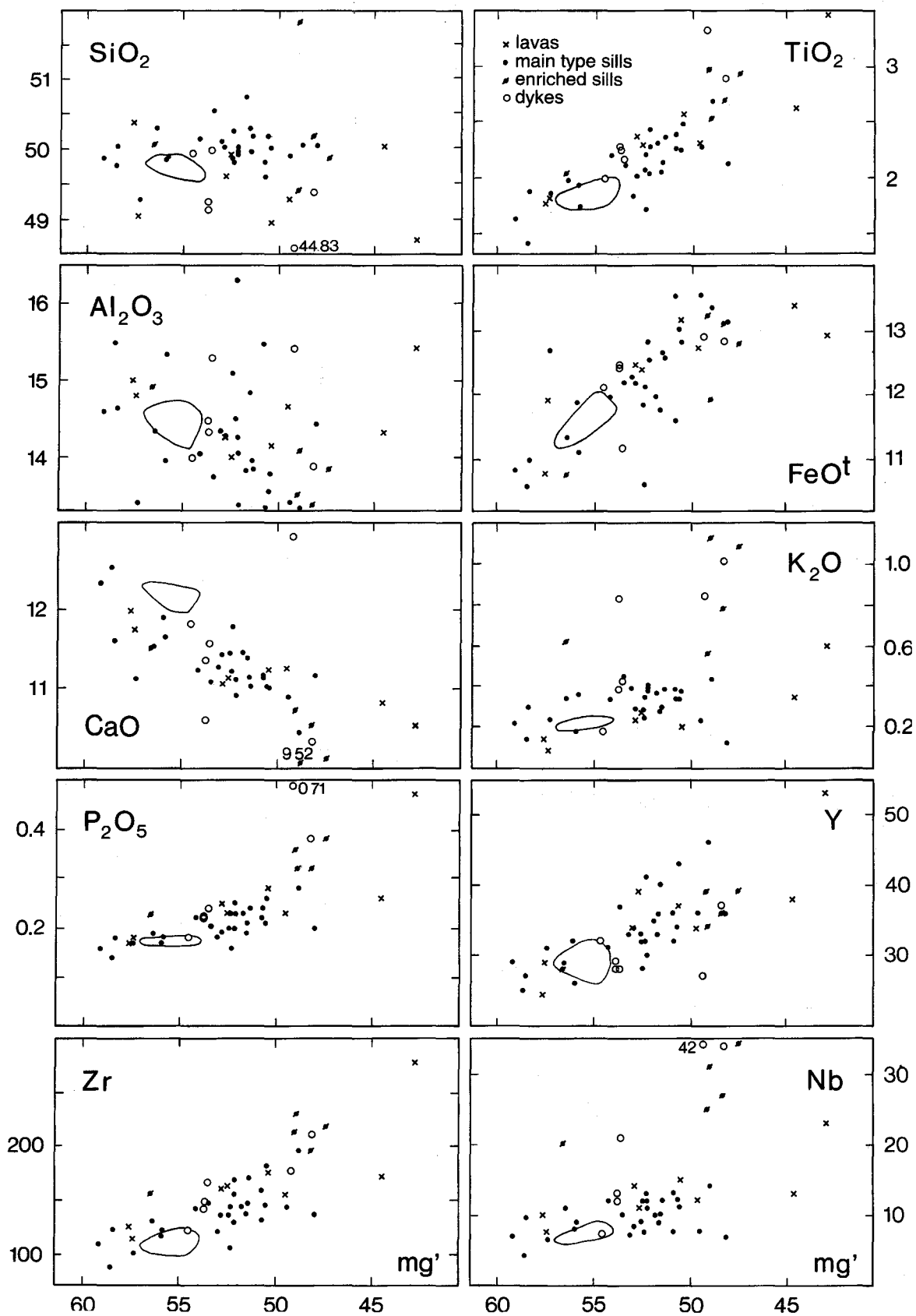
A few sills (GGU 239544, -47, -48, -70 and -72) and the dykes GGU 239540 and -41 plot outside the field of the 'main type' lavas in most diagrams. They are all enriched in incompatible elements and especially in the strongly incompatible elements: K, Rb, Ba, Nb, La and Ce (2–3 times the concentration in the 'main type' sills), while the enrichment is less marked for P, Zr and Ti.

As also indicated by the mineralogical investigations, the chemical variations in the sill on Leitch Bjerg (Fig. 5) are subtle, mg' ranges from 56.9 (sample collected 15 m above the base) to 54.0 (most coarse-grained sample 40 m above the base) and 53.6 (lower chilled margin).

Changes are much more pronounced in the thick Svinhufvud Bjerge sill. The lowermost sample has a basaltic composition, although slightly enriched in silica relative to the main field dolerites, while the three samples from 90 m, 85 m and 20 m below the upper contact are strongly iron-enriched, similar to the fractionated upper parts of the Skaergaard intrusion (Wager & Brown, 1968) and the Basistoppen sill (Naslund, 1989). The close chemical relations between samples from the fayalite diorite zone of the Basistoppen sill and from the upper part of the

→

Fig. 5. Major and trace elements versus mg' . The major elements have been recalculated assuming an oxide total of 100%. Encircled areas: five analyses of a sill on Leitch Bjerg, do not include analysis of the lower chill.



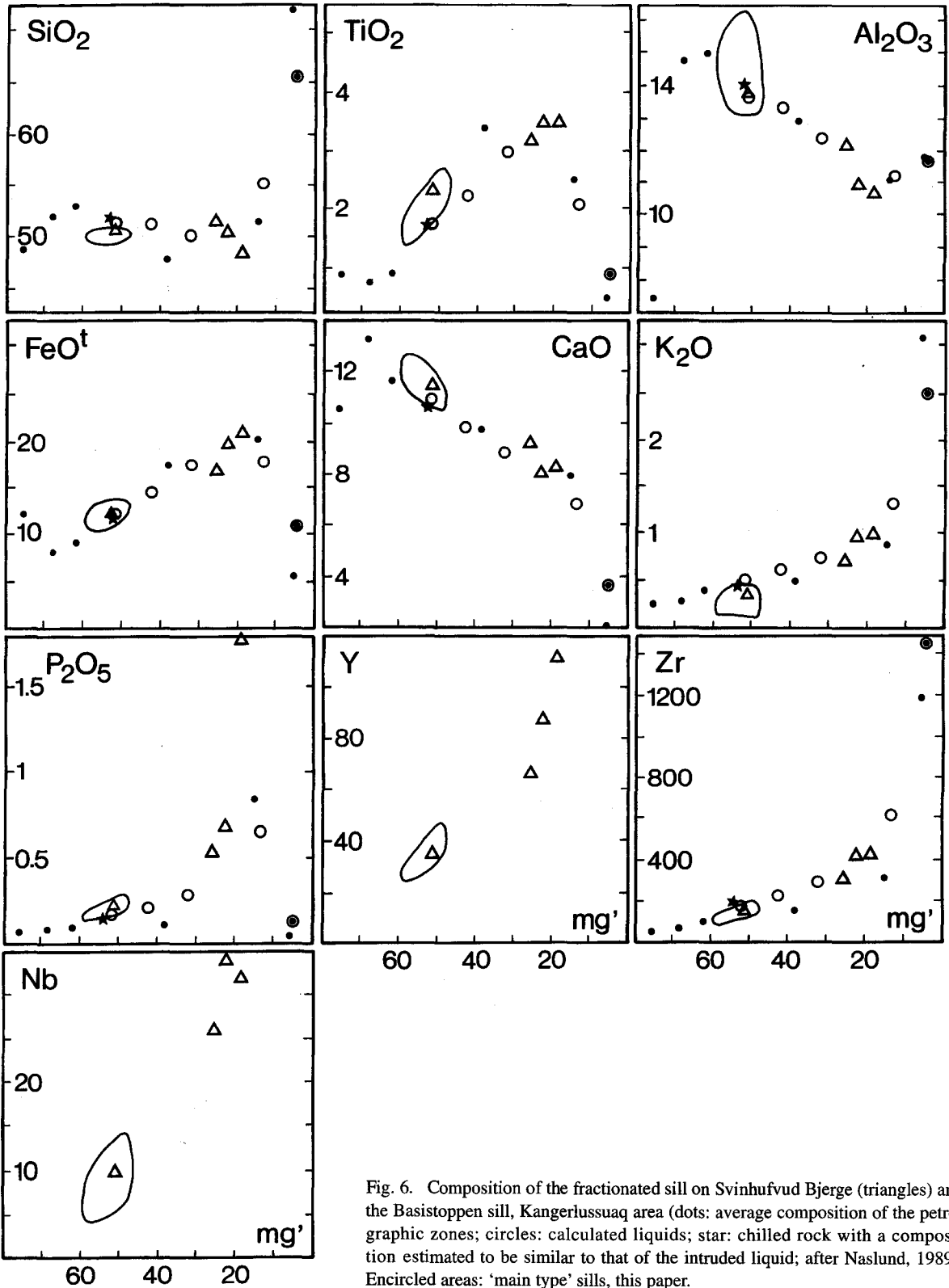


Fig. 6. Composition of the fractionated sill on Svinhufvud Bjerge (triangles) and the Basistoppen sill, Kangerlussuaq area (dots: average composition of the petrographic zones; circles: calculated liquids; star: chilled rock with a composition estimated to be similar to that of the intruded liquid; after Naslund, 1989). Encircled areas: 'main type' sills, this paper.

Svinhufvud Bjerge sill is demonstrated in Fig. 6. More detailed sampling is needed to determine whether the evolved composition of the upper part of the Svinhufvud Bjerge sill is caused by *in situ* fractionation or reflects multiple intrusions of magmas fractionated at depth. No internal boundaries were observed during field work.

Sr isotope analyses have been carried out on five samples. Two unfractionated 'main type' sills (GGU 239555 and -98) have $^{87}\text{Sr}/^{86}\text{Sr}$ ratios of 0.70355 and 0.70395 respectively. Similar ratios are found in both the basaltic and the dioritic part of the fractionated Svinhufvud Bjerge sill (0.70355 and 0.70384). A slightly increased ratio of 0.70471 is found in the enriched sill, GGU 239570.

'Main type' and enriched compositions

To judge from the variation diagrams (Fig. 5) the 'main type' sills and lavas in the region between Kong Oscar Fjord and Kejser Franz Joseph Fjord are closely related. Decreasing contents of Al_2O_3 , MgO and CaO with decreasing mg' suggest that the chemical trends are governed by fractionation of plagioclase in combination with one or more ferromagnesian minerals.

The role of fractional crystallisation has been tested using a least squares mixing program (Table 2). The sills GGU 239523 ($\text{mg}' = 59.1$) and GGU 239579 ($\text{mg}' = 50.5$) have been used as end members in the calculations. Mineral compositions were obtained from the microprobe analyses of phenocrysts from 'main type' lavas and fine-grained sills. The calculations show that the transition from dolerite GGU 239523 to dolerite GGU 239579 can be reproduced by subtracting 3.1% olivine, 13.6% plagioclase and 10.7% clinopyroxene. The solution agrees in general with the slight depletion of Ni, the enrichment of elements like Ti, K, P and Zr which all have low crystal/liquid distribution coefficients, and the steady level of Sc,

which is preferentially incorporated in clinopyroxene.

It is also clear from the variation diagrams that fractional crystallisation alone cannot account for the total spread in the content of incompatible elements. Fig. 7a and b present incompatible element diagrams ('spidergrams') for selected lavas and sills. The concentrations have been normalised to chondritic compositions after Thompson (1982). The main field sill samples all have similar patterns: relative concentrations rise from Ba to La and then fall slowly towards Y (Fig. 7b). The patterns of the enriched dolerites are different. They have steeper La to Y limbs whereas the Ba to La limbs are less steep.

The spidergrams demonstrate a close correlation between the concentrations of the non-mobile element Nb in the sills and the mobile elements Ba, Rb and K (cf. Fig. 4). This confirms that the concentration of these elements is not seriously influenced by alteration or crustal contamination. Conversely, the lower content of K and especially of Rb in the lavas (Fig. 7a) seen in connection with the scatter of the lavas in the K_2O versus Nb diagram (Fig. 4) may suggest a loss of these elements from some samples subsequent to the eruption. A similar divergence between the sills (high Rb and K) and the lower series lavas (low Rb and K) has been noticed by Upton *et al.* (1984a) on Hold with Hope.

Regional variations

Fig. 8 provides a comparison in terms of TiO_2 and mg' between the lavas and sills from Traill Ø and Geographical Society Ø, lavas from the Scoresby Sund region and lavas and sills from the area north of Kejser Franz Joseph Fjord. Larsen *et al.* (1989) demonstrated a range of TiO_2 levels among the Scoresby Sund lavas from MORB-type basalts to the so-called Ti-tholeiites. They also noticed that the variation in terms of TiO_2 appears to be much more restricted among the lower series lavas north of Kejser Franz Joseph Fjord: with a few exceptions analysed basalt flows from this area correlate with their low-Ti type from the Scoresby Sund region.

Among the eight lavas from Kap Mackenzie the seven 'main type' lavas have compositions similar to the lower lavas and to the sills north of Kejser Franz Joseph Fjord; only sample GGU 239531 has an off-trend composition. The same pattern emerges from a comparison between the sills on Traill Ø and Geographical Society Ø and the lavas and sills from the northern area: only the five enriched sills from the two islands plot off the main trend.

The lava GGU 239531 is characterised by a steep Ba to La limb in the spidergram and by a deep Sr anomaly, similar to the Ti-tholeiites of the Scoresby Sund region. The five sills, on the other hand, with their less steep Ba

Table 2. Least square tests of fractionation

Parent GGU 239523, daughter GGU 239579			
	Parent observed	Parent calculated	Calculated proportions weight percent
SiO_2	49.93	49.87	Olivine Fo_{74} 3.1%
TiO_2	1.63	1.67	Plagioclase An_{81} 13.6%
Al_2O_3	14.60	14.64	Clpx. $\text{Ca}_{43}\text{Mg}_{47}\text{Fe}_{10}$ 10.7%
FeO	10.86	10.97	
MnO	0.18	0.17	$\Sigma\text{R}^2 = 0.05$
MgO	7.75	7.74	
CaO	12.37	12.50	
Na_2O	2.30	2.17	
K_2O	0.21	0.24	
P_2O_5	0.16	0.16	

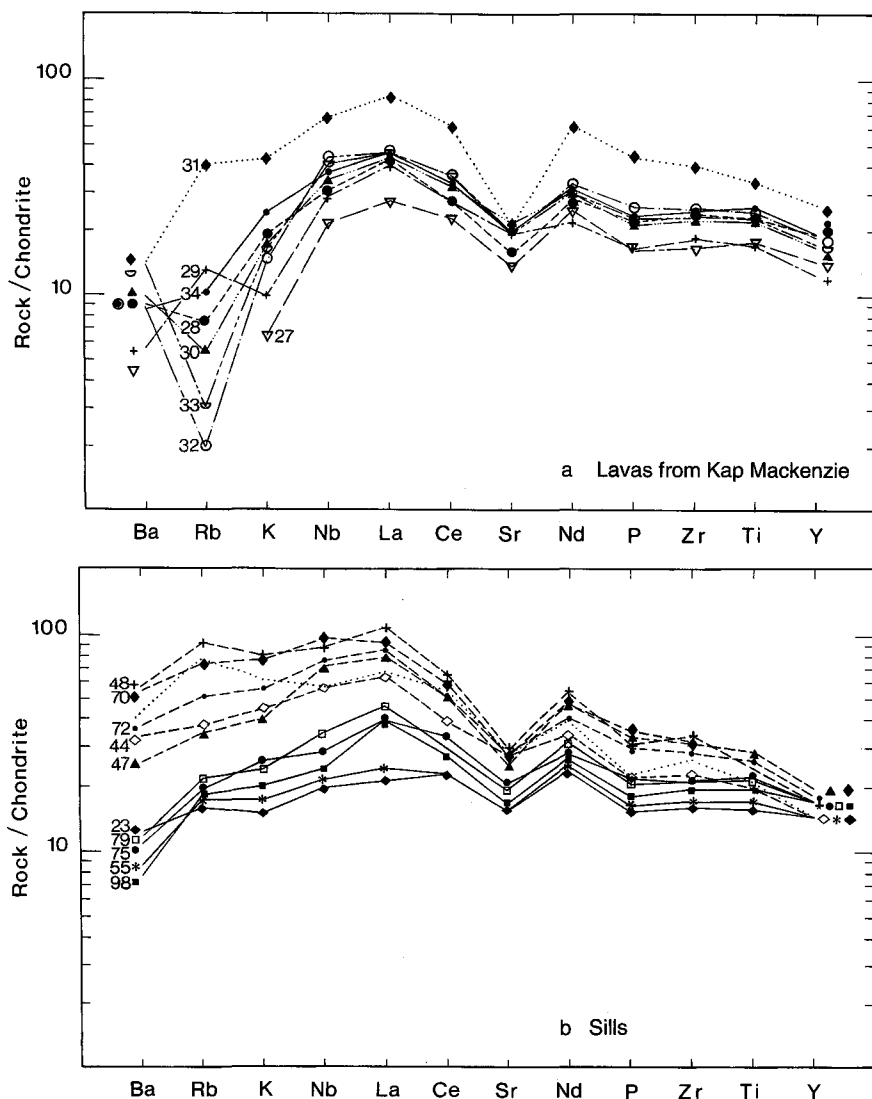


Fig. 7. Spidergrams for the incompatible elements. Normalisation factors from Thompson (1982). a. Lavas from Kap Mackenzie. b. Sills, full lines: 'main type' compositions, broken lines: enriched compositions, dotted line: average composition of normal type upper series lavas, Hold with Hope (Upton *et al.*, 1984b). GGU sample numbers are shown by their last two digits.

to La limbs, less distinct Sr anomalies and high $^{87}\text{Sr}/^{86}\text{Sr}$ ratios (sample GGU 239570) seem to be related to the hypersthene-normative lavas of the upper series of Hold with Hope and Giesecke Bjerge (Fig. 7). Independent evidence for this relationship comes from the preliminary palaeomagnetic analyses. Whereas the 'main type' sills appear to be reversely magnetised the analyses suggest that four of the five enriched sills were intruded during a period of normal polarity of the Earth's magnetic field as were the upper series lavas north of Kejser Franz Joseph Fjord.

In conclusion, the lavas and sills on Traill Ø and Geographical Society Ø are related in general to the basalts in the Scoresby Sund region and north of Kejser Franz Joseph Fjord; however, their restricted chemical variation, as shown e.g. in the TiO_2 versus mg' diagrams, points towards a closer relationship with the sills and lower lavas in the northern part of the province (Fig. 8).

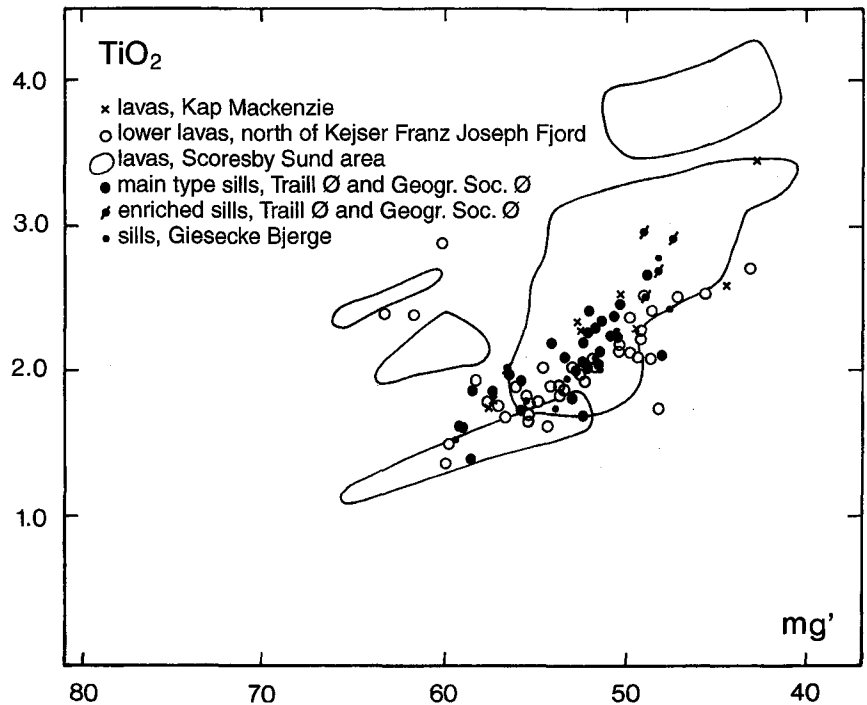
Discussion

Upton *et al.* (1984a) suggested that the source region of the lavas in the northern plateau was within a zone to the east of the present coastline where the lithosphere was greatly thinned prior to rifting. The scarcity of dykes on Traill Ø and Geographical Society Ø similarly suggests an offshore position of the feeders, also in this area.

In a detailed study of the Hold with Hope and Wollaston Forland lavas, Thirlwall *et al.* (1994) conclude that the lower lavas were probably derived from an Icelandic plume source with no component from MORB asthenosphere. They model around 20% melting, mostly in the spinel field, followed by substantial fractional crystallisation to form the lavas from the plume mantle.

The major and trace element compositions of the 'main type' lavas and sills studied here, and the few Sr isotope

Fig. 8. TiO_2 versus mg' for East Greenland lavas and sills. Data from Hald (1978) and unpublished; Larsen *et al.* (1989); Noe-Nygaard & Pedersen (1983); Thirlwall *et al.* (1994).



analyses of the sills, suggest that most of the magmas were of similar origin to those forming the lower lavas north of Kejser Franz Joseph Fjord. The composition of the few enriched sills indicates lithospheric contamination as suggested by Thirlwall *et al.* (1994) for the upper lavas.

Larsen *et al.* (1989) suggest that the magmas parental to the flood basalts in the Scoresby Sund region tended to collect near the mantle-crust boundary and that they were further fractionated in 'open' crustal magma chambers, where the Ti-enriched compositions were formed. The low-Ti basalts are found at two stratigraphic levels, and they are interpreted as being extruded during periods of increased replenishment of the upper crustal magma chambers and shortened residence time.

The apparent greater importance of mid-crustal magma chambers in the evolution of the melts in the Scoresby Sund region may reflect that the volcanic activity in this part of East Greenland took place along intra-plate fissures (Larsen & Watt, 1985) which probably reflected unsuccessful attempts to straighten the spreading axis, curving to the east between Kangerlussuaq and the initial Jan Mayen Fracture Zone (Larsen, 1988).

Candidates for mid-crustal magma chambers in the shape of thick sills intruded in a non-extensional environment have been mapped with seismic methods in the Jameson Land basin (Larsen & Marcussen, 1992). The Svinhufvud sill on nearby southern Traill Ø suggests that extensive fractionation may take place in such intrusions.

Acknowledgements. I wish to thank L. M. Larsen, T. F. D. Nielsen, A. K. Pedersen and L. Stemmerik for their constructive criticism of the manuscript. Thanks are also due to J. Kystøl, J. C. Bailey and P. M. Holm for major element, trace element and Sr-isotope analyses respectively and to J. Rønnsbo for help with the microprobe work.

References

- Anwar, Y. M. 1955: Geological investigations in East Greenland. Part V. The petrography of the Prinsen of Wales Bjerger lavas. *Meddr Grønland* **135**(1), 31 pp.
- Brooks, C. K. & Nielsen, T. F. D. 1982: The Phanerozoic development of the Kangerdlugssuaq area, East Greenland. *Meddr Grønland, Geosci.* **9**, 30 pp.
- Brooks, C. K. & Nielsen, T. F. D. & Pedersen, T. S. 1976: The Blossesville Coast basalts of East Greenland. Their occurrence, composition and temporal variation. *Contrib. Mineral. Petrol.* **58**, 279–292.
- Donovan, D. T. 1953: The Jurassic and Cretaceous stratigraphy and palaeontology of Traill Ø, East Greenland. *Meddr Grønland* **111**(4), 150 pp.
- Donovan, D. T. 1955: The stratigraphy of the Jurassic and Cretaceous rocks of Geographical Society Ø, East Greenland. *Meddr Grønland* **103**(9), 60 pp.
- Eldholm, O., Thiede, J. & Taylor, E. 1989: Evolution of the Vøring volcanic margin. In Eldholm, O., Thiede, J., Taylor, E. *et al.* (ed.) *Proc. ODP, Sci. Results* **104**, 1033–1065.
- Engell, J. 1975: The Kap Parry complex, central East Greenland. *Rapp. Grønlands geol. Unders.* **75**, 103–106.

- Fawcett, J. J., Gittins, J., Rucklidge, J. C. & Brooks, C. K. 1982: Petrology of Tertiary lavas from the western Kangerdlugssuaq area, East Greenland. *Mineralog. Mag.* **45**, 211–218.
- Frebold, H. & Noe-Nygaard, A. (1938): Marines Jungpalaeozoikum und Mesozoikum von der Traill-Insel (Ostgrönland). *Meddr Grønland* **119**(2), 37 pp.
- Hald, N. 1978: Tertiary igneous activity at Giesecke Bjerger, northern East Greenland. *Bull. geol. Soc. Denmark* **27**, 109–115.
- Hergt, J. M., Chappell, B. W., Faure, G. & Mensing, T. M. 1989: The geochemistry of Jurassic dolerites from Portal Peak, Antarctica. *Contrib. Mineral. Petrol.* **102**, 298–305.
- Koch, L. & Haller, J. 1971: Geological map of East Greenland 72°–76° N. Lat. 1:250 000. *Meddr Grønland* **183**, 26 pp.
- Larsen, H. C. 1988: A multiple and propagating rift model for the NE Atlantic. In Morton, A. C. & Parson, L. M. (ed.) Early Tertiary volcanism and the opening of the NE Atlantic. *Spec. Publ. geol. Soc. Lond.* **39**, 157–158.
- Larsen, H. C. 1990: The East Greenland shelf. In Grantz, A., Johnson, L. & Sweeney, J. F. (ed.) The Arctic Ocean region. *The geology of North America*, **L**, 185–210.
- Larsen, H. C. & Marcussen, C. 1988: Sill-intrusion, flood basalt emplacement and deep crustal structure of the Scoresby Sund region, East Greenland. In Storey, B. C., Alabaster, T. & Pankhurst, R. J. (ed.) Magmatism and the causes of continental break-up. *Spec. Publ. geol. Soc. Lond.* **68**, 365–386.
- Larsen, L. M. & Watt, W. S. 1985: Episodic volcanism during break-up of the North Atlantic: evidence from the East Greenland plateau basalts. *Earth planet. Sci. Lett.* **73**, 105–116.
- Larsen, L. M., Watt, W. S. & Watt, M. 1989: Geology and petrology of the Lower Tertiary plateau basalts of the Scoresby Sund area, East Greenland. *Bull. Grønlands geol. Unders.* **157**, 164 pp.
- Le Bas, M. J., Le Maitre, R. W., Streckeisen, A. & Zanettin, B. 1986: A chemical classification of volcanic rocks based on the total alkali-silica diagram. *J. Petrology* **27**, 745–750.
- Le Roex, A. P. & Reid, D. L. 1978: Geochemistry of Karroo dolerite sills in the Calvinia District, Western Cape Province, South Africa. *Contrib. Mineral. Petrol.* **66**, 351–360.
- Macdonald, G. A. & Katsura, T. 1964: Chemical composition of Hawaiian lavas. *J. Petrology* **5**, 82–133.
- Naslund, H. R. 1989: Petrology of the Basistoppen Sill, East Greenland: A calculated magma differentiation trend. *J. Petrology* **30**, 299–319.
- Nielsen, T. F. D., Soper, N. J., Brooks, C. K., Faller, A. M., Higgins, A. C. & Matthews, D. W. 1981: The pre-basaltic sediments and the Lower Basalts at Kangerdlugssuaq, East Greenland, their stratigraphy, lithology, palaeomagnetism and petrology. *Meddr Grønland, Geosci.* **6**, 25 pp.
- Noe-Nygaard, A. 1976: Tertiary igneous rocks between Shannon and Scoresby Sund, East Greenland. In Escher, A. & Watt, W. S. (ed.) *Geology of Greenland*, 386–402. Copenhagen: Geological Survey of Greenland.
- Noe-Nygaard, A. & Pedersen, A. K. 1983: Tertiary volcanic rocks from Bontekoe Ø, East Greenland. *Rapp. Grønlands geol. Unders.* **116**, 13 pp.
- Olsen, H. 1993: Sedimentary basin analysis of the continental Devonian basin in North-East Greenland. *Rapp. Grønlands geol. Unders.* **116**, 80 pp.
- Schaub, H. S. 1942: Zur Geologie der Traill Insel (Nordostgrönland). *Eclogae geol. Helv.* **35**(1), 54 pp.
- Smith, D. 1970: Mineralogy and petrology of the diabasic rocks in a differentiated olivine diabase sill complex, Sierra Ancha, Arizona. *Contrib. Mineral. Petrol.* **27**, 95–113.
- Stemmerik, L., Vigran, J. O. & Piasecki, S. 1991: Dating of late Paleozoic rifting events in the North Atlantic: new biostratigraphic data from the uppermost Devonian and Carboniferous of East Greenland. *Geology* **19**, 218–221.
- Stemmerik, L., Christiansen, F. G., Piasecki, S., Jordt, B., Marcussen, C. & Nøhr-Hansen, H. 1992: Depositional history and petroleum geology of the Carboniferous to Cretaceous sediments in the northern part of East Greenland. In Vorren, T. O., Bergsager, E., Dahl-Stamnes, Ø. A., Holter, E., Johansen, B., Lie, E. & Lund, T. B. (ed.) Arctic geology and petroleum potential. *Spec. Publ. Norweg. Petrol. Soc.* **2**, 67–87.
- Sun, S. S. 1980: Lead isotopic study of young volcanic rocks from mid-ocean ridges, ocean islands and island arcs. *Phil. Trans. R. Soc. London A* **297**, 409–445.
- Suryk, F. 1990: Timing, style and sedimentary evolution of Late Palaeozoic–Mesozoic extensional basins of East Greenland. In Hardmann, R. F. P. & Brooks, J. (ed.) Tectonic events responsible for Britain's oil and gas reserves. *Spec. Publ. geol. Soc. Lond.* **55**, 107–125.
- Suryk, F., Clemmensen, L. B. & Larsen, H. C. 1981: Post-Paleozoic evolution of the East Greenland continental margin. In Kerr, J. W. & Ferguson, A. J. (ed.) Geology of the North Atlantic borderlands. *Mem. Can. Soc. Petrol. Geol.* **7**, 611–645.
- Tarling, D. D., Hailwood, E. A. & Løvlie, R. 1988: A palaeomagnetic study of lower Tertiary lavas in E. Greenland and comparison with other lower Tertiary observations in the northern Atlantic. In Morton, A. C. & Parson, L. M. (ed.) Early Tertiary volcanism and the opening of the NE Atlantic. *Spec. Publ. geol. Soc. Lond.* **39**, 215–224.
- Thirlwall, M. F., Upton, B. G. J. & Jenkins, C. 1994: Interaction between continental lithosphere and the Iceland plume – Sr-Nd-Pb isotope geochemistry of Tertiary basalts, NE Greenland. *J. Petrology* **35**, 839–879.
- Thompson, R. N. 1982: Magmatism of the British Tertiary volcanic province. *Scot. J. Geol.* **18**, 49–107.
- Upton, B. G. J. 1988: History of Tertiary igneous activity in the N Atlantic borderlands. In Morton, A. C. & Parson, L. M. (ed.) Early Tertiary volcanism and the opening of the NE Atlantic. *Spec. Publ. geol. Soc. Lond.* **39**, 429–453.
- Upton, B. G. J., Emeleus, C. H. & Beckinsale, R. D. 1984a: Petrology of the northern East Greenland flood basalts: evidence from Hold with Hope and Wollaston Forland. *J. Petrology* **25**, 151–184.
- Upton, B. G. J., Emeleus, C. H. & Beckinsale, R. D. & Macintyre, R. M. 1984b: Myggbukta and Kap Broer Ruys: the most northerly of East Greenland Tertiary centres(?). *Mineralog. Mag.* **48**, 323–343.
- Upton, B. G. J., Emeleus, C. H. & Hald, N. 1980: Tertiary volcanism in northern E Greenland: Gauss Halvø and Hold with Hope. *J. Geol. Soc. Lond.* **137**, 491–508.
- Vischer, A. 1943: Die postdevonische Tektonik von Ostgrönland zwischen 74° und 75° N. Br. Kuhn Ø, Wollaston Forland, Clavering Ø und angrenzende Gebiete. *Meddr Grønland* **133**(1), 195 pp.

- Wager, L. R. & Brown, G. M. 1968: *Layered igneous rocks*. 588 pp. Edinburgh & London: Oliver & Boyd.
- Walker, K. R., Ware N. G. & Lovering J. F. 1973: Compositional variations in the pyroxenes of the differentiated Palisades Sill, New Jersey. *Bull. Geol. Soc. Amer.* **84**, 89–110.
- Watt, W. S., Larsen, L. M. & Watt, M. 1986: Volcanic history of the Lower Tertiary plateau basalts in the Scoresby Sund region, East Greenland. *Rapp. Grønlands geol. Unders.* **128**, 147–156.



Stratigraphy and depositional evolution of the Upper Palaeozoic sedimentary succession in eastern Peary Land, North Greenland

Lars Stemmerik, Eckart Håkansson, Lena Madsen, Inger Nilsson, Stefan Piasecki¹, Sylvie Pinard² and Jan A. Rasmussen

The Upper Palaeozoic Foldedal and Kim Fjelde formations in eastern Peary Land are redefined on the basis of new biostratigraphic data, including fusulinids, conodonts, palynomorphs and small foraminifera. The Foldedal Formation in its new definition includes all late Moscovian to Gzelian deposits in the region. It is separated by a major hiatus from the redefined Kim Fjelde Formation which includes mid-Permian (late Artinskian – Kungurian) carbonates and chert deposits. The Upper Carboniferous succession is dominated by cyclically interbedded siliciclastics and carbonates with minor tabular build-ups. The mid and Upper Permian succession consists of cool-water carbonates, spiculitic chert and shales.

L. S., S. P.¹ & J. A. R., Geological Survey of Denmark and Greenland, Thoravej 8, DK-2400 Copenhagen NV, Denmark.

E. H. & L. M., Geological Institute, University of Copenhagen, Øster Voldgade 10, DK-1350 Copenhagen K, Denmark.

I. N., Saga Petroleum a.s., Postboks 1134, N-9400 Harstad, Norway.

S. P.², 7146–119th Street N.W., Edmonton T6G 1V6, Canada (formerly of the Geological Survey of Canada).

In eastern Peary Land, the marine Upper Palaeozoic deposits of the Wandel Sea Basin have been included in the upper Moscovian to Upper Carboniferous Foldedal Formation of mixed carbonates and siliciclastics, the Upper Carboniferous to (?) Kungurian carbonate-dominated Kim Fjelde Formation and the shale-dominated, mid to Upper Permian Midnatfjeld Formation (Håkansson, 1979; Stemmerik & Håkansson, 1989). Originally it was suggested these formations formed a continuous sedimentary succession of mid-Carboniferous to Late Permian age (Håkansson, 1979; Håkansson & Stemmerik, 1984; Stemmerik & Håkansson, 1989, 1991). However, field work in the area in 1991 proved the presence of a major subaerial exposure surface within the Kim Fjelde Formation in the southern part of the outcrop area. Later, field work in Amdrup Land and Holm Land further to the east has shown that this exposure event is of regional significance (Stemmerik & Elvebakk, 1994). Biostratigraphic data indicate that the exposure surface represents a major hiatus

spanning most of the Early Permian, and accordingly, the originally proposed lithostratigraphic scheme has to be revised.

This paper revises the lithostratigraphy of the Upper Palaeozoic deposits in eastern Peary Land in accordance with new sedimentological and sequence stratigraphic information, and provides new biostratigraphic data from the succession (Figs 1, 2). Age dating is based on fusulinids in the Carboniferous part of the succession with some additional data from conodonts, and on conodonts, small foraminifera and palynomorphs in the Permian part of the succession. The boundary between the Foldedal Formation and Kim Fjelde Formation is an erosional unconformity while the boundary between the Kim Fjelde Formation and the Midnatfjeld Formation is a major flood surface.

The Foldedal Formation is redefined to include a succession of mixed siliciclastics and shallow shelf carbonates of late Moscovian to Gzelian (?earliest Asselian)

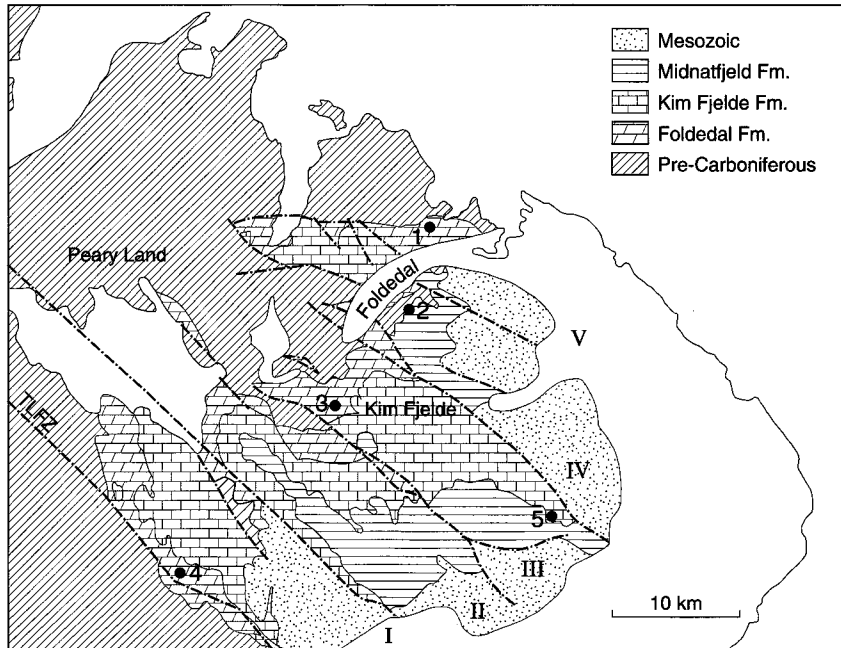


Fig. 1. Geological map of eastern Peary Land showing distribution of Upper Palaeozoic formations and location of measured sections (1–5). I to V are major fault blocks within the Trolle Land Fault System. TLFZ: Trolle Land Fault Zone.

age. It includes the lower part of the Kim Fjelde Formation as it was defined by Håkansson (1979) and Stemmerik & Håkansson (1989). The Kim Fjelde Formation is defined to include a succession of normal marine shallow to deeper shelf carbonates of late Artinskian to Kungurian age. The Midnattfjeld Formation is composed of two shallowing upward successions of Kazanian age.

Biostratigraphy

The Carboniferous part of the succession has been dated by fusulinids, while the Permian sediments have been dated by a combination of conodonts, small foraminifera and palynomorphs. The fusulinid assemblages identified in the Moscovian–Gzelian succession are comparable to assemblages previously described from the Wandel Sea Basin (Petryk, 1977; Nilsson *et al.*, 1991; Nilsson, 1994; Stemmerik *et al.*, 1995a; Dunbar *et al.*, 1962), and they can be correlated to the fusulinid zones in the Russian stratotype area.

Biostratigraphic zonation is less firmly established in the late Artinskian and younger Permian sediments due to lack of fusulinids in the Arctic region. Conodonts, small-foraminifera and palynomorphs have been compared to local zonation in the Sverdrup Basin, Svalbard and the Barents Sea to establish the best possible correlation.

Upper Carboniferous

Fusulinids. In the lower part of the Foldedal Formation

in northern Foldedal (sections 1 and 3 in Fig. 2) a fusulinid assemblage characterised by *Beedeina* aff. *B. paradiستا*, *Parawedekindellina* sp., *Fusulinella eopulchra*, *F. pulchra*, *Pseudostafella* sp., *Ozawinella* spp., *Eostafella* sp., *Schubertella* sp. and *Pseudoendothyra* sp. occurs. This assemblage shows close similarities with the late Moscovian *Wedekindellina* assemblage of Dunbar *et al.* (1962) and it is regarded as being of the same age. An assemblage composed of *Protriticites* spp., *Fusulinella* aff. *F. eopulchra* and *Quasifusulinoides fusiformis* is regarded as slightly younger and has been assigned to the latest Moscovian–?early Kasimovian. Upper Kasimovian strata are characterised by a *Rauserites* ex. gr. *simplex* assemblage with *R. simplex*, *R.* aff. *R. irregularis*, *Pseudofusulinella usvae* and *Schubertella transitoria*. This fauna can be correlated to the *R.* ex. gr. *simplex* assemblage of Nilsson (1994). Sediments belonging to the early–middle Gzelian *Rauserites* ex. gr. *rossicus* assemblage occur in the upper part of the Foldedal Formation in section 1 of northern Foldedal (Fig. 2). This assemblage is characterised by *R.* ex. gr. *rossicus*, *Rugosofusulina* aff. *R. prisca*, *R.* aff. *R. moderata*, *R.* aff. *R. elliptica*, *Daixina?* sp. and *Schubertella transitoria*. The youngest fusulinid-bearing sediments so far recognised in eastern Peary Land are characterised by a fauna including *Daixina* ex. gr. *navicullaeformis* of late Gzelian age.

Two conodont assemblages have been observed in the Foldedal Formation. The oldest, which is a monospecific assemblage of *Idiognathodus incurvus*, was found in limestones 5 m above the Kap Bunch Member at locality 3

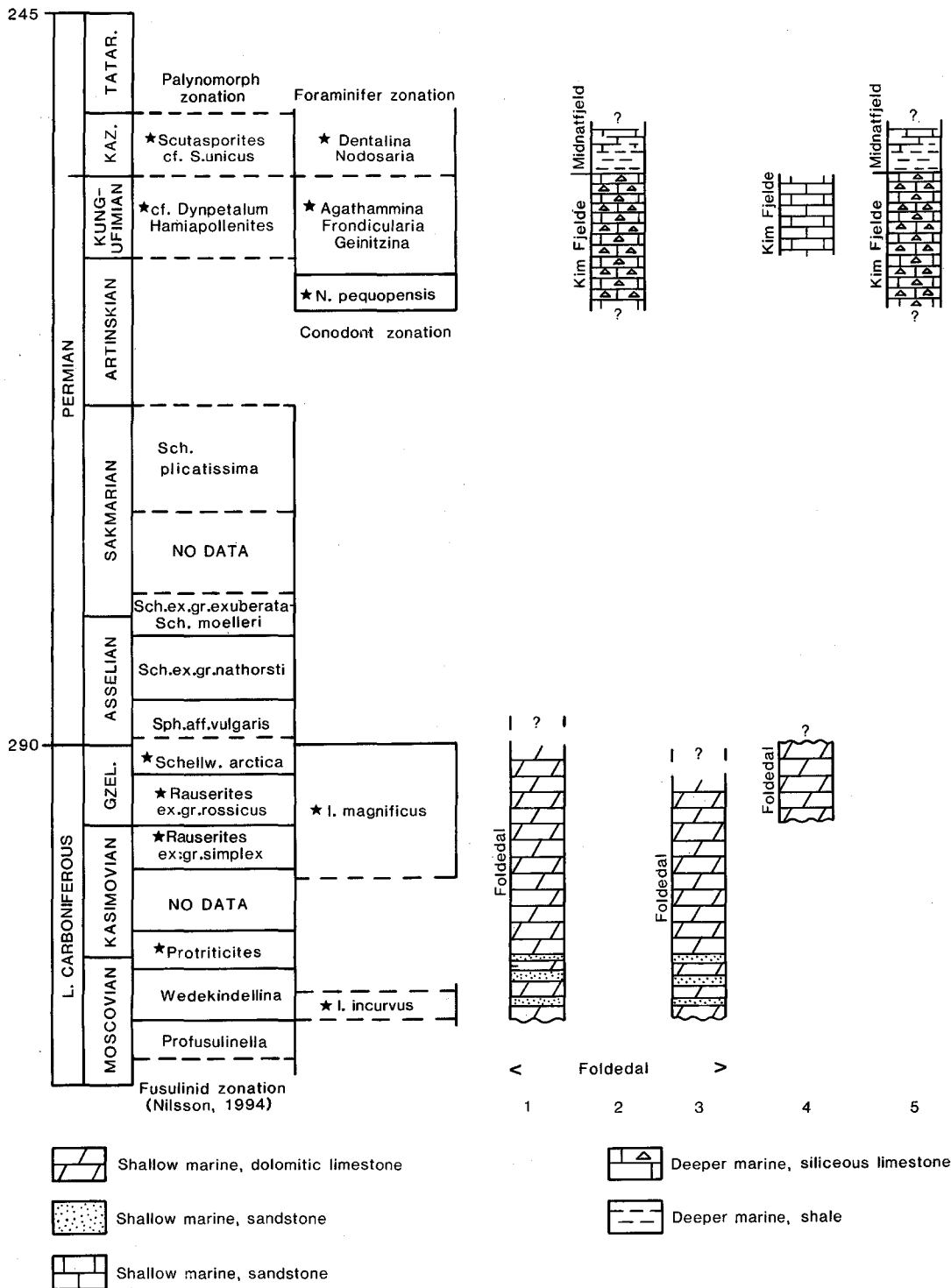


Fig. 2. Correlation of Upper Palaeozoic sediments in eastern Peary Land. Locations of sections 1 to 5 are given in Fig. 1.

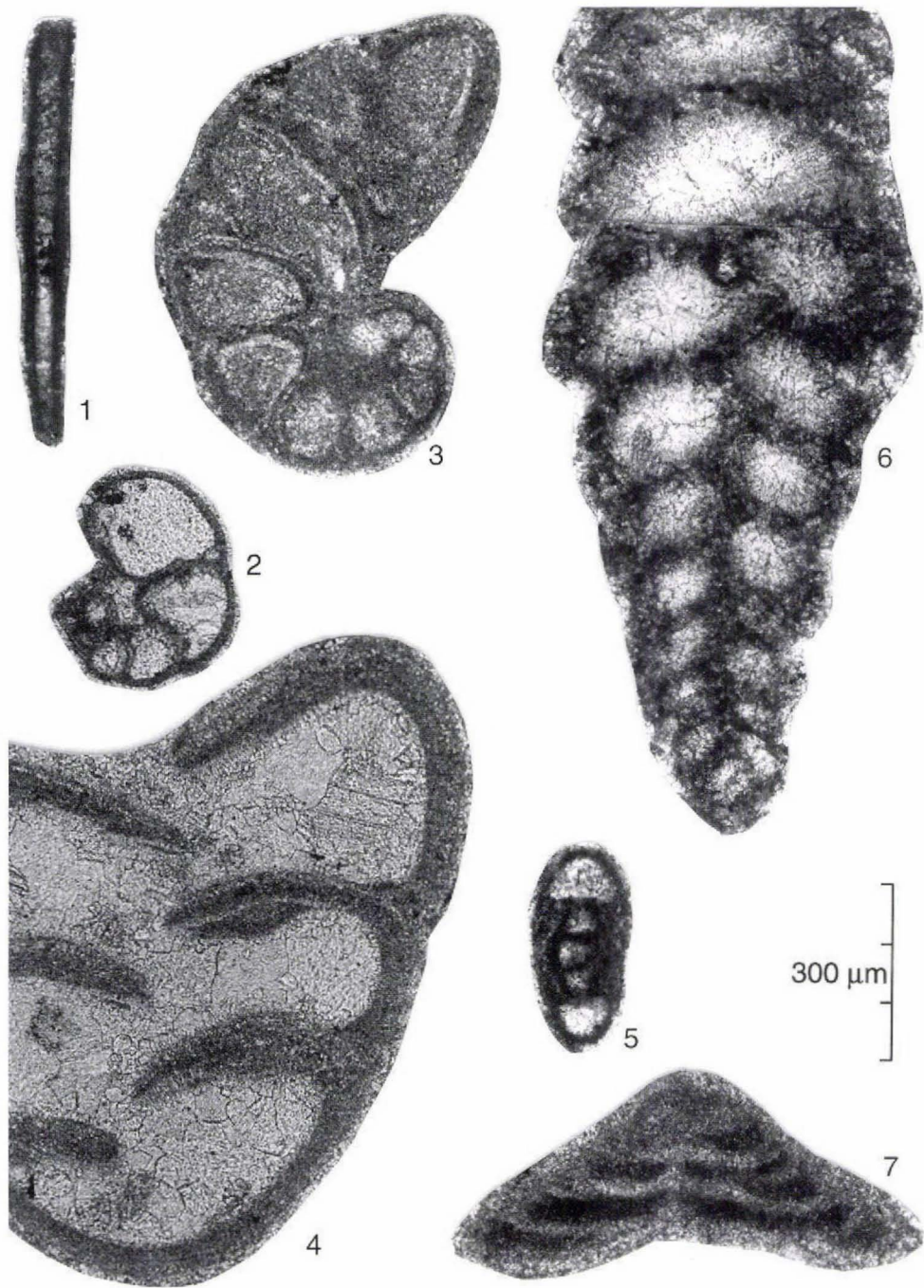


Fig. 3. Small foraminifera from the Kim Fjelde Formation. Fig. 3.1: *Earlandia* ex. group *elegans*. Longitudinal section. MGUH 23642 from GGU 334521A. Fig. 3.2: *Globivalvulina* sp. 1. Equatorial oblique section. MGUH 23643 from GGU 334647B. Fig. 3.3: *Globivalvulina* sp. 2. Equatorial section. MGUH 23644 from GGU 334513B. Fig. 3.4: *Globivalvulina* sp. 2. Para-axial section. MGUH 23645 from GGU 334513A. Fig. 3.5: *Neoendothyra*? sp. Para-axial section slightly oblique. MGUH 23646 from GGU 334521A. Fig. 3.6: *Deckerella*? sp. Longitudinal frontal section. MGUH 23647 from GGU 334521A. Fig. 3.7: *Tetrataxis* sp. Longitudinal oblique section. MGUH 23648 from GGU 334648A.

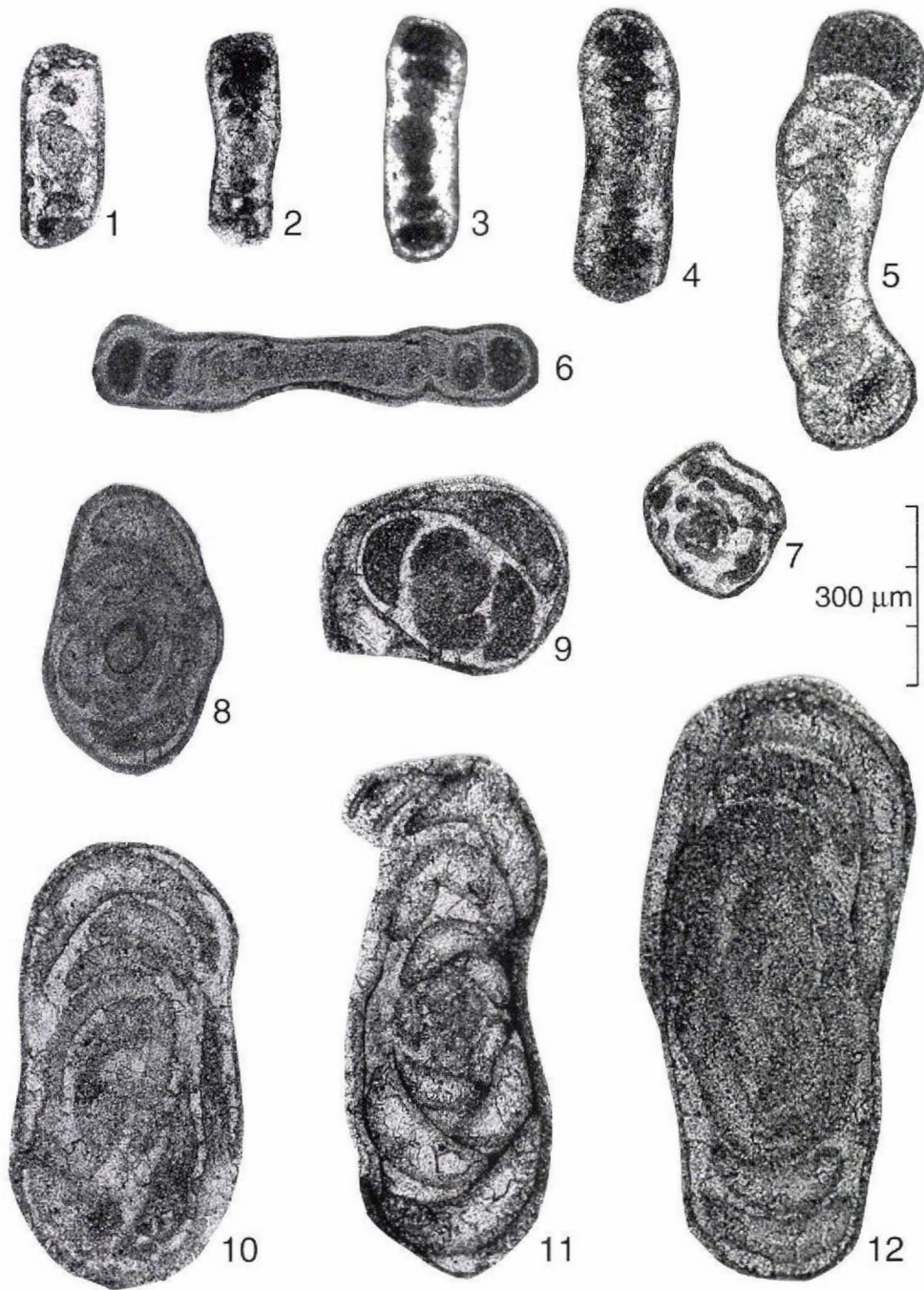


Fig. 4. Small foraminifera from the Kim Fjelde Formation. Figs 4.1–4.5: '*Neohemigordius*' aff. *saranensis* (Baryshnikov in Baryshnikov, Zolotova & Koscheleva, 1982). Fig. 4.1: Axial section. MGUH 23649 from GGU 334648B. Fig. 4.2: Para-axial section. MGUH 23650 from GGU 334648B. Fig. 4.3: Axial section. MGUH 23651 from GGU 334648A. Fig. 4.4: Para-axial section. MGUH 23652 from GGU 334648B. Fig. 4.5: Para-axial section. MGUH 23453 from GGU 334648B. Fig. 4.6: '*Cornuspira*' sp. Para-axial section. MGUH 23654 from GGU 334657. Fig. 4.7: '*Glomospira*' sp. MGUH 23655 from GGU 334646A. Figs 4.8–4.12: '*Agathammina*' *mandulaensis*? Xia & Zhang (1984). Fig. 4.8: Transversal oblique section. MGUH 23656 from GGU 334646. Fig. 4.9: Transversal section. MGUH 23657 from GGU 334646B. Fig. 4.10: Oblique longitudinal section. MGUH 23658 from GGU 334646B. Fig. 4.11: Oblique longitudinal section. MGUH 23659 from GGU 334646B. Fig. 4.12: Longitudinal para-axial section. MGUH 23660 from GGU 334646B.

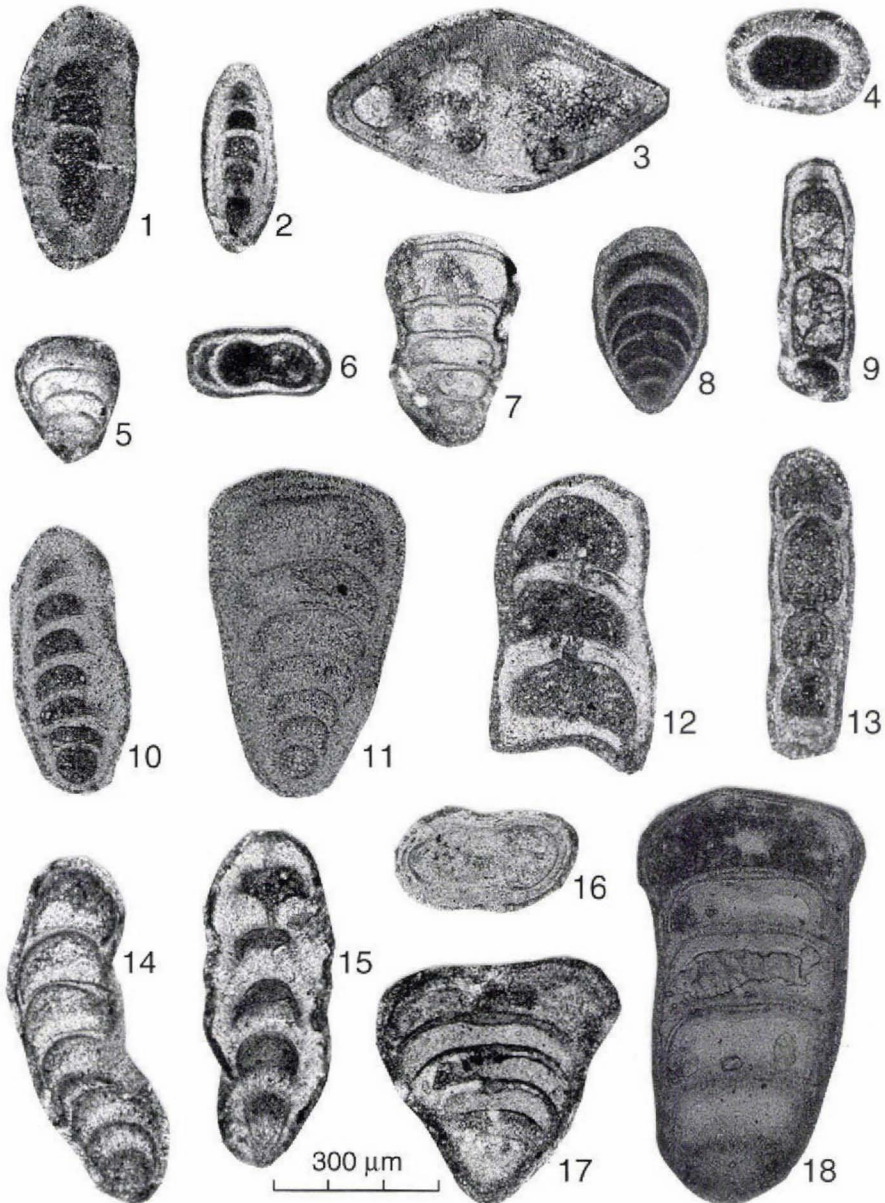


Fig. 5. Small foraminifera from the Kim Fjelde Formation. Figs 5.1–5.2: '*Langella*'? sp. Fig. 5.1: Oblique section. MGUH 23661 from GGU 334646B. Fig. 5.2: Oblique section. MGUH 23662 from GGU 334646A. Fig. 5.3: *Pachyphloia*? sp. Transversal section. MGUH 23663 from GGU 334657A. Fig. 5.4: Ornamented frondicularid. Transversal section. MGUH 23664 from GGU 334646B. Figs 5.5–5.7: '*Geinitzina*' sp. 1. Fig. 5.5: Frontal oblique section. MGUH 23665 from GGU 334513B. Fig. 5.6: Transversal section. MGUH 23666 from GGU 334646A. Fig. 5.7: Longitudinal frontal section. MGUH 23667 from GGU 334523B. Fig. 5.8: '*Fronicularia*' sp. 1. MGUH 23668 from GGU 334646. Fig. 5.9: *Tezaquina*? sp. Axial section. MGUH 23669 from GGU 334521A. Figs 5.10–5.11: '*Geinitzina*' sp. 2. Fig. 5.10: Longitudinal oblique section. MGUH 23670 from GGU 334646A. Fig. 5.11: Longitudinal oblique section. MGUH 23671 from GGU 334646B. Fig. 5.12: Undetermined Genus A. Longitudinal oblique section. MGUH 23672 from GGU 334646B. Fig. 5.13: '*Nodosaria*' sp. Longitudinal section. MGUH 23673 from GGU 334657B. Fig. 14. '*Lenticulina*' sp. Longitudinal section. MGUH 23674 from GGU 334646A. Fig. 15: '*Fronicularia*' sp. (cf. *Gerkeina* sp. nov. in Sosipatrova, 1967, pl. 12, fig. 33) MGUH 23675 from GGU 334523B. Fig. 16: '*Geinitzina*' sp. 3?. Transversal section. MGUH 23676 from GGU 334646B. Fig. 17: *Pachyphloia*? sp. Longitudinal frontal section. MGUH 23677 from GGU 334509A. Fig. 18: '*Geinitzina*' sp. 3 (cf. *Geinitzina gigantea* Miklukho-Maklai *sensu* Sosipatrova, 1967, pl. 12, fig. 40). Longitudinal frontal non-axial section. MGUH 23678 from GGU 334657.

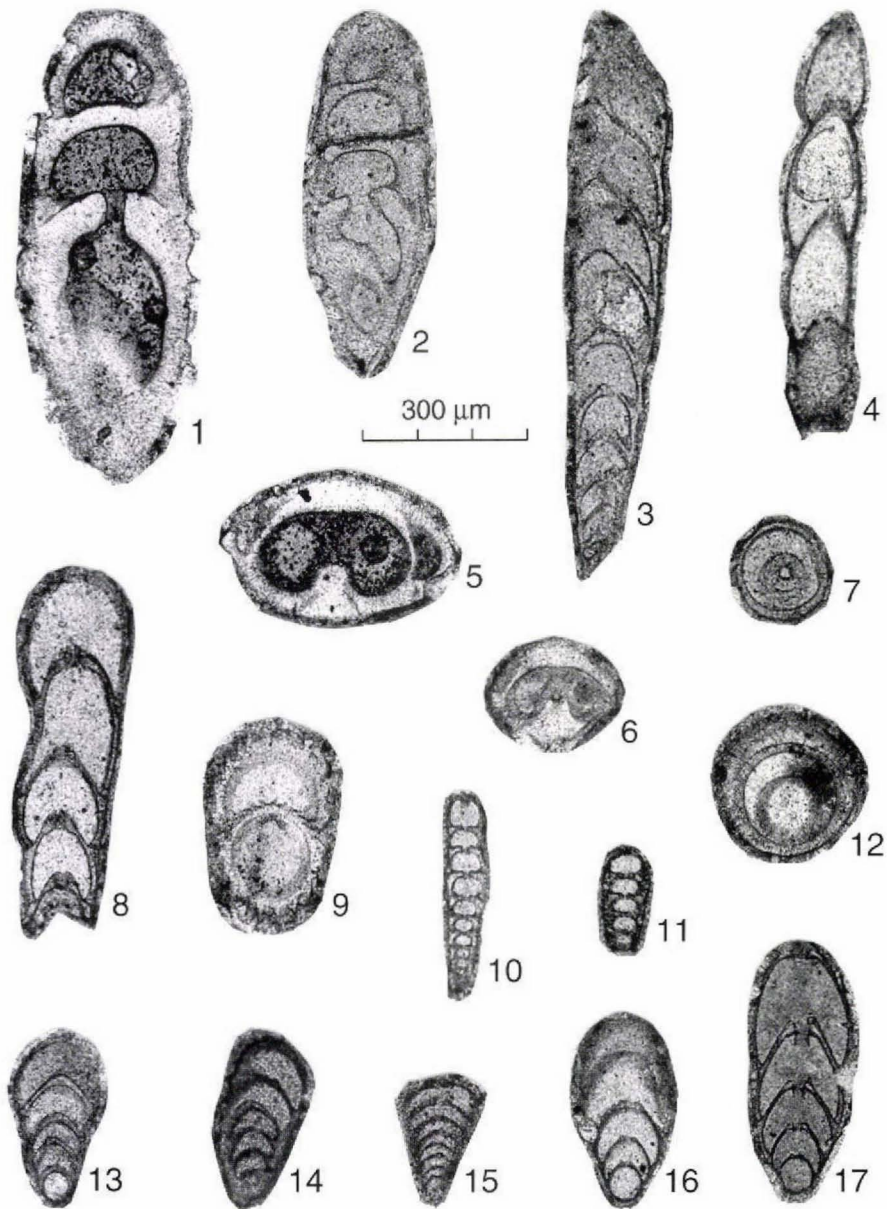


Fig. 6. Small foraminifera from the Midnatsfjeld Formation. Figs 6.1–6.2: Undetermined Genus B. Fig. 6.1: Oblique section. MGUH 23679 from GGU 334506A. Fig. 6.2: Oblique section. MGUH 23680 from GGU 334511B. Fig. 6.3: '*Fronidularia*' sp. 2. Para-frontal section? MGUH 23681 from GGU 334506A. Fig. 6.4: '*Dentalina*' *siliquaformis sensu* Sosipatrova (1967). Axial section. MGUH 23682 from GGU 334505A. Figs 6.5–6.6: '*Fronidularia*' sp. 2?. Fig. 6.5: Transversal section. MGUH 23683 from GGU 334506A. Fig. 6.6: Transversal section slightly oblique showing partly the opening. MGUH 23684 from GGU 334511A. Fig. 6.7: '*Dentalina*' *siliquaformis sensu* Sosipatrova (1967). Transversal section passing by the opening. MGUH 23685 from GGU 334506A. Fig. 6.8: '*Fronidularia*' sp. 2?. Lateral axial section? MGUH 23686 from GGU 334506B. Fig. 6.9: *Echinodosaria* sp. Transversal oblique section. MGUH 23687 from GGU 334511A. Figs 6.10–6.11: Nodosarid? sp. or lateral section of '*Fronidularia*' sp. 4. Fig. 6.10: Longitudinal section. MGUH 23688 from GGU 334511A. Fig. 6.11: Longitudinal section. MGUH 23689 from GGU 334505B. Fig. 6.12: '*Pseudonodosaria*'? sp. (= *Rectoglandulina* of most authors). Oblique section. MGUH 23690 from GGU 334506A. Figs 6.13–6.14: '*Fronidularia*' sp. 3. Fig. 6.13: Para-frontal section. MGUH 23691 from GGU 334506A. Fig. 6.14: Para-frontal section. MGUH 23692 from GGU 334506. Fig. 6.15: '*Fronidularia*' sp. 4. Frontal section. MGUH 23693 from GGU 334505B. Figs 6.16–6.17: '*Pseudonodosaria*' sp. (= *Rectoglandulina* of most authors). Axial section. MGUH 23694 from GGU 334511. Fig. 6.17: Axial section. MGUH 23695 from GGU 334511A.

(Fig. 1). The species characterises the Atokan (mid-Moscovian) of the southwestern United States (Dunn, 1966) and the 'Aegiranum Marine Band' (Westphalian C) of the Netherlands, Belgium and England (van den Boogaard & Bless, 1985).

A younger conodont assemblage comprising *Idiognathodus magnificus* and *Hindeodus minutus* was identified within the upper part of the Foldedal Formation near locality 4 (Fig. 1). *I. magnificus* has been reported from Missourian and Virgilian strata of the United States (Grayson *et al.*, 1990, with earlier references) and the Kasimovian and Gzelian of the Dneprovsko–Donetskaya depression (Kozitskaya, 1983; reported as *Idiognathodus lobulatus*, *I. toreticianus*, *I. saggitalis*, *Streptognathodus alekseevi*, *S. firmus* and *S. luganicus*). *H. minutus* is long-ranging and has been described from the Kasimovian (Baesemann, 1973) to the late Artinskian (Nakrem, 1991).

Permian

Conodonts. In the lower part of the Kim Fjelde Formation, as defined in this paper, a conodont assemblage occurs characterised by *Neostreptognathodus pequopenis* and *Ellisonia conflexa*. *N. pequopenis* is regarded as a late Artinskian index fossil in the Arctic region. It occurs in upper Artinskian strata of the Sverdrup Basin (Beauchamp *et al.*, 1989; Beauchamp & Henderson, 1994). *N. pequopenis* also occurs in the upper Artinskian, lower part of the Kapp Starostin Formation and upper part of the Hambergfjellet Formation in Svalbard (Nakrem, 1991; Nakrem *et al.*, 1992). In these areas it co-occurs with *S. jenkinsi*; this fusulinid has so far not been recorded from Greenland. *Ellisonia conflexa* is a long ranging species which disappears in the latest Artinskian.

Small foraminifera. Two different assemblages of small foraminifera have been identified in the Permian part of the succession (Figs 3, 4, 5, 6). The oldest assemblage is confined to the Kim Fjelde Formation, and contains '*Agathammina*' *mandulaensis*?, '*Cornuspira*' sp., *Deckerella*? sp., *Earlandia* ex.gr. *elegans*, '*Fron dicularia*' sp. 1, *Fron dicularia* sp., *Geinitzina* sp. 1, *Geinitzina* sp. 2, *Geinitzina* sp. 3, *Globivalvulina* sp. 1, *Globivalvulina* sp. 2, '*Glomospira*' sp., '*Langella*' sp., '*Lenticulina*' sp., *Neendothyra*? sp., '*Neohemigordius*' aff. *saranensis*, '*Nodosaria*' sp., '*Pachypholia*'? sp., *Tetrataxis* sp. and *Tezaquina* sp. This fauna resembles late Artinskian – Kungurian foraminifer assemblages described from the lower part of the Kapp Starostin Formation on Spitsbergen (Sosipatrova, 1967). '*Neohemigordius*' aff. *N. saranensis* was originally described from the Sarininian, uppermost Artinskian of the pre-Ural (Baryshnikov *et al.*, 1982). In Russia and the Sverdrup Basin of Arctic Canada, *Fron dicularia* has its

first appearance in the Artinskian together with forms like *Geinitzina* and *Pachypholia*. *Agathammina* has its acme in beds of Kungurian–Kazanian age (Pronina, 1990). It is restricted to post-Artinskian beds in the Sverdrup Basin while *Agathammina* ?*mandulaensis* occurs in proposed Artinskian–Kungurian strata in Mongolia (Xia & Zhang, 1984). Based on these comparisons it is suggested that the assemblage is of late Artinskian – Kungurian age (Fig. 2).

An assemblage dominated by '*Dentalina*' *siliquaformis*, *Echinodosaria* sp., '*Fron dicularia*' sp. 2, '*Fron dicularia*' sp. 3, '*Fron dicularia*' sp. 4, undetermined Genus B (Fig. 6.1), *Nodosarid*? sp. and '*Pseudonodosaria*' sp. occurs in the Midnatfjeld Formation. This assemblage resembles the fauna described from the late Kungurian–?Kazanian, middle and upper parts of the Kapp Starostin Formation on Spitsbergen (Sosipatrova, 1967) and the Kazanian Degerbøls and Trolld Fiord formations in the Sverdrup Basin. This points towards a late Kungurian to Kazanian age for this assemblage.

Palynomorphs. Two distinctive palynomorph assemblages are identified in the Permian succession (Figs 7, 8). In the basal part of the Kim Fjelde Formation on the southernmost fault block in Peary Land (section 4 in Fig. 2), the flora is dominated by terrestrial palynomorphs with rare acritachs. The flora contains both bisaccate pollen and spores but stratigraphically significant species are rare (Fig. 7). The presence of *Maculatasporites* sp. (cf. *Reticulina bilateralis*) and *Hamiapollenites* sp. in combination with the absence of any *Taeniaesporites*, *Lunatisporites*, *Scutasporites* and *Lueckisporites* and the absence of the *Unellium*–*Starostina* acritarch assemblage suggest that the flora has affinities to the *Dynpetalum* sp. – *Hamiapollenites bullaeformis* assemblage from the Finnmark Platform (Mangerud, 1994). This assemblage by comparison to the Sverdrup Basin is considered as Kungurian–Ufimian in age, and a similar age is suggested for the North Greenland flora.

In the Midnatfjeld Formation, the flora is dominated by acritachs such as *Unellium starostina*, *U. permica* and *Starostina reinodderis* (Fig. 8). The terrestrial sporomorphs comprise *Vittatina*, *Scutasporites* sp., *Krauselisporites* sp. and a variety of trilete spores. The Midnatfjeld Formation assemblage resembles the flora found in the lower part of the *Scutasporites* sp. cf. *S. unicus* – *Lunatisporites* sp. Concurrent Range Zone from the Finnmark Platform (Mangerud, 1994), the flora in the *Unellium* zone and the *Krauselisporites* sp. assemblage of Spitsbergen (Konieczny, 1987; Mangerud & Konieczny, 1993). The abundance of *Unellium* sp. and *Starostina* spp. and the occurrence of *Scutasporites* cf. *S. unicus* suggest a Kazanian age for this assemblage.

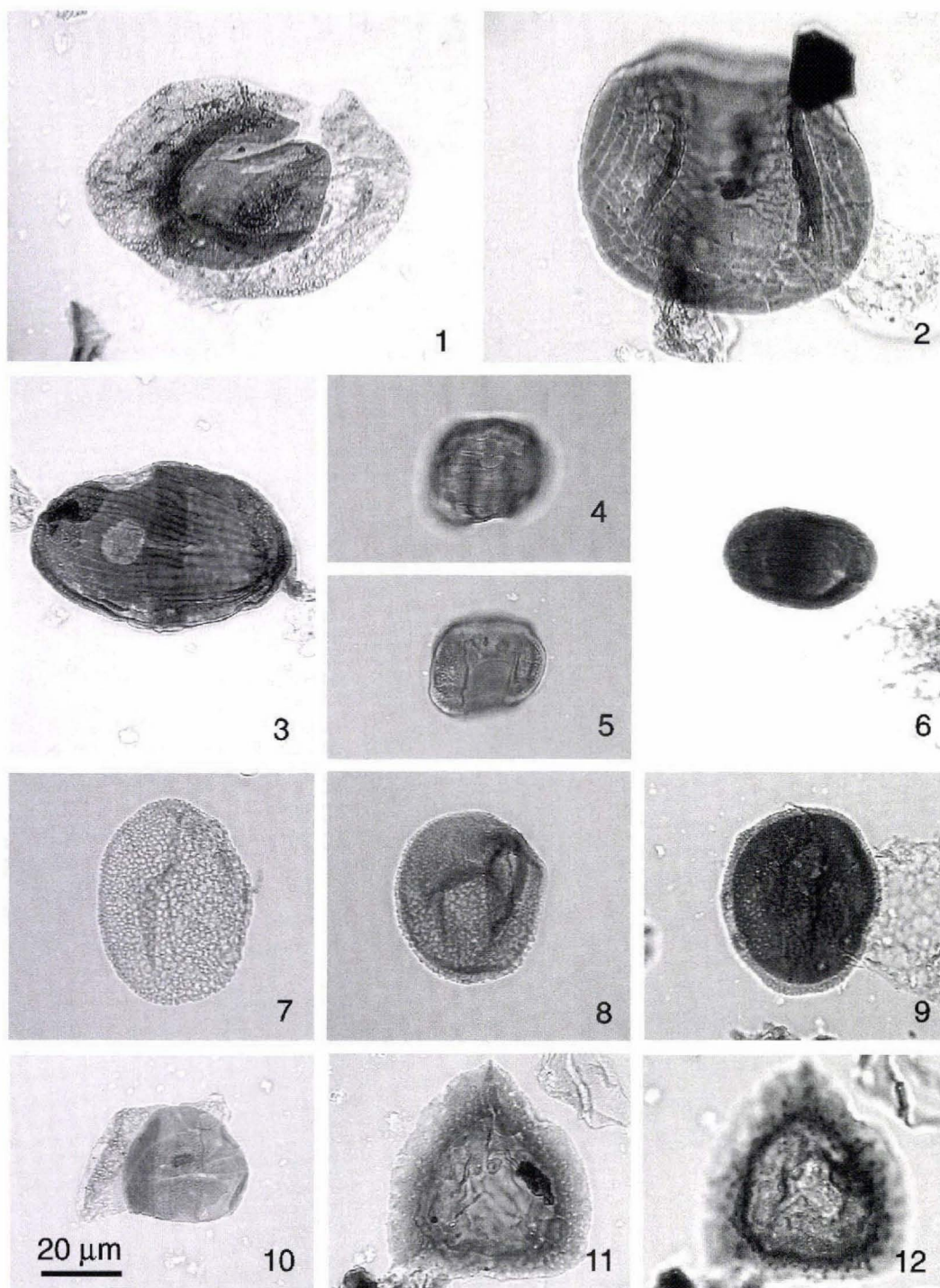


Fig. 7. Palynomorphs from the Kim Fjelde Formation. Fig. 7.1: *Potonieisporites* sp., MGUH 23696 from GGU 334600. Fig. 7.2: *Vittatina striata*, MGUH 23697 from GGU 334644. Fig. 7.3: *Vittatina costabilis*, MGUH 23698 from GGU 334603. Fig. 7.4 and 7.5: *Vittatina saccifer*, MGUH 23699–23700 from GGU 334603. Fig. 7.6: *Vittatina subsaccata*, MGUH 23701 from GGU 334603. Figs 7.7–7.9: *Maculatasporites* sp. (aff. '*Reticulina bilateralis*'), MGUH 23702–23704 from GGU 334600 and 334603. Fig. 7.10: *Hamiapollenites* sp., MGUH 23705 from GGU 334603. Figs 7.11–7.12: *Kraeuselisporites spinosus*, MGUH 23706–23707 from GGU 334 600. NB: Figs 7.1 and 7.2 are 1.3 times larger than figs 7.3–7.12 and the 20 micron bar.

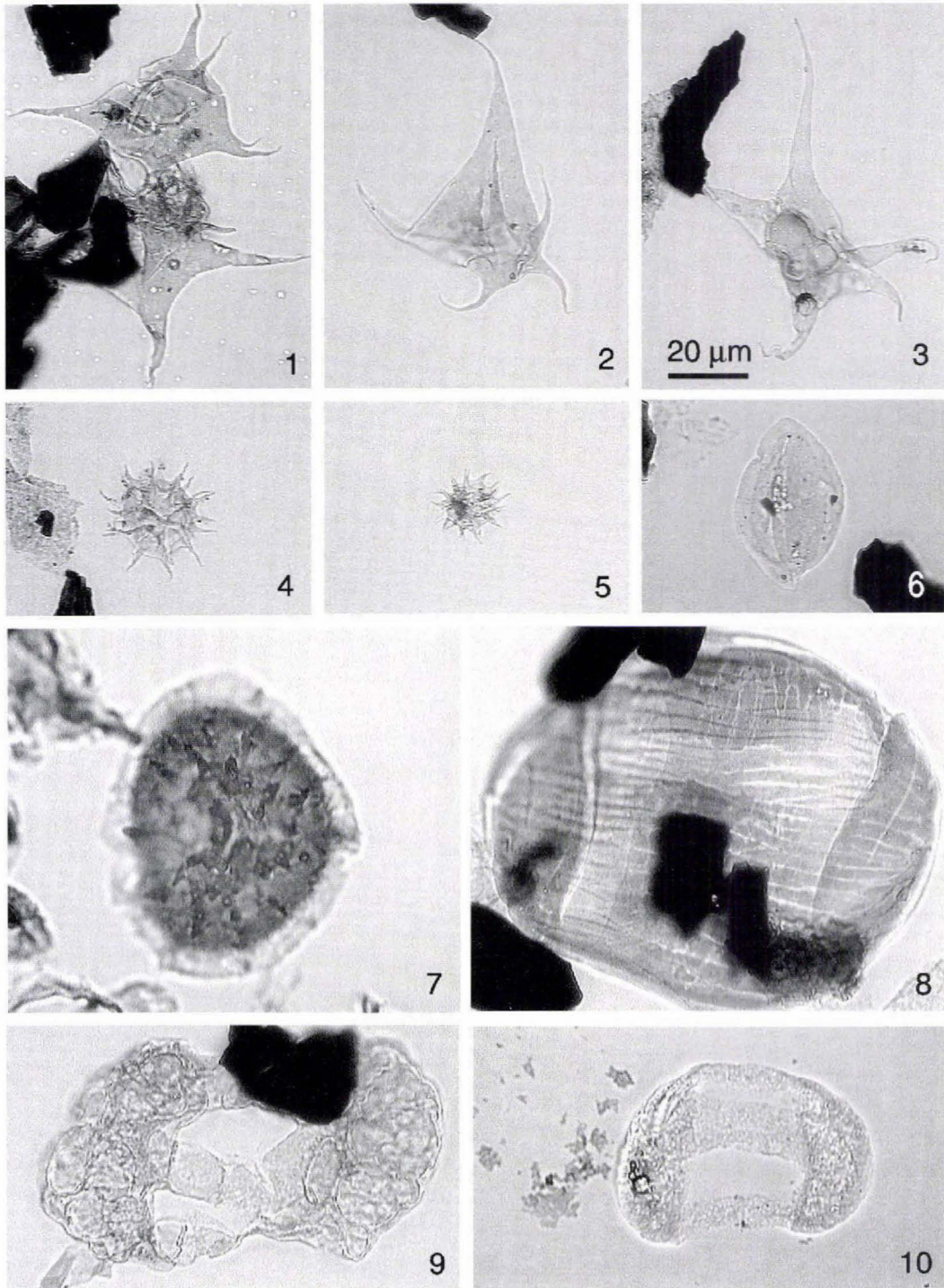
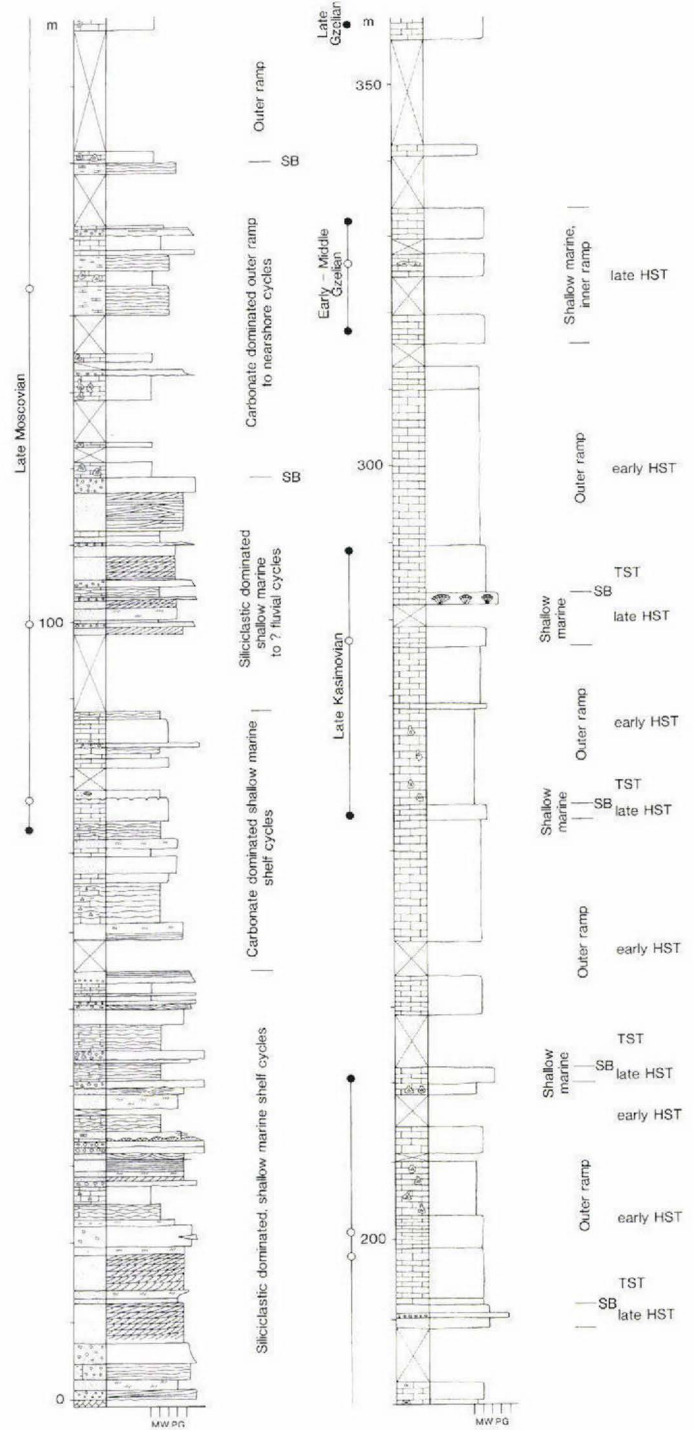


Fig. 8. Palynomorph from the Midnatsfjeld Formation. Fig. 8.1: *Unellium starostinum*, MGUH 23708 from GGU 361781. Fig. 8.2: *Unellium permicum*, MGUH 23709 from GGU361781. Fig. 8.3: *Unellium* sp. (aff. *Veryhachium crucitum*), MGUH 23710 from GGU 361781. Fig. 8.4: *Statostinum reinoddensis*, MGUH 23711 from GGU 361781. Fig. 8.5: *Michrystridium* sp., MGUH 23712 from GGU 361781. Fig. 8.6: *Preticolpipollenites* sp., MGUH 23713 from GGU 361725. Fig. 8.7: *Kraeuselisporites apiculatus*, MGUH 23714 from GGU 361781. Fig. 8.8: *Vittatina persecta*, MGUH 23715 from GGU 361725. Fig. 8.9: *Scutasporites* sp., MGUH 23716 from GGU 361781. Fig. 8.10: *Scutasporites* sp. cf. *S. unicus*, MGUH 23717 from GGU 361725.
 N.B.: Figs 8.7–8.10 are 1.3 times larger than Figs 8.1–8.6 and the 20 micron bar.

Fig. 9. Sedimentological log of the upper Moscovian to Gzelian Foldedal Formation in western Foldedal. Location 1 in Fig. 1.



Age. Based on the biostratigraphic evidence presented here, the Foldedal Formation is dated as late Moscovian–Gzelian. The Kim Fjeld Formation is regarded as being of late Artinskian to late Kungurian age and the Midnat-

fjeld Formation most likely is late Kungurian to Kazanian in age (Fig. 2).

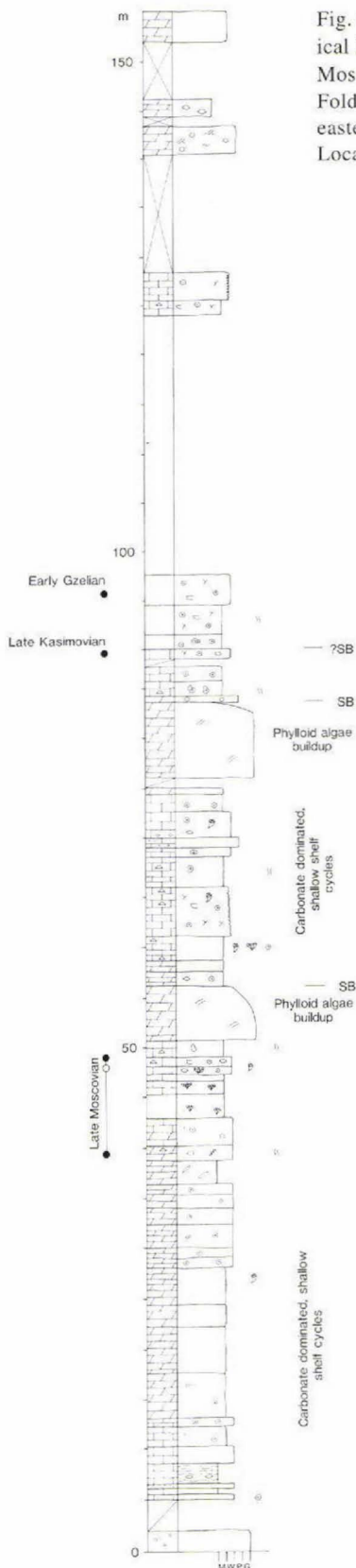


Fig. 10. Sedimentological log of the upper Moscovian to Gzelian Foldedal Formation in eastern Foldedal. Location 3 in Fig. 1.

Lithostratigraphy

To keep the lithostratigraphic scheme as simple as possible no new lithostratigraphic units have been erected, but when necessary, the lithostratigraphic units defined by Stemmerik & Håkansson (1989) have been redefined. In contrast to Håkansson (1979) and Stemmerik & Håkansson (1989) we prefer to include the Midnatfjeld Formation in the Mallemuk Mountain Group rather than, as originally proposed, the Trolle Land Group. This is due to the conformable relation between the Kim Fjelde and Midnatfjeld formations and the extensive occurrence of carbonates in the upper part of the Midnatfjeld Formation.

Foldedal Formation

History. This name was originally introduced by Håkansson (1979) for a succession of conglomerates and interbedded sandstones and carbonates which form the base of the Wandel Sea Basin succession around Foldedal in eastern Peary Land. Later, Stemmerik & Håkansson (1989) also included comparable sequences in Holm Land, Am-drup Land and the Lockwood Ø area in the formation. The formation is here defined also to include an Upper Carboniferous succession of shallow shelf carbonates previously assigned to the basal part of the Kim Fjelde Formation.

Type section. The new type section (Fig. 9) is situated on the north side of Foldedal (Locality 1 in Fig. 1) and corresponds to section A in figure 17 of Stemmerik & Håkansson (1989).

Thickness. Highly variable due to variations in the underlying basement relief and the transgressive nature of the formation. In eastern Peary Land the thickness of the formation ranges from less than 30 m in the south to more than 450 m in the Foldedal area in the north.

Lithology. The lower part of the formation consists of interbedded reddish weathering conglomerates, sandstones and biogenic limestones in Peary Land. The siliciclastic sediments become less common upwards, and the upper part of the formation is dominated by shallowing upward cycles of shallow to deeper subtidal carbonates locally with thin tabular carbonate build-ups (Fig. 10) (Stemmerik *et al.*, 1995a).

Boundaries. In eastern Peary Land the formation rests unconformably on a variety of rocks from the North Greenland fold belt (Håkansson, 1979). It is disconformably overlain by Permian sediments of the Kim Fjelde

Fig. 11. Transition between the Foldedal Formation and Kim Fjelde Formation in the southernmost part of the Wandel Sea Basin in eastern Peary Land. Location 5 in Fig. 1.



Formation in the southernmost fault block, and here the boundary between the two formations is placed above the uppermost reddish weathering, karstified carbonates (Fig. 11). The boundary is not exposed in Kim Fjelde proper and Foldedal.

Distribution. The formation has a limited distribution in eastern Peary Land around Clarence Wyckoff Bjerg and along Foldedal southwards to locality 4 in Fig. 1.

Age. The formation is of late Moscovian to Gzelian age based on fusulinids with some additional conodont data (Fig. 2). It possibly ranges into the Early Permian.

Kim Fjelde Formation

History. This name was originally given by Håkansson (1979) to a thick series of marine limestones of proposed Late Carboniferous to Early Permian age found in eastern Peary Land. Later, it was defined to include the Upper Marine Group of Grönwall (1916) in Holm Land and Amdrup Land (Stemmerik & Håkansson, 1989). The formation is here redefined to include a succession of chert-rich carbonates of late Artinskian to Kungurian age. The lower part of the formation, as originally defined, is now included in the underlying Foldedal Formation.

Type section. The new type section (Figs 12, 13) is located in northern Foldedal (Locality 2 in Fig. 1) and corresponds to the upper part of section A in figure 20 of Stemmerik & Håkansson (1989).

Thickness. The formation varies in thickness along the NW–SE striking Trolle Land Fault System, from less than 30 m in the southwestern Peary Land fault block to more than 380 m in the north.

Lithology. In northern Kim Fjelde, the formation is composed of well-bedded, chert-rich and biogenic limestones with a fauna dominated by resedimented brachiopods and trepostome bryozoans. Towards the south, these deeper water sediments pass into shallow water biogenic limestones also dominated by brachiopods and trepostome bryozoans, and with abundant *Zoophycos*. The formation contains minor siliciclastic intervals towards the south.

Boundaries. The lower boundary is a subaerial exposure surface and corresponds to the upper boundary of the Foldedal Formation. The upper boundary is a major flood surface and marks the transition to the dominantly siliciclastic lithologies of the Midnatfjeld Formation.

Age. Late Artinskian to Kungurian based on conodonts, small foraminifera and palynomorphs (Fig. 2). The lower boundary appears diachronous being oldest in the northern part of Kim Fjelde.

Midnatfjeld Formation

History. This formation was erected by Håkansson (1979) to include siliciclastic sediments of late Permian age in eastern Peary Land. Later fieldwork shows that the formation consists of two shallowing upward megacycles

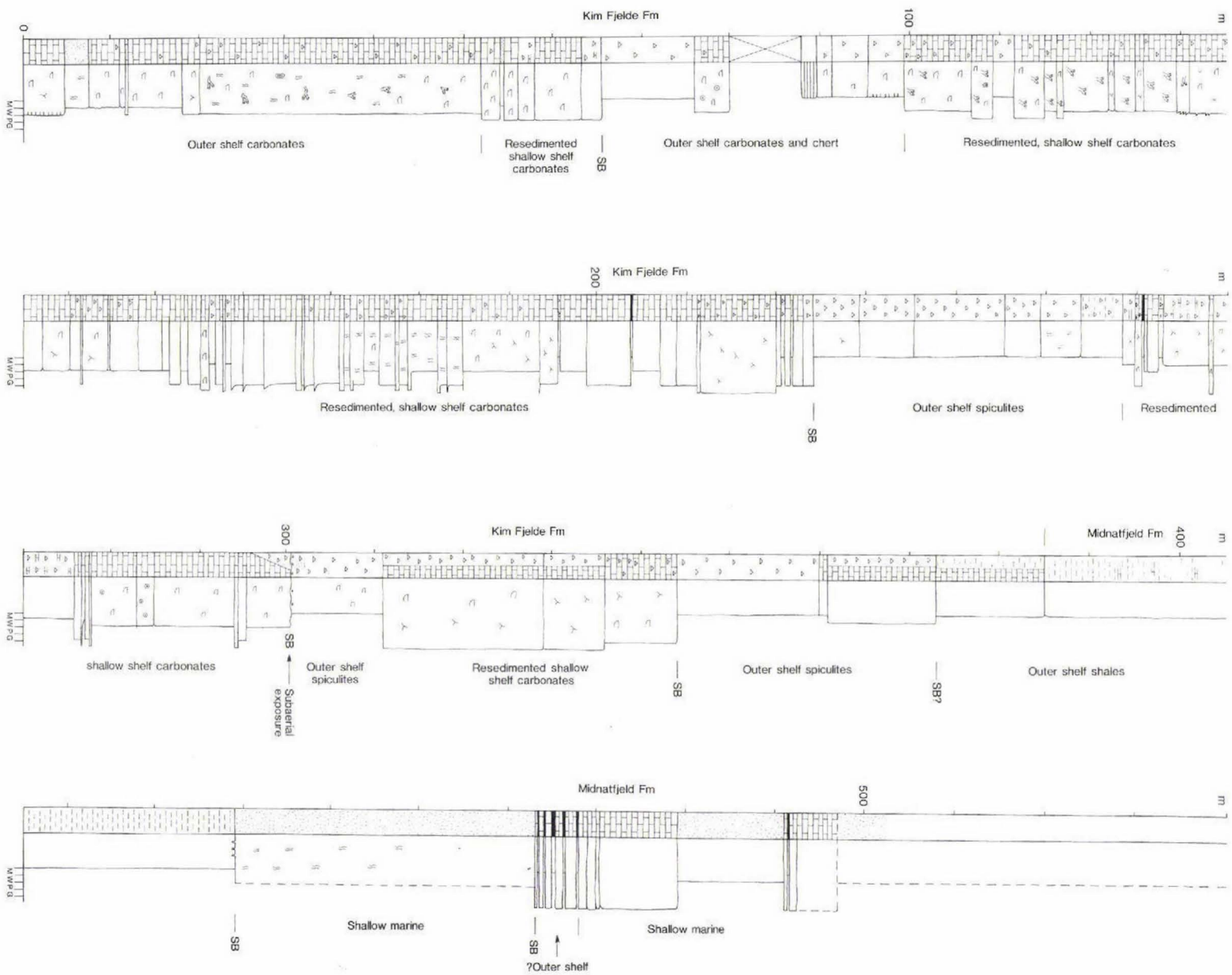
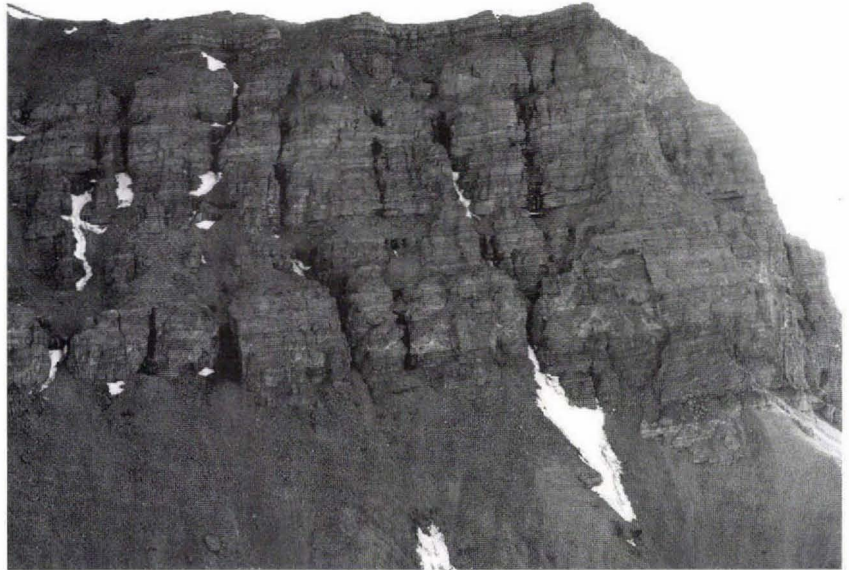


Fig. 12. Sedimentological log of the upper Artinskian to Kungurian Kim Fjelde Formation and the Kazanian Midnatfjeld Formation in northern Fuldal. Location 2 in Fig. 1.

Fig. 13. Kim Fjelde Formation in northern Foldedal. The sediments are dominated by resedimented brachiopod and bryozoan-rich limestones. Note internal disconformities.



dominated by shales and carbonates in eastern Kim Fjelde and shales and sandstones in northern Kim Fjelde. The abundance of carbonates in the upperpart of the formation, and the conformable relation to the underlying Kim Fjelde Formation led us to include this formation in the Mallebuk Mountain Group.

Type section. The new type section is in northern Foldedal (Fig. 12).

Thickness. The formation is more than 160 m thick in

northern Foldedal and more than 200 m thick in eastern Kim Fjelde (Fig. 12).

Lithology. The basal part of the formation is composed of laminated and bioturbated shales. These shales pass into a thick succession of bioturbated sandstone in northern Foldedal. In eastern Kim Fjelde the shales pass into bedded biogenic limestones.

Boundaries. The lower boundary is placed at the base of a thick shale unit (Figs 12, 14). It is a major flood surface.

Fig. 14. Bedded chert-rich carbonates of the Kim Fjelde Formation overlain by black laminated shales with slumped carbonates of the Midnatfjeld Formation. The cliff face in the background is composed of bedded limestones of the Midnatfjeld Formation.





Fig. 15. Karstified Silurian limestone overlain by Moscovian dolomitic limestones. Location 3, eastern Foldedal.

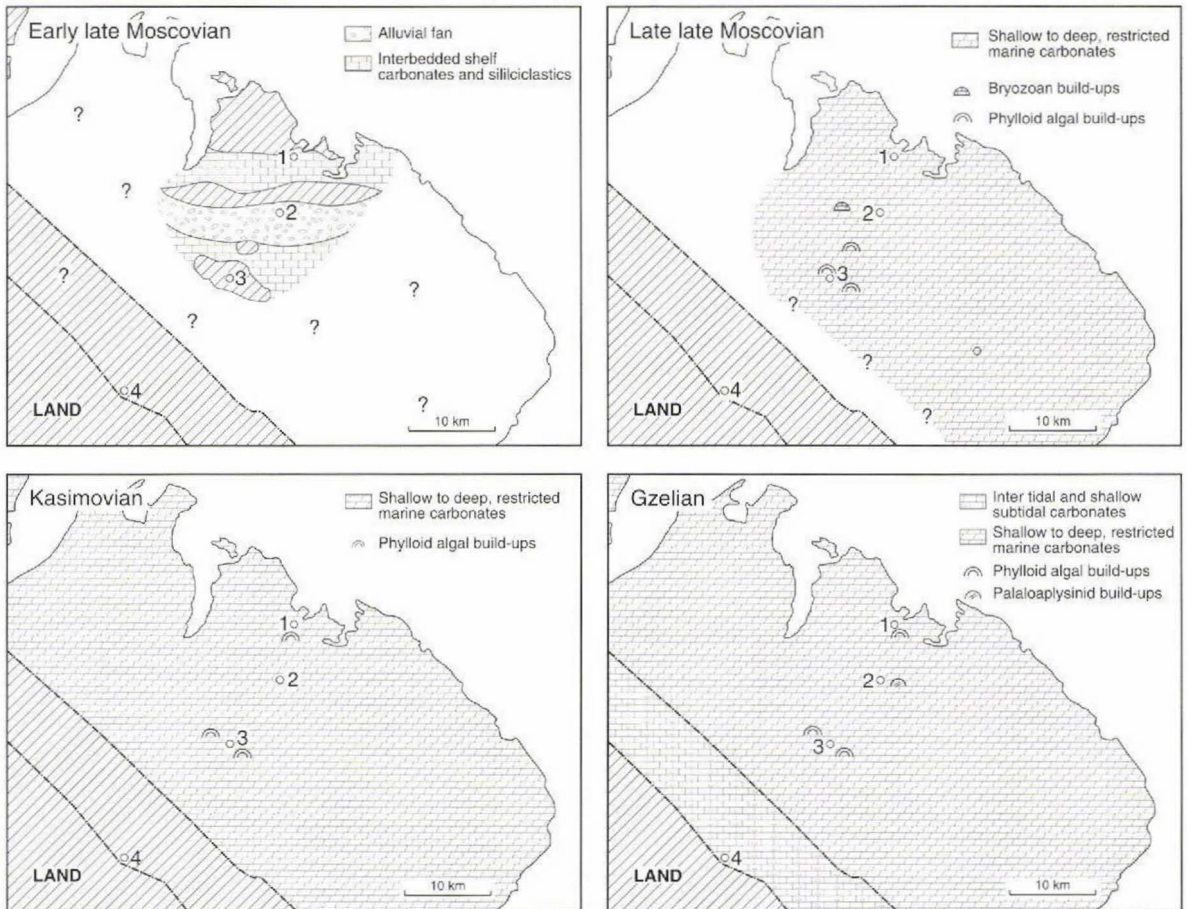


Fig. 16. Palaeogeographic reconstructions of the Foldedal Formation.

The upper boundary is defined by a low-angle unconformity. In northern Foldedal, the formation is overlain by the Triassic Parish Bjerg Formation and in eastern Kim Fjelde, the formation is overlain by the Parish Bjerg Formation or the Jurassic Ladegårdsåen Formation (Håkansson, 1979).

Age. The formation most likely is of late Kungurian to Kazanian age based on small foraminifera and palynomorphs (Fig. 2).

Depositional evolution

The sedimentary succession records a number of distinctive depositional phases within the Wandel Sea Basin. These depositional events are controlled by large scale tectonism and overall changes in relative sea level and climate, and they can be correlated with depositional events elsewhere in the Arctic region (e.g. Stemmerik & Worsley, 1995). During the Upper Palaeozoic, the Wandel Sea Basin shifted northwards as part of the Laurasian plate (Scotese & McKerrow, 1990). Deposition took place in a warm and semiarid climate during the Moscovian to Sakmarian. The fauna is dominated by foraminifera and algae, and fusulinids are common during this time interval. Evaporites are common locally in the Wandel Sea Basin, although very little evidence of evaporite sedimentation is found in eastern Peary Land. During late Artinskian time a marked change in climate occurred throughout the region. This, together with changing palaeohydrographic conditions, probably related to Proto-Atlantic rifting (cf. Stemmerik & Worsley, 1995) led to deposition in cold temperate water. The fauna is dominated by brachiopods and bryozoans. The continuous northwards migration in combination with an overall climatic cooling towards the end of the Permian (e.g. Beauchamp, 1994) led to even colder depositional conditions during the Kungurian–Kazanian where siliceous sponges became important.

Moscovian

In eastern Peary Land, Moscovian sediments rest directly on karstified Lower Palaeozoic limestones and Proterozoic sandstones (Fig. 15). The Moscovian sea thus transgressed a highly irregular topography with more than 100 m of relief in Foldedal, and the entire Foldedal area was not flooded until latest Moscovian – earliest Kasimovian time (Fig. 16). Moscovian deposits are not found on the southernmost fault block and apparently this block marked the southern limit of the depositional basin during the Moscovian (Fig. 16).

The upper Moscovian succession forms one large scale

transgressive unit of cyclic shelf deposits. It ranges in thickness from more than 220 m in the Foldedal-1 section situated in a palaeogeographic low to less than 90 m in the Foldedal-3 section measured on a palaeohigh (Figs 9, 10).

Early late Moscovian. During early late Moscovian time, siliciclastic material was shed from palaeotopographic highs in western Foldedal into adjacent lows, and thick piles of alluvial conglomerates and interbedded siliciclastics and carbonates were deposited (Figs 9, 16). In a ?fault-controlled subs basin in central Foldedal an approximately 100 m thick succession of up to 5 m thick layers of reddish weathering, matrix supported conglomerates forms the basal part of the Moscovian (Fig. 17). These alluvial conglomerates form one large, upward fining unit where individual beds become thinner and more fine-grained upwards. In the lower part of the succession there is evidence of subaerial exposure with karst related cementation.

Further to the north, in the Foldedal-1 section, the basal 20 m of the Moscovian succession is dominated by

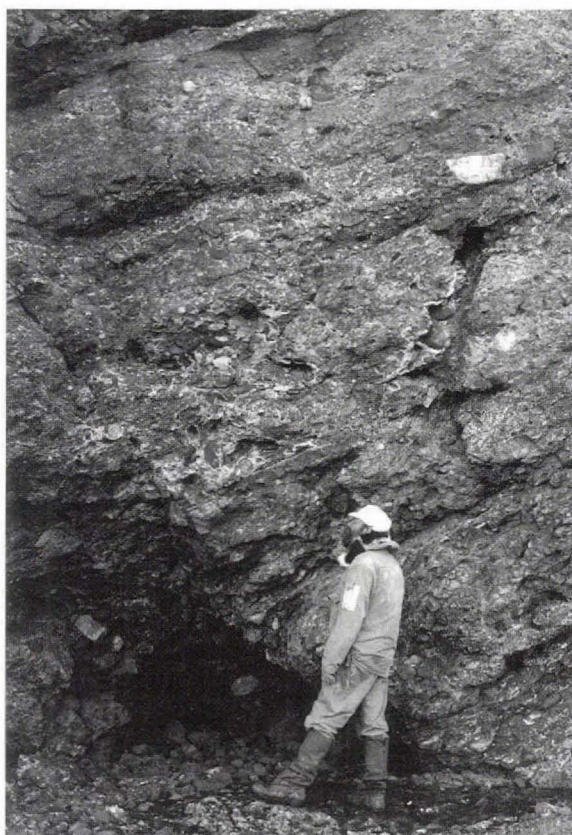


Fig. 17. Alluvial conglomerate with karst-related calcite cement. Lowermost part of Foldedal Formation, southwestern Foldedal.



Fig. 18. Cross-bedded sandstone, lower Foldedal Formation, western Foldedal.

interbedded marine conglomerates, planar cross-bedded medium- to coarse-grained sandstones and siltstones (Fig. 14). This siliciclastic unit passes up into a succession of stacked 1–8 m thick shallowing upward cycles of marine carbonates, cross-bedded sandstone and conglomerates (Figs 9, 18, 19). Deposition took place on a shallow shelf during high frequency fluctuations in sea level. The siliciclastic material was kept in the nearshore areas during sea level rises and fine-grained carbonates were deposited on the shelf. During sea level highstand and falling sea level, siliciclastic shoreline deposits

prograded across the shelf and in rare cases, the cycles are terminated by fluvial conglomerates.

Also in this area, the lowermost approximately 100 m of the upper Moscovian forms an overall transgressive unit. This is reflected in a gradual decrease in the proportion of siliciclastic material within individual cycles and by an upward deepening of the transgressive deposits at the base of individual cycles. Pure carbonate shelf cycles occur in the upper part (Fig. 14).



Fig. 19. Conglomerate overlain by marine limestone. Basal part of Foldedal Formation, western Foldedal.

Fig. 20. Bioturbated carbonate mudstone, Moscovian part of Foldedal Formation, western Foldedal.



Late late Moscovian. During the middle part of the late Moscovian there was a brief increase in siliciclastic supply in northern Foldedal and approximately 20 m of cyclic interbedded nearshore sandstones and fluvial conglomerates were deposited in the Foldedal-1 section (Fig. 14). The remaining part of the late Moscovian was dominated by cyclic shelf carbonates both in the palaeotopographic lows and on the newly transgressed palaeotopographic highs. At this time eastern Peary Land formed a broad carbonate ramp where facies distribution, to some degree, was still controlled by the pre-depositional relief

(Fig. 16). In the palaeogeographic lows, bioturbated carbonate mudstones and wackestones with chert-filled *Thalassinoides* burrows were deposited during sea level rise (Fig. 20). During sea level highstand and falling sea level foraminifera-dominated grainstones were deposited. These sediments contain a somewhat restricted fauna and were most likely deposited in slightly agitated restricted shelf environments. Above palaeogeographic highs, cyclic interbedded fusulinid-dominated grainstones and dolomitised mudstones with replaced gypsum crystals and nodules were deposited during initial flooding. Later



Fig. 21. *Palaeoaplysina* boundstone overlain by dolomitic mudstone. Upper Foldedal Formation, northern Foldedal.



Fig. 22. Crinoid dominated packstone. Gzelian part of Foldedal Formation, location 4 in Fig. 1.

in the late Moscovian, more open marine conditions were established over the highs, and the transgressive part of the cycles became dominated by open marine packstones with a fauna of crinoids, brachiopods and corals. The highstand deposits are usually completely dolomitised and primary textures can only rarely be identified. Occasionally, the highstand deposits are composed of tabular phylloid algae mounds or bryozoan mounds with abundant early marine cement.

Kasimovian

The Kasimovian succession ranges in thickness from 25–40 m above palaeotopographic highs to 85 m in the palaeotopographic lows. The greater part of the succession belongs to the late Kasimovian *Rauserites* ex.gr. *simplex* zone, and early Kasimovian sediments have only rarely been identified.

The Kasimovian succession is composed of 10–30 m thick upward shoaling cycles with a thick transgressive unit of bioturbated carbonate mudstone and wackestone



Fig. 23. Karstified upper part of the Foldedal Formation. Location 4 in Fig. 1.

Fig. 24. Karst breccia in the uppermost part of the Foldedal Formation. Location 4 in Fig. 1.



and a thin highstand unit composed of fusulinid-rich packstones (Fig. 14).

The cycles have a much longer duration than the underlying Moscovian cycles and deposition most likely took place on the outer part of a deep carbonate ramp (Fig. 16) (Stemmerik *et al.*, 1995a).

Gzelian

During Gzelian times the southwestern fault block in the Trolle Land Fault System also became flooded and a

broad carbonate shelf was established extending somewhat onto the stable craton. The Gzelian succession ranges in thickness from 30–50 m and in northern Foldedal it comprises thin shoaling upward cycles of bioturbated wackestones with chert-filled *Thalassinoides* burrows, biogenic packstones or phylloid algae build-ups. These cycles resemble the underlying Kasimovian cycles, although they are thinner, and most likely they were deposited in an outer ramp setting. Locally in northern Foldedal *Palaeoaplysina* build-ups occur (Fig. 21). In the newly transgressed areas to the south, the lower part



Fig. 25. Bryozoan dominated rudstone. Kim Fjelde Formation, northern Foldedal.



Fig. 26. Brachiopod dominated rudstone. Kim Fjelde Formation, southern Kim Fjelde.

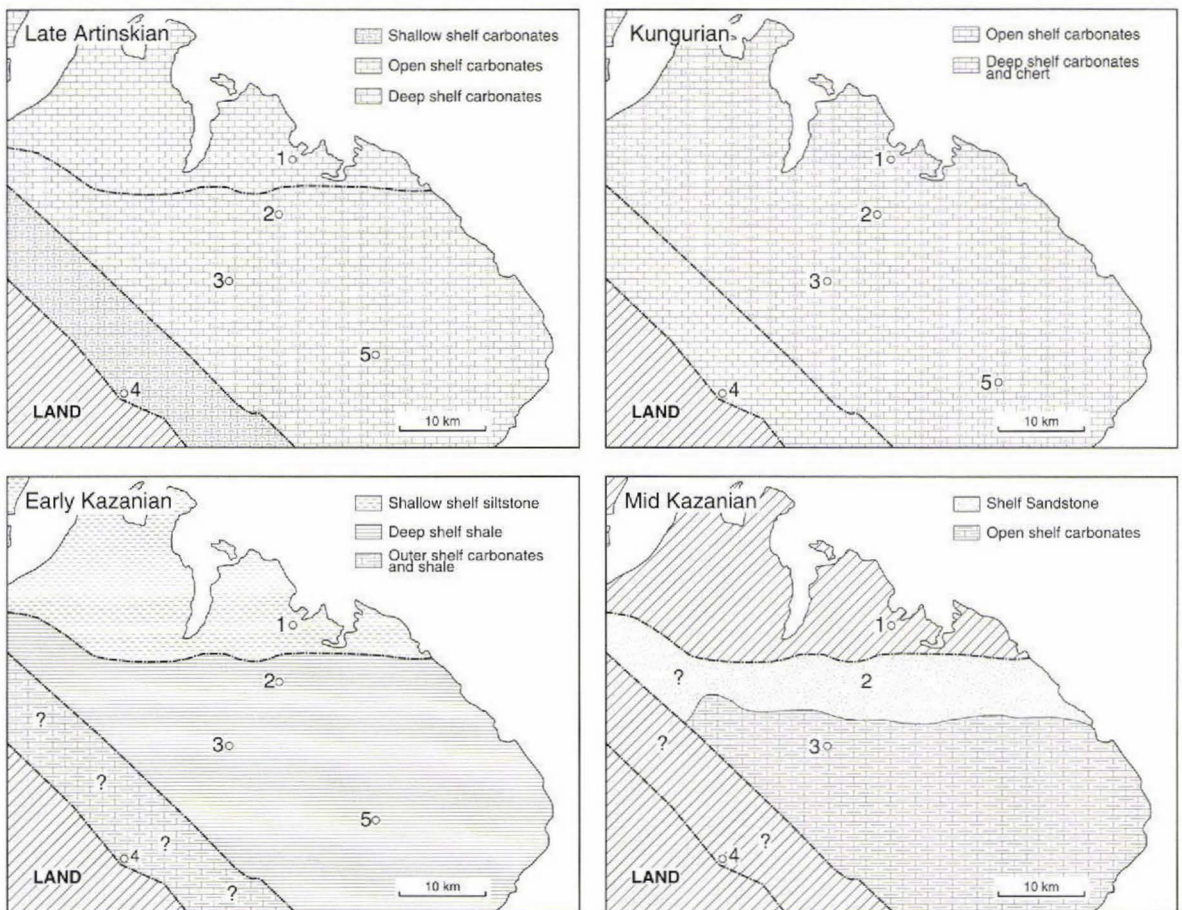


Fig. 27. Palaeogeographic reconstructions of the Kim Fjelde and Midnatfjeld formations.

of the Gzelian succession is composed of shallow marine, foraminifer-dominated grainstones, packstones and wackestones and sandstones (Fig. 22). The upper part of the succession is karstified and shows evidence of evaporite dissolution, and apparently more restricted marine conditions prevailed in the area during this time interval (Figs 16, 23, 24).

Late Artinskian – Kungurian

During late Artinskian time eastern Peary Land became flooded again for the first time since the end of the Gzelian. The transition between the Gzelian and late Artinskian sediments is not exposed in the Foldedal area. In the southern part of Kim Fjelde (Locality 4 in Fig. 1), the late Artinskian sea transgressed over a relatively flat karstified surface (Fig. 11).

During late Artinskian, *N. pequopensis* zone time, only the northern part of the area was flooded. There the succession consists of well-bedded carbonate gravity flows with a fauna of brachiopods and large trepostome bryozoan (Figs 13, 25, 26). The sediments form small, 5–10 m fining upward packages where individual beds become thinner and more fine-grained upwards. These units are often separated by disconformities, and occasionally low relief erosional scoups occur. The sediments in northern Foldedal are most likely turbidites derived from a northern carbonate platform (Fig. 27). Judging from the fauna, the source area was a relatively shallow, well-agitated shelf.

In latest Artinskian time the southwestern fault block in the Trolle Land Fault System became flooded and also

this flooding event reached the stable craton. The basal transgressive deposits contain reworked caliche nodules and other clasts of the underlying carbonates (Fig. 28). The overlying sedimentary succession consists of shallow marine carbonate with a fauna dominated by brachiopods and bryozoans, and shallow marine bioturbated sandstones. The sediments resemble the Kim Fjelde Formation on Amdrup Land (Stemmerik & Håkansson, 1989) and apparently a broad carbonate platform was established along the northern and northeastern margins of the Greenland craton at this time.

In the southern part of the basin, shallow carbonate platform deposition continued into the Kungurian. In northern Peary Land, the sedimentary basin became gradually deeper and during the later parts of the Kungurian, deep water spiculitic chert and shale were deposited over most of eastern Peary Land (Fig. 27).

Kazanian

The base of the Kazanian is marked by a major flooding event. Deep water conditions prevailed throughout eastern Peary Land, possibly with the exception of the southernmost fault block and an isolated area to the north (Fig. 27). In southern Kim Fjelde, the deepening is associated with tectonically induced slumped carbonate beds (Fig. 14). The Kazanian is composed of two large scale shallowing upwards successions, each more than 100 m thick. Following initial flooding and deposition of bioturbated and laminated shales, shallow water carbonates started to prograde from the southwestern basin margin into the basin and a thick succession of shallow water,



Fig. 28. Biogenic packstone with reworked caliche nodules, lowermost Kim Fjelde Formation. Location 4 in Fig. 1.



Fig. 29. Bryozoan packstone in the limestone dominated part of the Midnatfjeld Formation. Hammer head for scale, southern Kim Fjelde.

bryozoan and brachiopod dominated carbonates was deposited in southern and eastern Kim Fjelde (Fig. 29). In northern Foldedal a thick succession of bioturbated shelf sandstones was deposited during this time interval. The source for these sandstones was most likely an uplifted area to the northeast (Fig. 27).

During later Kazanian time a new deepening event took place and deeper water shale sedimentation was re-established throughout the area. The final shallowing of the eastern Peary Land part of the basin is marked by renewed progradation of shallow marine carbonates, this time both from the south and the north.

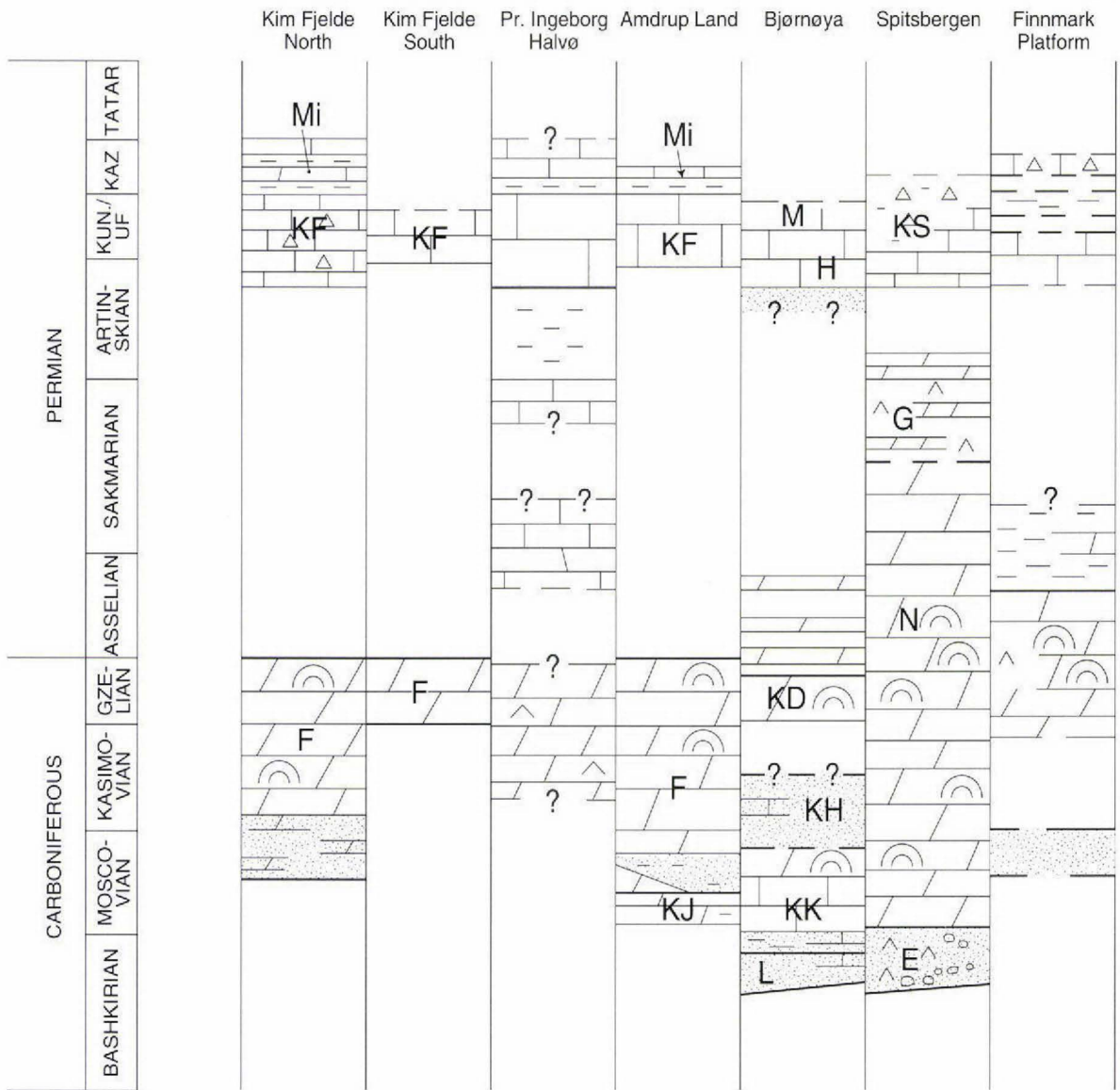
Comparison to adjacent areas

The marine mid-Carboniferous to Late Permian succession in eastern Peary Land is among the stratigraphically most complete in the Wandel Sea Basin (Fig. 30). The mid-Carboniferous transgression reached Foldedal in northeastern Peary Land in late Moscovian time, slightly later than it reached southern Holm Land and southern Amdrup Land where the basal part of the marine succession is dated as late early Moscovian (Dunbar *et al.*, 1962; Stemmerik & Håkansson, 1989; Nilsson, 1994). The late Moscovian transgression in eastern Peary Land corresponds in time to the transgression of northern Holm Land and northern Amdrup Land and apparently the Finnmark Platform was also transgressed at this time (Fig. 30; Bugge *et al.*, 1995). Elsewhere in the western Barents Sea, the initial mid-Carboniferous transgression took place during the late Bashkirian, and on Svalbard

thick syn-rift successions were deposited prior to the flooding of North Greenland (Fig. 30; Steel & Worsley, 1984; Stemmerik & Worsley, 1989; Johannessen & Steel, 1992).

The overall Moscovian to Gzelian facies development recognised in eastern Peary Land compares with that described from elsewhere in the Wandel Sea Basin and on Spitsbergen and Bjørnøya, although the Moscovian succession in North Greenland is much thicker than the time equivalent successions on Spitsbergen and Bjørnøya (Stemmerik & Worsley, 1989). In all these areas cyclic shelf deposits were deposited during the late Carboniferous. Throughout the region, the supply of siliciclastic material decreased during the Moscovian, and the Kasimovian and Gzelian successions are dominated by restricted marine carbonate cycles with localised *Palaeoaplysina*-phylloid algae build-ups (Stemmerik *et al.*, 1994, 1995a; Stemmerik & Elvebakk, 1994; I. Nilsson, unpublished data).

The early Permian hiatus separating the Foldedal and Kim Fjelde formations in eastern Peary Land also occurs elsewhere in the Wandel Sea Basin (Fig. 30). In eastern Peary Land as well as on Holm Land and Amdrup Land, the hiatus spans the Asselian to mid-Artinskian (Fig. 30). Late Sakmarian deposits have been recognised on Prinsesse Ingeborg Halvø and a local Sakmarian to ?early Artinskian subbasin apparently existed in that area (Håkansson *et al.*, 1989; Nilsson *et al.*, 1991). On Bjørnøya the early Permian hiatus spans the Asselian to mid-Artinskian with the exception of a brief marine incursion during the mid- to late Asselian (Fig. 30). On Spitsbergen



E : Ebbadalen Fm.
 F : Foldedal Fm.
 G : Gipsdalen Fm.
 H : Hambergfjellet Fm.
 L : Landnordingsvika Fm.

M : Miseryfjellet Fm.
 N : Nordenskiöldbreen Fm.
 KD : Kapp Duner Fm.
 KF : Kim Fjælde Fm.
 KH : Kapp Hanna Fm.

KJ : Kap Jungersen Fm.
 KK : Kapp Kåre Fm.
 KS : Kapp Starostin Fm.
 Mi : Midnatfjeld Fm.

Fig. 30. Correlation of Upper Palaeozoic successions in North Greenland and the Barents Sea area.

and on the Finnmark Platform, sedimentation continued in the Asselian and Sakmarian, and a much shorter late Sakmarian to mid-Artinskian break in sedimentation is present.

The late Artinskian transgression falls within the

N. pequopenis conodont zone and the *Schwagerina jenkinsi* fusulinid zone throughout the region (Nakrem *et al.*, 1992; Bugge *et al.*, 1995). In most areas, shallow marine limestones similar to those described from the southern part of Peary Land were deposited. The succes-

sion in northern Kim Fjelde is comparable to sediments deposited in deep basins, like the Nordkapp Basin in the Barents Sea (Stemmerik & Worsley, 1995). The gradual deepening in the Kim Fjelde area during the late Artinskian and Kungurian has also been recognised on Spitsbergen and elsewhere in the Barents Sea (Stemmerik & Worsley, 1989, 1995).

The earliest Kazanian flooding event that separates the Kim Fjelde Formation from the Midnatfjeld Formation in eastern Peary Land has also been recognised on Amdrup Land (Stemmerik *et al.*, 1995b) and on Prinsesse Ingeborg Halvø (Fig. 30). In the Barents Sea, the Kungurian–Kazanian transition is also marked by a major flooding event and large scale shoaling upwards cycles like those seen in eastern Peary Land occur (e.g. Stemmerik & Larssen, 1992).

Summary and conclusions

The Upper Palaeozoic succession in eastern Peary Land is divided into the upper Moscovian to Gzelian Foldedal Formation, the upper Artinskian to Kungurian Kim Fjelde Formation and the upper Kungurian to Kazanian Midnatfjeld Formation. Ages are based on fusulinids in the Foldedal Formation and on a combination of conodonts, small foraminifera and palynomorphs in the Kim Fjelde and Midnatfjeld formations. The succession rests unconformably on Silurian and older rocks. The Foldedal Formation and Kim Fjelde Formation are separated by a major hiatus while the boundary between the Kim Fjelde Formation and the Midnatfjeld Formation is a major, most likely tectonically controlled flood surface.

The large scale depositional pattern seen in eastern Peary Land fits the patterns seen elsewhere in the Arctic region:

The large scale transgressive-regressive pattern seen in the Foldedal Formation is also recognised in Amdrup Land and Holm Land in eastern North Greenland, on Bjørnøya and in the Sverdrup Basin of Arctic Canada.

The early Permian, Asselian to mid-Artinskian hiatus in eastern Peary Land corresponds to a hiatus on Holm Land and Amdrup Land in eastern North Greenland and on Bjørnøya. Elsewhere in the Arctic region, Asselian and Sakmarian deposits are widespread, and apparently the hiatus in eastern Peary Land is related to tectonic inversion of this area. Time equivalent tectonic inversion is also seen in Amdrup Land and Holm Land and on Bjørnøya.

The late Artinskian transgression at the base of the Kim Fjelde Formation corresponds to a major transgres-

sion throughout the Arctic region. This event is related to major tilting in the Sverdrup Basin and in the western Barents Sea (Beauchamp, 1993; Johansen *et al.*, 1994), and judging from the facies patterns this transgression is also related to tectonic tilting in eastern Peary Land.

The early Kazanian flooding event at the base of the Midnatfjeld Formation is associated with major slumping and is most likely associated with renewed tectonism in the area. The Kazanian succession is composed of two large scale transgressive-regressive units. Similar large scale transgressive-regressive units occur in the Barents Sea.

References

- Baesemann, J. F. 1973: Missourian (Upper Pennsylvanian) conodonts of northeastern Kansas. *J. Paleontology* **47**, 689–710.
- Baryshnikov, V. V., Zolotova, V. P. & Koscheleva, V. F. 1982: [New species of foraminifers from the Artinskian stage of the Pre-Ural of Perm.] *Akademiia Nauk SSSR, Ural'ski Nauchnii Tsentr. Institut Geologii i Geokhimii, Sverdlovsk, Nauchnye Doklady*, 3–54. (In Russian.)
- Beauchamp, B. 1993: Carboniferous and Permian reefs of the Sverdrup Basin, Canadian Arctic: an aid to Barents Sea exploration. In Vorren, T. O., Bergsager, E., Dahl-Stamnes, Ø. A., Holter, E., Johansen, B., Lie, E. & Lund, T. B. (ed.) *Arctic Geology and Petroleum Potential. Norwegian Petrol. Soc. Spec. Publ.* **2**, 217–241.
- Beauchamp, B. 1994: Permian climatic cooling in the Canadian Arctic. In Klein, G. D. (ed.) *Pangea: paleoclimate, tectonics and sedimentology during accretion, zenith and breakup of a supercontinent. Geol. Soc. Amer. Spec. Pap.* **228**, 229–245.
- Beauchamp, B. & Henderson, C. M. 1994: The Lower Permian Raanes, Great Bear Cape and Trappers Cove formations, Sverdrup Basin, Canadian Arctic: stratigraphy and conodont zonation. *Bull. geol. Surv. Canada*, **42**, 562–597.
- Beauchamp, B., Harrison, J. C. & Henderson, C. M. 1989: Upper Paleozoic stratigraphy and basin analysis of the Sverdrup Basin, Canadian Arctic Archipelago: Part 2, Transgressive-regressive sequences. *Pap. geol. Surv. Canada* **89-1G**, 105–113.
- van den Boogaard, M. & Bless, M. J. M. 1985: Some conodont faunas from Aegiranum marine band. *Pal. Proceed. Ser.* **B 8**, 133–154.
- Bugge, T., Mangerud, G., Elvebakk, G., Mørk, A., Nilsson, I., Fanavoll, S. & Vigran, J. O. 1995: The Upper Palaeozoic succession on the Finnmark Platform, Barents Sea. *Norsk geol. Tidsskr.* **75**, 3–30.
- Dunbar, C. P., Troelsen, J., Ross, C., Ross, J. P. & Norford, B. 1962: Faunas and correlation of the Late Paleozoic rocks of northeast Greenland. *Meddr Grønland* **167**(4), 16 pp.
- Dunn, D. L. 1966: New pennsylvanian conodonts from southwestern United States. *J. Paleontology* **40**, 1294–1303.
- Grayson, R. C., Merrill, G. K. & Lambert, L. L. 1990: Carboniferous gnathodontid conodont apparatuses: evidence of a dual origin for Pennsylvanian taxa. *Courier Forschungsinstitut Senckenberg* **118**, 353–396.

- Grönwall, K. G. 1916: The marine Carboniferous of North-East Greenland and its brachiopod fauna. *Meddr Grønland* **43** (20), 110 pp.
- Håkansson, E. 1979: Carboniferous to Tertiary development of the Wandel Sea Basin, eastern North Greenland. *Rapp. Grønlands geol. Unders.* **85**, 11–15.
- Håkansson, E. & Stemmerik, L. 1984: Wandel Sea Basin – the North Greenland equivalent to Svalbard and the Barents Shelf. In Spencer, A. M. *et al.* (ed.) *Petroleum geology of the North European margin*, 97–107, London: Graham & Trotman (for Norwegian Petroleum Society).
- Håkansson, E., Madsen, L. & Pedersen, S. A. S. 1989: Geological investigations of Prinsesse Ingeborg Halvø, eastern North Greenland. *Rapp. Grønlands geol. Unders.* **145**, 113–118.
- Johannessen, E. P. & Steel, R. J. 1992: Mid-Carboniferous extension and rift-infill sequence in the Billefjorden Trough, Svalbard. *Norsk geol. Tidsskr.* **72**, 35–48.
- Johansen, S. E., Gudlaugsson, S. T., Svånå, T. A. & Faleide, J. I. 1994: Late Palaeozoic evolution of the Loppa High, Barents Sea. In Johansen, S. E. (ed.) *Geological evolution of the Barents Sea with special emphasis on the late Palaeozoic development*. Unpublished Dr.Science Thesis, Univ. Oslo, 49 pp.
- Koniczny, R. M. 1987: Permian palynostratigraphy of Svalbard. Confidential Report. *Inst. KontinentalsokkelUnders. Sintefgruppen*, 1–194. (Unpublished.)
- Kozitskaya, R. I. 1983: [Conodonts in the Upper Carboniferous sediments of Dneprovsko–Donetskaya depression.] *Izv. Akad. Nauk. SSSR, Ser. Geol.* **11**, 69–76. (In Russian)
- Mangerud, G. 1994: Palynological assemblages from the Permian and lowermost Triassic succession on the Finnmark Platform, Barents Sea. *Rev. Palaeobot. Palynol.* **82**, 317–349.
- Mangerud, G. & Koniczny, R. M. 1993: Palynology of the Permian succession of Spitsbergen, Svalbard. *Polar Research* **9**(2), 155–167.
- Nakrem, H. A. 1991: Conodonts from the Permian succession of Bjørnøya (Svalbard). *Norsk geol. Tidsskr.* **71**, 235–248.
- Nakrem, H. A., Nilsson, I. & Mangerud, G. 1992: Permian biostratigraphy of Svalbard (Arctic Norway) – A review. *Intern. Geol. Rev.* **34**(9), 933–959.
- Nilsson, I. 1994: Upper Palaeozoic fusulinid assemblages, Wandel Sea Basin, North Greenland. *Rapp. Grønlands geol. Unders.* **161**, 45–71.
- Nilsson, I., Håkansson, E., Madsen, L., Pedersen, S. A. S. & Stemmerik, L. 1991: Stratigraphic significance of new fusulinid samples from the Upper Palaeozoic Mallemuk Mountain Group, North Greenland. *Rapp. Grønlands geol. Unders.* **150**, 29–32.
- Petryk, A. A. 1977: Upper Carboniferous (Late Pennsylvanian) microfossils from the Wandel Sea Basin, eastern North Greenland. *Rapp. Grønlands geol. Unders.* **85**, 16–21.
- Pronina, G.P. 1990: [Stratigraphic significance of small foraminifers from Late Permian of Transcaucasia.] *Vsesoyuznyi Ordena Lenina Nauchno-issledovatel'skii, Geologicheskii Institut, Leningrad*, 1–22. (In Russian.)
- Scotese, C. R. & McKerrow, W. S. 1990: Revised world maps and introduction. In McKerrow, W. S. & Scotese, C. R. (ed.) *Palaeozoic palaeogeography and biogeography. Geol. Soc. London. Mem.* **12**, 1–21.
- Sosipatrova, G. P. 1967: [Upper Paleozoic foraminifera of Spitsbergen.] In Sokolev, V. N. & Vasilevskaja, N. (ed.) *Stratigraphy of Spitsbergen*. Leningrad: NIIGA (In Russian.) English version: British Library, Lending Division, Boston Spa. (1977; 125–163).
- Steel, R.J. & Worsley, D. 1984: Svalbard's post-Caledonian strata. An atlas of sedimentational patterns and palaeogeographic evolution. In Spencer, A. M. *et al.* (ed.) *Petroleum Geology of the North European Margin*, 109–135. Graham & Trotman for Norwegian Petroleum Society.
- Stemmerik, L. & Elvebakk, G. 1994: A newly discovered mid-Carboniferous – ?early Permian reef complex in the Wandel Sea Basin, eastern North Greenland. *Rapp. Grønlands geol. Unders.* **161**, 39–44.
- Stemmerik, L. & Håkansson, E. 1989: Stratigraphy and depositional history of the Upper Palaeozoic and Triassic sediments in the Wandel Sea Basin, central and eastern North Greenland. *Rapp. Grønlands geol. Unders.* **143**, 21–45.
- Stemmerik, L. & Håkansson, E. 1991: Carboniferous and Permian history of the Wandel Sea Basin, North Greenland. *Bull. Grønlands geol. Unders.* **160**, 141–151.
- Stemmerik, L. & Larssen, G. B. 1992: Upper Palaeozoic geology in the Barents Sea and adjacent areas: Upper Palaeozoic carbonate studies in the Loppa High – Stappen High area, western Barents Sea. *Inst. KontinentalsokkelUnders. Report 23.1438.00/08/92. Reg.no. 92.155.* (Unpublished.)
- Stemmerik, L. & Worsley, D. 1989: Late Palaeozoic sequence correlations, North Greenland, Svalbard and the Barents Shelf. In Collinson, J. D. (ed.) *Correlation in hydrocarbon exploration*, 99–111. Graham & Trotman for Norwegian Petroleum Society.
- Stemmerik, L. & Worsley, D. 1995: Permian history of the Barents Shelf area. In Scholle, P. A., Peryt, T. M. & Ulmer-Scholle, D. S. (ed.) *The Permian of northern Pangea 2: Sedimentary basins and economic resources*. Berlin: Springer Verlag, 81–97.
- Stemmerik, L., Larson, P. A., Larssen, G. B., Mørk, A. & Simonsen, B. T. 1994: Depositional evolution of Lower Permian *Palaeoaplysina* build-ups, Kapp Duner Formation, Bjørnøya, Arctic Norway. *Sedimentary Geology* **92**, 161–174.
- Stemmerik, L., Nilsson, I. & Elvebakk, G. 1995a: Gzelian–Asselian depositional sequences in the western Barents Sea and North Greenland. In Steel, R. *et al.* (ed.) *Sequence stratigraphy on the Northwest European margin. Norwegian Petroleum Society, Special Publication 5*, 529–544.
- Stemmerik, L., Dalhoff, F. & Nilsson, I. 1995b: Petroleum geology and thermal maturity of eastern North Greenland – a new petroleum energy research project. *Rapp. Grønlands geol. Unders.* **165**, 49–52.
- Xia G. & Zhang Z. 1984: Foraminifera. In Tianjin Institute of Geology and Mineral Resources (ed.) *Paleontological Atlas of North China. III. Micropaleontological Volume.* (In Chinese) Beijing: Geological Publishing House, 5–59, 726–736.



Upper Permian foraminifera from East Greenland

Jack Pattison & Lars Stemmerik

Foraminiferal assemblages recorded from limestones of the Upper Permian Wegener Halvø Formation in the Wegener Halvø, Karstryggen and Clavering Ø areas of East Greenland mostly consist of the nodosariid genera *Dentalina*, *Fronidina*, *Geinitzina* and *Ichtyolaria*, and the miliolid genera *Agathammina* and *Calcitornella*. More limited assemblages dominated by *Agathammina* were recorded from the underlying Karstryggen Formation. The foraminifera are all benthonic, mostly shallow-water forms. The fauna is of Zechstein aspect and suggests a broad correlation with Zechstein 1 and younger strata in the Zechstein basin of North-West Europe.

Solid specimens of agglutinated foraminifera, mostly referable to *Ammobaculites* and *Ammodiscus*, were recorded from the youngest Permian strata, the Schuchert Dal Formation, in the Schuchert Dal.

J. P., 372 Loughborough Road, West Bridgford, Nottingham, NG2 7FD, U.K. (formerly of the British Geological Survey).

L. S., Geological Survey of Denmark and Greenland, Thoravej 8, DK-2400 Copenhagen NV, Denmark.

The Upper Permian basin in East Greenland has been studied intensively over the last ten years in association with onshore hydrocarbon activity in the region, and the overall depositional history is well described (Surlyk *et al.*, 1986; Scholle *et al.*, 1991; 1993; Stemmerik, 1987; 1991; Stemmerik *et al.*, 1988; 1993; Stemmerik & Piasecki, 1991; Christiansen *et al.*, 1993). However, studies of the Upper Permian fauna have been very limited since the pioneer work by Dunbar (1955) on the brachiopods and Newell (1955) on the bivalves. Recent stratigraphic studies include work by Piasecki (1984) and Utting & Piasecki (1995) on the palynostratigraphy and by Rasmussen *et al.* (1990) on the conodont fauna.

The East Greenland Basin is situated midway between, to the south, the evaporitic Zechstein basin and adjacent Bakevellia Sea basin in north-west Europe, and, to the north, the cold temperate basins of North Greenland, Spitsbergen and the Barents Sea. It thus provides important information on the Late Permian faunal provinces in the North Atlantic region. This paper describes, for the first time, the Upper Permian foraminiferal fauna from East Greenland and discusses its relationships with those in the Zechstein and Bakevellia Sea basins (Fig. 1).

Regional setting and stratigraphy

The Upper Permian basin in East Greenland is more than 400 km long and at least 80 km wide (Fig. 2). The

western limit is a major fault system which separated the depositional basin from the stable Greenland craton during the Carboniferous and subsequent periods (Surlyk *et al.*, 1986). Structural elements which influenced the Late Permian sedimentation are the Liverpool Land and Wegener Halvø highs to the south-east and the Clavering Ø high to the north (Figs 1, 2). The Liverpool Land high is inferred to have formed the south-eastern limit of the basin and, as suggested by Maync (1961), the basin was most likely closed towards the south.

The depositional succession starts with fluviatile conglomerates of the Huledal Formation. They are followed by shallow-water, restricted marine limestones and evaporites of the Karstryggen Formation deposited during the initial Late Permian transgression of the basin. The Karstryggen Formation was eroded to produce a palaeo-karst terrain. During the succeeding overall rise in sea level the platform carbonates of the Wegener Halvø Formation were deposited along the basin margins and over structural highs while shales of the Ravnefeld Formation were deposited in the central parts of the basin (Fig. 3). Following another marked fall in relative sea level, sedimentation changed dramatically and the entire basin was filled by shallow-water siliciclastics of the Schuchert Dal Formation (Fig. 3).

The most likely correlation between the East Greenland succession and the Zechstein sediments of North-West Europe equates the base of the Zechstein succession

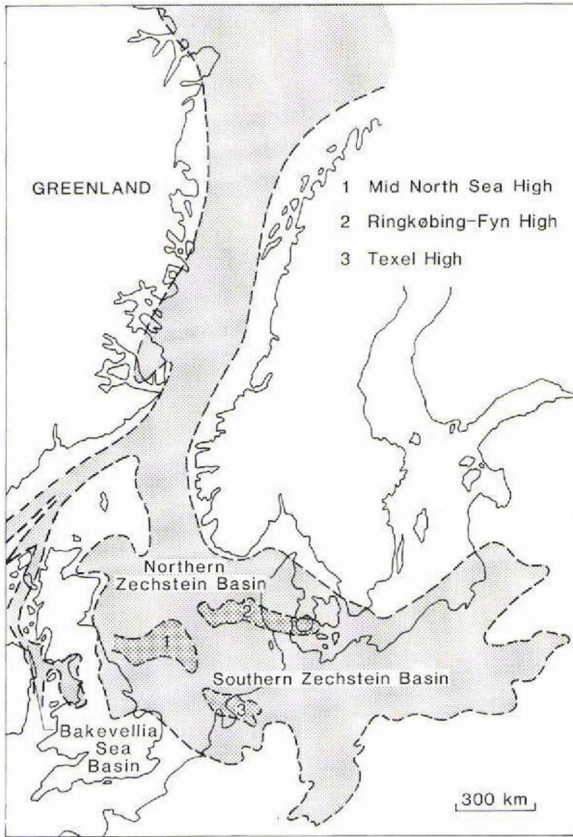


Fig. 1. Late Permian palaeogeography of the North Atlantic rift system.

with the base of the Wegener Halvø and Ravnfjeld formations (Rasmussen *et al.*, 1990; Stemmerik & Piasecki, 1991). The boundary is regarded as roughly equivalent to the Ufimian–Kazanian boundary in the Russian zonation (Stemmerik, 1995).

General description of the fauna

The majority of the foraminifera described in this paper were seen in thin-sectioned limestones, largely from the Wegener Halvø Formation (Tables 1–3). Most of these are from the carbonate platform succession on Wegener Halvø along the eastern basin margin, where foraminifera most commonly occur in the more marginal parts of bryozoan build-ups and in biogenic grainstone deposits associated with bryozoans and brachiopods (Stemmerik, 1991). Other foraminifera recorded in Wegener Halvø Formation limestones include a few specimens from deposits of more protected platform environments in the Karstryggen area along the western basin margin and larger assemblages from marginal parts of bryozoan build-ups on the Clavering Ø high to the north (Figs 1, 2).

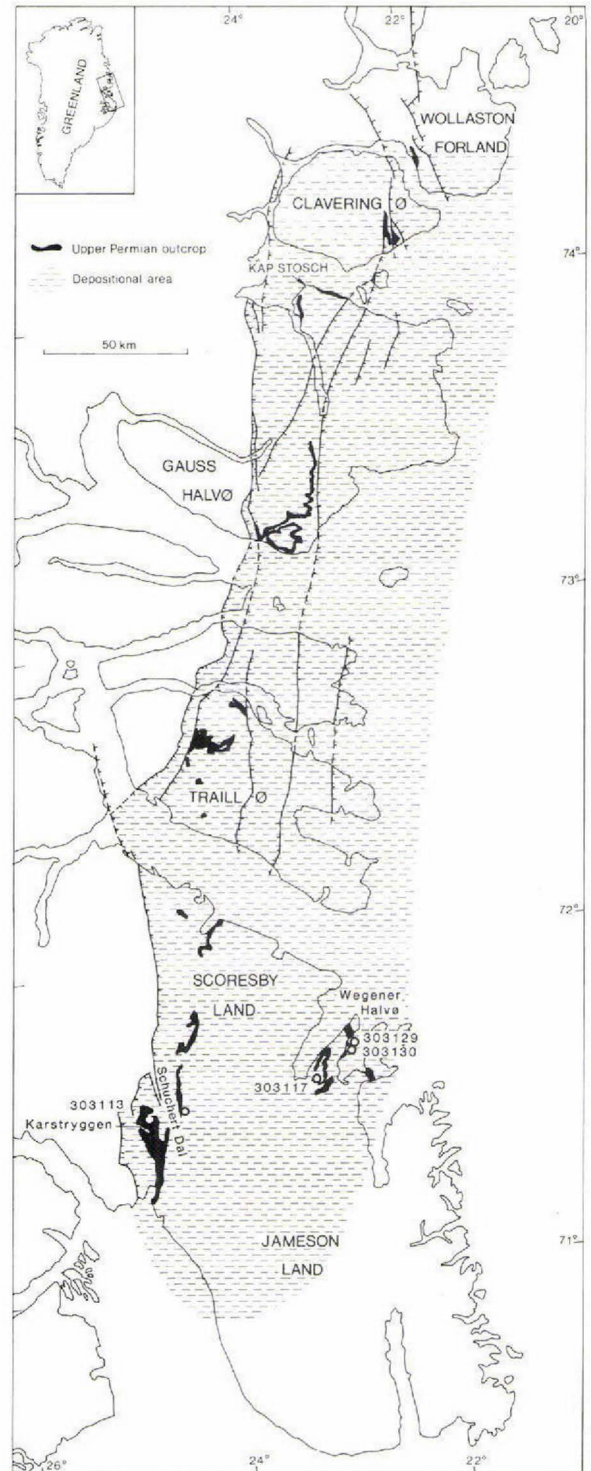


Fig. 2. Outcrops of Upper Permian strata in East Greenland.

Foraminifera have also been noted in two thin sections of limestone from the Karstryggen Formation. In addition, a

Table 2. Foraminifera recorded from GGU shallow core 303129 on Wegener Halvø

Depth below top of Wegener Halvø Fm	Sample number 303129-	<i>Agathammina pusilla</i>	<i>Dentalina permiana</i>	<i>Dentalina</i> cf. <i>siliqueaeformis</i>	<i>Geinitzina acuta</i>	<i>Ammodiscus roesslereri</i>	<i>Nodosaria permiana</i>	<i>Fronolina</i> spp.	<i>Ammobaculites eiseli</i>	<i>Reophax?</i>	<i>Geinitzina postcarbonica</i>	<i>Ichthyolaria</i> cf. <i>permotaurica</i>	<i>Calcitornella</i> spp.	indeterminate nodosarids	
0.44	8	X	•	•	•	•	•	•	•	•	•	•	•	X	
4.74	9	A	X	X	•	•	•	•	•	•	•	•	•	X	Assemblage A
5.64	10	A	•	•	X	•	•	•	•	•	•	•	•	•	
6.44	11	A	X	•	•	•	•	•	•	•	•	•	•	•	
7.33	12	A	?	•	•	•	•	•	•	•	•	•	•	X	
7.95	13	A	•	?	•	X	•	•	•	•	•	•	•	X	
9.36	14	X	X	•	•	•	•	•	•	•	•	•	•	•	Assemblage B
9.91	15	X	•	•	•	•	•	•	•	•	•	•	•	X	
10.20	16	X	•	•	•	•	X	X	•	•	•	•	•	•	
11.20	17	X	X	•	•	•	?	•	•	•	•	•	•	X	
11.76	18	X	•	•	•	•	•	•	•	•	•	•	•	•	
11.88	19	X	•	•	•	•	•	•	•	•	•	•	•	X	
13.01	20	X	•	•	•	•	•	•	•	•	•	•	•	X	
13.70	21	X	•	X	•	•	•	•	•	•	•	•	•	•	
14.78	22	X	•	•	•	•	•	•	•	•	•	•	•	•	
17.27	23	X	•	•	•	•	•	•	•	•	•	•	•	X	
17.92	24	X	•	•	?	•	X	•	?	•	•	•	•	X	Assemblage C
19.01	25	X	•	•	?	•	?	•	?	X	•	•	•	X	
19.65	26	X	•	•	?	•	•	•	?	?	•	•	•	•	
20.14	27	•	•	•	•	•	X	•	•	•	•	•	•	•	
21.61	28	A	•	•	X	•	X	•	•	•	X	•	•	X	Assemblage A
23.13	29	X	•	•	•	•	•	X	•	•	•	•	•	•	
24.07	30	•	•	•	•	•	•	•	•	•	•	•	•	X	
24.94	31	•	•	•	•	•	X	•	•	•	•	•	•	X	
26.33	32	•	•	•	X	•	•	•	•	•	•	•	•	X	Assemblage D
27.05	33	•	•	•	X	•	•	•	•	•	•	X	•	X	
28.28	34	•	•	•	X	•	•	•	•	•	•	X	•	X	
29.30	35	•	•	?	?	•	•	•	•	•	X	•	•	•	
29.70	36	•	•	•	•	•	X	•	•	•	•	•	•	X	
30.02	37	•	•	•	?	•	•	•	•	•	•	•	X	•	
34.27	41	•	•	•	•	•	•	•	•	•	•	•	X	X	Assemblage E
35.06	42	•	•	•	•	•	•	•	•	•	•	•	X	•	
41.63	48	•	•	•	•	•	•	X	•	•	•	•	?	X	

X = recorded, A = abundant

Table 3. Foraminifera recorded from GGU shallow cores 303113, 303117 and 303130 on Karstryggen and Wegener Halvø

GGU shallow core 303113 Karstryggen							GGU shallow core 303117 Wegener Halvø							
Depth in metres below top of Wegener Halvø Fm	Sample No. 303113-	<i>Agathammina pusilla</i>	<i>Geinitzina</i> spp.	<i>Geinitzina acuta</i>	other nodosariids	<i>Calcitornella</i> spp.	Depth in metres below top of Wegener Halvø Fm	Sample No. 303117-	<i>Agathammina pusilla</i>	<i>Ichtyolaria</i> cf. <i>permotaurica</i>	nodosariids (incl. <i>Pachyphloia</i> ?)	<i>Nodosaria permiana</i>	<i>Ammobaculites</i>	<i>Geinitzina</i>
8.48	76	X	X	•	•	•	25.54	103	X	X	X	•	•	•
10.28	55	X	•	•	•	•	26.31	104	X	•	X	•	•	•
16.70	86	X	•	•	•	•	33.91	115	X	•	X	•	•	•
17.70	88	X	•	•	•	•	34.66	116	X	•	X	X	•	•
18.61	91	A	•	•	•	X	36.04	117	X	•	•	•	•	•
18.96	59	A	•	X	•	•	36.51	118	X	•	•	•	?	•
19.06	92	A	•	•	•	•	42.08	126	X	•	X	•	?	•
19.50	93	A	•	•	•	•	42.91	127	X	•	X	•	•	?
19.70	70	A	•	•	•	•	44.53	132	X	•	X	•	•	•
19.87	94	A	•	•	•	•								
20.24	95	A	•	•	•	•								
20.94	96	A	•	•	X	•								
21.46	97	X	•	•	•	•								
22.02	98	X	•	•	•	•								
23.37	61	A	•	•	•	•								
23.63	101	X	•	•	•	•								
24.02	102	X	•	•	•	•								
24.80	103	A	•	•	•	•								
25.53	104	A	•	•	•	•								
25.95	105	A	•	•	•	•								
26.96	62	A	•	•	•	•								
27.64	108	X	•	•	X	•								
28.29	109	X	•	•	•	•								
31.12	114	X	•	•	•	•								
31.41	64	X	•	•	•	•								

GGU shallow core 303130 Wegener Halvø						
Depth below top of Wegener Halvø Fm	Sample No. 303130-	<i>Nodosaria permiana</i>	<i>Geinitzina</i> (incl. <i>G. acuta</i>)	nodosariid	<i>Froncina</i> spp.	<i>Calcitornella</i> spp.
	2	X	X	•	•	•
11.60	15	•	•	X	X	•
15.15	26	•	X	X	•	X
15.26	27	•	X	X	•	X
16.85	30	•	•	X	X	X
21.40	37	•	X	•	•	•
21.80	39	•	X	X	•	?
46.69	87	•	•	•	•	?

X = recorded A = abundant

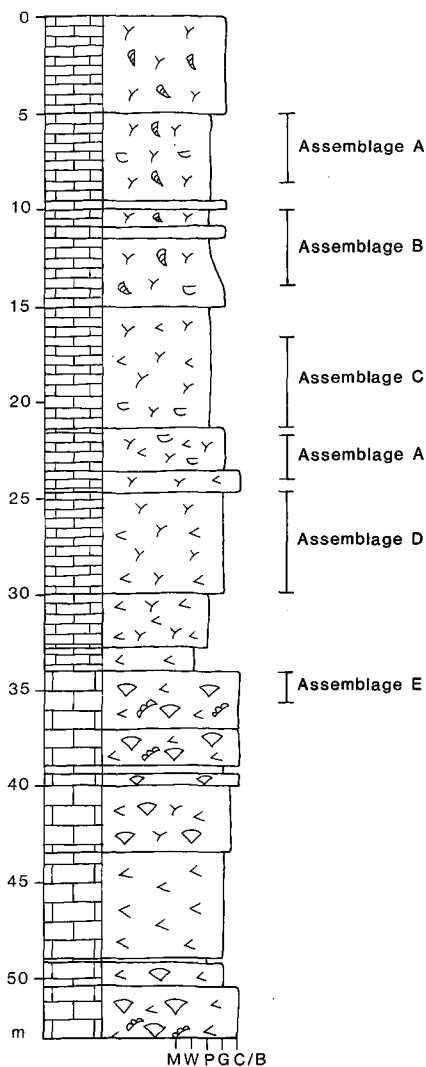


Fig. 4. Sedimentological log of GGU shallow core 303129 on Wegener Halvø with distribution of foraminifera assemblages.

build-up and reached the build-up core in the basal part (Fig. 4; Stemmerik, 1991). The cored succession contains five distinct assemblages that can be correlated to various carbonate facies (Fig. 4; Table 2).

Assemblage A contains numerous large *Agathammina pusilla* as well as mostly simple-walled nodosariids, notably *Dentalina*. It occurs in bryozoan-foraminifer packstones together with abundant cryptostome bryozoans in the interval from 4.75 m to 8.00 m and 21.60 m to 23.15 m (Fig. 4; Table 2).

Assemblage B contains *Agathammina pusilla*, although fewer in *Assemblage A*, and a limited nodosariid fauna. It

occurs in bryozoan-foraminifer packstones and grainstones together with cryptostome bryozoans in the interval from 9.40 m to 13.70 m (Fig. 4; Table 2).

Assemblage C is comparable to *assemblage B* but includes some doubtful forms which might be fragmentary *Ammobaculites* and *Reophax*. This assemblage occurs in a bryozoan-bivalve packstone with both cryptostome and trepostome bryozoans, and some brachiopods from 17.90 m to 19.65 m (Fig. 4; Table 2).

Assemblage D contains a varied nodosariid fauna including *Geinitzina* and other double-walled forms, such as *Ichtyolaria* and possibly *Pachyphloia*. No *Agathammina* were recorded in this assemblage. *Assemblage D* occurs in bryozoan-bivalve grainstones from 24.95 m to 29.70 m (Fig. 4; Table 2).

Assemblage E contains *Calcitornella* and nodosariids. It occurs in marine cementstones with comminuted organic debris from 34.25 m to 35.10 m.

The other two boreholes in the Wegener Halvø area also yielded foraminiferal faunas with a Zechstein aspect (Table 3). The collection from 303130, near 303129, resembles that of *Assemblages D* and *E*. It includes *Geinitzina*, *Fronndina* and abundant *Calcitornella*, but no *Agathammina*. This core was drilled through a build-up core, and the fauna occurs in depositional facies similar to those of *Assemblage E* (cf. Stemmerik, 1991). Borehole 303117, farther south, was drilled through the flanks of a large bryozoan build-up. The fauna yields *Agathammina* and thick-walled nodosariids and is comparable with *Assemblage C* of 303129.

Surface samples examined from Wegener Halvø were mostly from the north-eastern end of the peninsula near boreholes 303129 and 303130. The overall fauna includes the same calcareous porcellanous and nodosariid forms recorded in the boreholes plus the agglutinated *Ammodiscus roessleri* and *Glomospira*. One surface sample from the southern part of the area yielded, in addition to the characteristic Zechstein species *Geinitzina acuta*, an indistinct probable *Endothyra*, a genus unrecorded in North-West European Zechstein strata.

Karstryggen (Wegener Halvø and Karstryggen Formations)

Most of the material examined came from the Wegener Halvø Formation on the western side of the area and included a number of samples from the borehole 303113. They yielded a monotonous fauna in which *Agathammina pusilla* was ubiquitous but otherwise only contained

a few nodosariids, including *Dentalina* and *Geinitzina* (Table 3). One other borehole (303101), and surface sampling, from the Wegener Halvø Formation in the western side of the area yielded comparable limited assemblages including *Agathammina*, *Calcitornella* and a few nodosariids.

Two samples from the Karstryggen Formation farther east in the area yielded only *Agathammina pusilla*.

Clavering Ø (Wegener Halvø Formation)

A total of only six samples from this area yielded a sufficiently large number of species to suggest the presence of a relatively rich foraminiferal fauna with distinct characteristics. No specimens of *Agathammina* were recorded but the agglutinated genera *Ammodiscus*, *Glomospira* and a possible *Ammobaculites* were seen. The nodosariids, which constitute most of the foraminifera seen, include a greater proportion of broad-tested forms such as *Fronidina*, *Geinitzina* and *Ichtyolaria* than in the faunal collections from the Wegener Halvø Formation farther south. In addition, a coiled, chambered foraminifer was seen which might be referred to *Globivalvulina*, a taxon not recorded elsewhere in East Greenland or in the European Zechstein.

Schuchert Dal (Schuchert Dal Formation and Wordie Creek Group)

Both palynomorphs and solid foraminifera have been extracted from samples collected from a surface section on the east side of Schuchert Dal. The palynomorphs suggest that the section crosses the Permian–Triassic boundary (S. Piasecki, personal communication), which is taken as the boundary between the Schuchert Dal Formation and the overlying Wordie Creek Group (Fig. 5).

The foraminifera collected from the section are all agglutinated forms which are comparable with European Zechstein material but cannot be regarded as diagnostic of age. The samples from below the postulated boundary are richer than those from above: the latter yielded no *Ammobaculites*, a genus well-represented in the lower part of the section (Fig. 5). The most prolific sample proved to be that from what is taken to be the top of the Schuchert Dal Formation; specimens from that sample are illustrated in Fig. 6.

Discussion

These foraminiferal faunas, as might be expected by analogy with the East Greenland Upper Permian brachiopod and bivalve faunas, are comparable with those of the Zechstein and Bakevellia Sea basins. The North-West

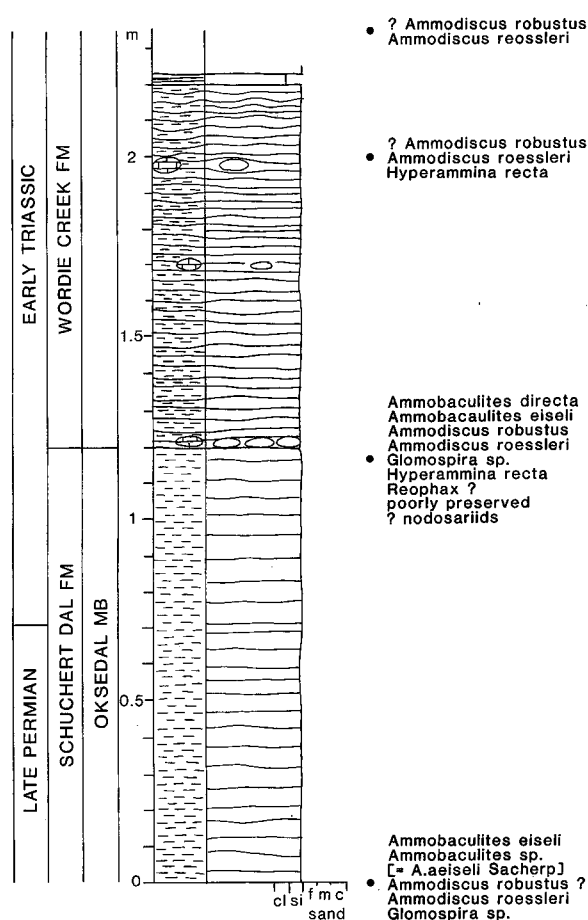


Fig. 5. Distribution of agglutinated and siliceous foraminifera across the Permian–Triassic boundary in Schuchert Dal.

European Zechstein foraminifera are among the most intensively studied Permian populations of smaller foraminifera (see e.g. Scherp, 1962; Woszczyńska, 1968; Pattison, 1989), although much about them remains problematic, especially factors related to test wall structure and composition, and thus to their supra-generic taxonomy. Therefore, inferences about the environmental, stratigraphical and evolutionary significance of the East Greenland foraminifera necessarily draw upon lessons learnt about Zechstein foraminifera but those inferences are limited by similar doubts relating to wall structures and nomenclature.

Palaeoenvironments

The fauna consist of benthonic, probably epifaunal, relatively shallow-water, assemblages with some indications of varying depths and substrates. The variations of environment inferred from the collections seen, however,

are limited in range compared with those indicated by known Zechstein foraminiferal faunas.

In Zechstein strata, the foraminiferal assemblage (E) of core 303129, with predominant *Calcitornella*, would be regarded as indicative of relatively shallow-water facies. The overlying assemblage (D), with *Geinitzina* but without *Agathammina*, accompanied by bivalves, is also broadly indicative of shallow water but includes more nodosariid forms than might be expected. Assemblages C, B and A contain *Agathammina* throughout and declining numbers of *Geinitzina*, associated with bryozoans (both cryptostome and tepostome) and brachiopods. The interpreted trend towards increased water depth is in line with observations of foraminiferal distribution in Polish Zechstein strata by Peryt & Peryt (1977). The deepening upward trend inferred from the changes in the foraminifer fauna is supported by microfacies studies of the core (Stemmerik, 1991). Assemblages E and D occur in high energy facies which represent the core of the bryozoan build-ups. Assemblages C, B and A occur in flank deposits surrounding the build-up core, and are accordingly associated with more protected environments. The microfacies indicate a trend towards more protected environments, and abundance of *Agathammina* seems to be restricted to mud-supported facies.

Analogous inferences can be made from the foraminiferal assemblages yielded by the other two cores of the bryozoan build-ups in the Wegener Halvø area (Table 3). The foraminifera from core 303130 are comparable with assemblages (D) and (E) of 303129 and are similarly associated with abundant marine cement, bivalves and probable algal debris, supportive of a shallow-water, reef core origin (Stemmerik, 1991). The foraminifera, comparable with those of assemblage C of 303129, yielded by core 303117 occur in build-up flank deposits associated with brachiopods and bryozoans and indicate a deeper water shelf-sea environment. The rest of the material collected from the Wegener Halvø area is broadly indicative of relatively deep, shelf-sea waters.

The limited number of foraminiferal forms yielded by core 303113 (Table 3) in the Karstryggen area together are broadly comparable with the relatively deep-water assemblage (A) of core 303129. They are associated with brachiopods, bryozoans, bivalves and gastropods.

The rich assemblages collected from Claving Ø are less easy to characterise. The species represent considerable variations of water depth, substrate and turbulence and most likely they are reworked from different parts of the bryozoan build-ups.

The presence in North-West European Zechstein strata of agglutinated foraminifera such as those recorded from the section through the top of the Schuchert Dal Formation (Fig. 5), is usually an indication of the availability of

suitable adventitious material for incorporation in the test wall. They are most commonly recorded in marginal marine environments where the introduction of terrigenous sediment by rivers can be inferred.

Biostratigraphical correlation

The established view of what are broadly termed Zechstein rocks in north-west Europe is that they are the products of four or five cycles of mostly evaporitic deposition although this cyclic character is only distinct in the southern part of the main Zechstein basin. There, the first three of those cycles include carbonate units which, together with some associated mudstones, have yielded most of the known marine Zechstein fossils. The first Zechstein cycle carbonate (Z1) contains a fairly rich brachiopod/bryozoan/bivalve/gastropod fauna and varied foraminiferal assemblages. There are considerable lateral variations in the faunal content of the Z1 carbonate strata due to both palaeoenvironmental and diagenetic factors.

The carbonate units of the next two Zechstein cycles (Z2 and Z3) in the southern part of the Zechstein basin contain faunas which are more limited, both in total numbers and in diversity. The differences between these faunas and those of the first cycle result largely from the elimination of Z1 species rather than the introduction of new ones and this kind of change is characteristic of the foraminifera as well as the other groups.

In the northern sub-basin of the Zechstein Sea and the contemporaneous Bakevellia Sea to the west the cyclic nature of the deposition is less uniform in character and, in the Bakevellia Sea basin, more difficult to correlate between sub-basins. There is commonly only one marine fossil-bearing carbonate unit in any area and that unit can usually be correlated, in part or in whole, with the first cycle carbonate of the southern part of the main Zechstein basin.

Overall, the North-West European Zechstein faunas lack representatives of several groups of organisms which occur in late Permian marine strata of other parts of the world; notably no ammonoids or fusulinaceans have been recorded. These deficiencies can be largely attributed to postulated land barriers between the Tethyan Ocean, where those groups flourished, and the Zechstein Sea. Consequently, Zechstein faunas, despite their inferred low-latitude origins, can be regarded as belonging to the Boreal Province, in common with those of the late Permian rocks in East Greenland and other depositional basins associated with the proto-North Atlantic. This distinctive paucity of the Permian Boreal faunas which occur around the present-day North Atlantic and Arctic oceans as well as the Russian Platform was noted by both Gobbett (1973) and Stehli (1973) with reference to the fusulinaceans and brachiopods respectively.

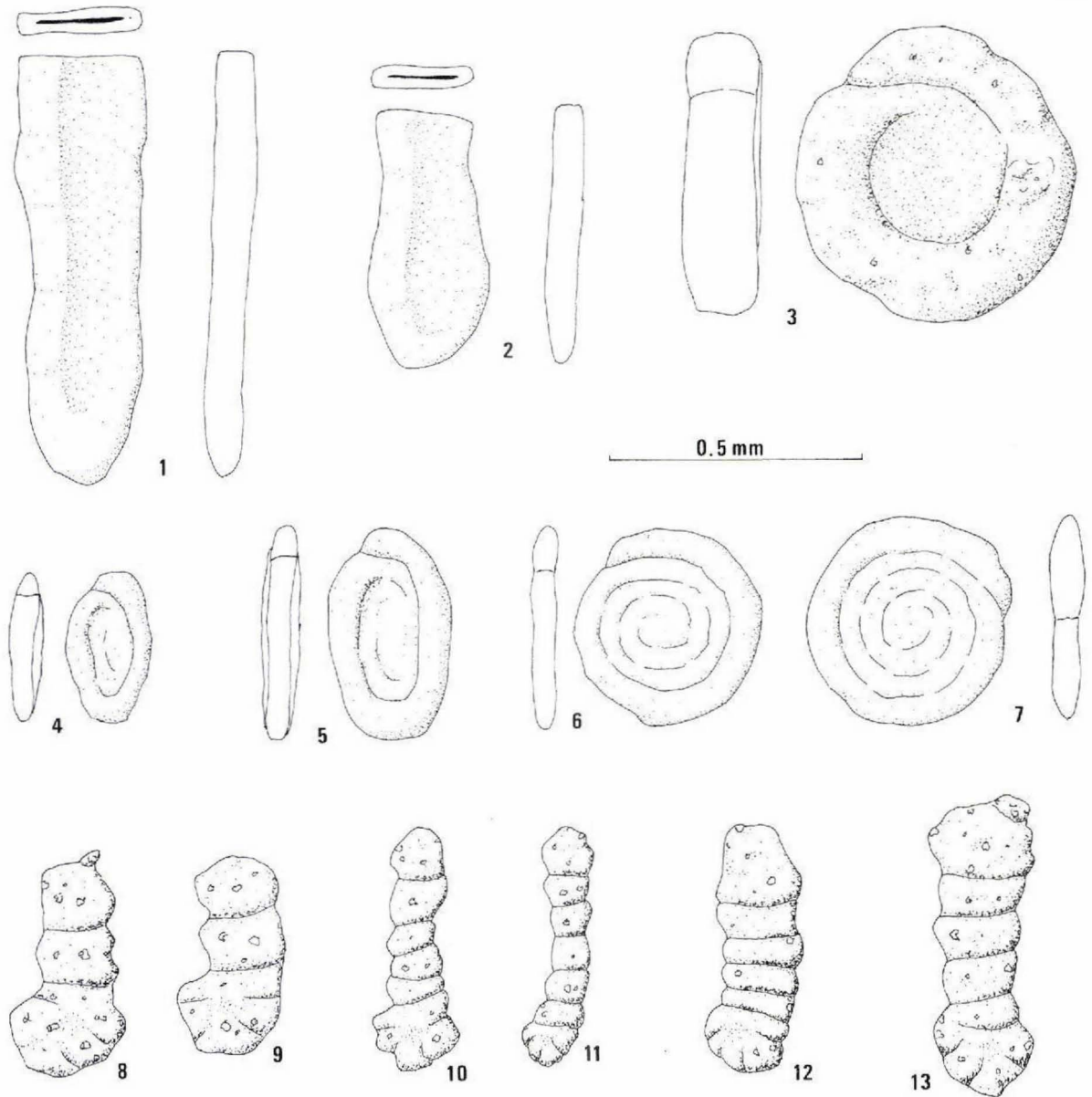


Fig. 6. Agglutinated and siliceous foraminifera, extracted as solid tests, from the top of the Oksedal Member of the Schuchert Dal Formation in Schuchert Dal.

(1) *Hyperammina recta* Scherp; MGUH 23598. (2) *H. recta*; MGUH 23599. (3) *Ammodiscus robustus* Vangerow; MGUH 23600. (4) *Ammodiscus roessleri ellipticus* (Spandel); MGUH 23601. (5) *A. roessleri ellipticus*; MGUH 23602. (6) *Ammodiscus roessleri* (Schmid); MGUH 23603. (7) *A. roessleri*; MGUH 23604. (8) *Ammobaculites* sp. [= *A. eiseli* Scherp, 1962]; MGUH 23605. (9) *Ammobaculites* sp. [as previous fig.]; MGUH 23606. (10) *Ammobaculites eiseli* (Paalzow); MGUH 23607. (11) *A. eiseli*; MGUH 23608. (12) *Ammobaculites directa* Scherp; MGUH 23609. (13) *A. directa*; MGUH 23610.

It must be emphasised that taxonomic uncertainties at both supra-generic and species levels make biostratigraphical correlation between the Zechstein, East Greenland and other late Permian Boreal foraminiferal faunas a somewhat speculative exercise. Broad comparisons between whole assemblages appear to be more useful than

correlations based on possibly dubious records of individual species. The numerically best-represented suborders of foraminifera in the East Greenland Upper Permian appear to be the calcareous porcellanous Miliolina and the calcareous, multilocular, uniserial forms here regarded as nodosariids within the Lagenina. Also present are the

finely siliceous genera *Ammodiscus*, *Glomospira* and *Hyperammmina*, and the coarsely agglutinated *Ammobaculites*. This general composition is entirely comparable with that of the north European Zechstein and other late Permian, non-Tethyan, foraminiferal faunas.

Another similarity with the north European Zechstein fauna is the widespread presence of *Agathammina pusilla*. The previously noted significance of that species as an indicator of a relatively deep water environment may diminish its biostratigraphical value, but it should be noted that within the Zechstein it is almost diagnostic of a Z1 age. If it does occur in younger Zechstein strata it is extremely rare in them. The species, in its dominance among Z1 foraminifera, and absence or rarity in Z2 or Z3 rocks, is analogous with *Bakevella binneyi* among Zechstein bivalves and suggests a correlation of the Wegener Halvø Formation with the first Zechstein cycle. Other miliolids in the Zechstein are more facies-controlled and their absence from the East Greenland samples probably results merely from comparable facies not being represented. They include *Cyclogyra* and partly planispirally-coiled *Agathammina* species, characteristic of low-energy, shallow water with mud substrates in the Zechstein; and tightly streptospirally coiled *Calcitornella* or *Orthovertella*, common in the core of Z1 barrier reefs.

The nodosariid assemblages are also broadly comparable with those of the first Zechstein cycle including both thin simple-walled *Dentalina* and *Fronndina*, and more complex, double-layer walled forms referred to *Geinitzina*, *Ichtyolaria* and *Nodosaria*. Woszczyńska (1981) reviewed the stratigraphical distribution of nodosariids recorded from Zechstein strata in Europe. All the species she listed from post-Z1 rocks were forms also recorded in first cycle strata. Similar nodosariid assemblages have been described from Z1 and Z2 strata in the British Isles, where again, no new forms appeared after the first cycle (Z1). What appear to be comparable nodosariid assemblages were described by Sosipatrova (1972) from Spitsbergen in strata correlated with the Upper Permian Ufimian and Kazanian stages of the Russian Platform.

The nodosariids offer the most promise as biostratigraphical tools among the Boreal late Permian small foraminifera but at present their potential cannot be realised because of the taxonomic confusion surrounding the group. The confusion partly derives from the transitional nature of the group in the late Permian but has been compounded by some inadequate original descriptions of the genera and species to which these foraminifera are usually assigned. Because they include both tests with single-layered and multiple-layered walls they have been variously assigned to two different suborders, the Fusulinina and the Lagenina, but not always with the care that such a major distinction should justify. Mamet &

Pinard (1990) have described uniserial, rectilinear, calcareous foraminifera from early Permian rocks of the Canadian Arctic Sverdrup Basin which may represent an earlier phase of the transition between these two major groups. In particular, their new genus *Nodosinelloides*, within the Fusulinina, could include several double-walled species recorded from East Greenland and the European Zechstein, which have been referred to *Nodosaria*, both here and in previous work. However, the late Permian faunas also include species with thinner, single-layered walls, including some of the *Dentalina* in this paper, which appear to be more closely related to Mesozoic Lagenina, or may be referable to the genus *Protonodosaria*, also within the Fusulinina. The authors prefer to retain the mixed generic taxonomy used by most earlier authors for these Permian forms until the wall structures of all the relevant generic type species have been re-examined.

The siliceous or agglutinated forms recorded mostly in the Schuchert Dal section mentioned above, across what is taken to be the Permian–Triassic boundary, are of even less stratigraphical value as they are all long-ranging forms similar to or comparable with foraminifera found in many mudstones of Upper Palaeozoic or later age.

Pending a thorough re-examination of Permian 'nodosariid' taxonomy, the biostratigraphical usefulness of the foraminifera described here must be limited to a general support for the broad correlations already based on the macrofaunas. That is to equate the transgression which initiated the Wegener Halvø and Ravnefjeld formations with that of the first Zechstein cycle (Z1) and to assign a Kazanian age to both. The impact of the transgression was so profound in East Greenland and so sudden and widespread in Europe, where it resulted in the deep-water Kupferschiefer-Marl Slate sea, that a major eustatic sea-level rise seems the probable cause. Given a sea-level rise of such apparent magnitude, it is reasonable to expect that other late Permian marine strata in the Boreal Province were also initiated by it. The faunal evidence suggests that the latter include the earliest marine strata in the various sub-basins of the Bakevella Sea and contemporaneous marine deposition might be expected to have taken place in half-grabens aligned parallel to the late

Fig. 7.

Magnification $\times 77$

- 7.1 *Agathammina pusilla* (Geinitz); [longitudinal section] MGUH 23611 from GGU 303129–8
- 7.2 *Agathammina pusilla*; [transverse section]; MGUH 23612 from GGU 303129–9
- 7.3 *Agathammina pusilla*; [transverse section]; MGUH 23613 from GGU 303129–10
- 7.4 *Agathammina pusilla*; [diagonal section]; MGUH 23614 from GGU 303129–13



Palaeozoic rift north-west and north of the British Isles and west of Norway.

Outside this simplistic correlation of all the main Permian marine fossil-bearing stratigraphical units in the north Atlantic region the age of several less organically-rich marine formations is more doubtful. They include older strata such as the Karstryggen Formation in East Greenland and the Banderschiefer, the Mutterflos and the Zechstein Konglomerat in Germany and Poland. The last three are commonly regarded as local and minor precursors of the Zechstein proper as their faunas have a Zechstein aspect although the brachiopods of the Zechstein Konglomerat form a distinct assemblage. However, a broad correlation between some or all of those three formations and the Karstryggen Formation is possible.

The Z1 and Z2 carbonate units, are stratigraphically separate in the southern Zechstein sub-basin, and are usually mutually distinguishable because of the distinctiveness of the Z3 biota. However, they are not so easily correlated with deposits in the northern sub-basin of the Zechstein or of the Bakevellia Sea. Therefore precise correlation with strata in East Greenland is not feasible and the Wegener Halvø and Ravnefjeld formations must be regarded as broadly equivalent to the unified Halibut carbonate formation of the northern North Sea and all three of the older cycles (Z1-Z3) in the more distal parts of the southern Zechstein sub-basin and the Bakevellia Sea basin.

Brief systematic descriptions

Suborder Textulariina

(Mostly seen as solid specimens)

Ammobaculites directa Scherp

Fig. 6.12, 6.13 = *Ammobaculites directa* Scherp, 1962.

Remarks. The early coiled part is roughly in line with the rectilinear part and less than 1.5 times its width. The chambers in the coiled part are indistinct. There are 4 to 5 chambers in the rectilinear part; all except the final one are much wider than long. The test wall is coarse-grained with a probable siliceous cement.

Ammobaculites eiseli (Paalzow)

Fig. 6.10, 6.11 = *Ammobaculites eiseli* (Spandel) Paalzow, 1936.

Remarks. The early coiled part is slightly offset from the line of the rectilinear part. The chambers in the coiled part are indistinct but less so than in *A. directa*. There are 5 to 6 chambers in the rectilinear part; they are almost as

long as wide. Sutures are distinct. The test wall is like that of *A. directa*.

Ammobaculites sp.

Fig. 6.8, 6.9 = *Ammobaculites eiseli* (Spandel) Scherp, 1962.

Remarks. The early coiled part is at least 1.5 × the width of the rectilinear part and distinctly offset. The chambers in the coiled part are indistinct. There are 2 to 3 chambers in the rectilinear part; their width and length about equal. The test wall is like those of *A. directa* and *A. eiseli*.

Ammodiscus robustus Vangerow

Fig. 6.3 = *Ammodiscus robustus* Vangerow, 1962.

Remarks. The test consists of a planispirally coiled tube. Coiling is involute; the inner whorls and aperture are indistinct. The final whorl is thick. The test wall is fairly coarse-grained; the cement probably siliceous.

Ammodiscus roessleri (Schmid)

Fig. 6.6, 6.7, 8.2 = *Serpula roessleri* Schmid, 1867.

Remarks. The test is discoid and consists of a proloculus followed by a planispirally coiled, tubular second chamber. The tubular chamber increases slowly in width. The aperture is indistinct. The test wall is fine-grained and probably siliceous. The species has been seen both as solid specimens and in thin section.

Ammodiscus roessleri ellipticus (Spandel)

Fig. 6.4, 6.5 = *Trochammina bradyana elliptica* Spandel, 1898.

Remarks. The test consists of a planispirally coiled tube but has an overall ovoid shape. This form is possibly a

Fig. 8

Magnification × 77

8.1 *Calcitornella* sp.; MGUH 23615 from GGU 292697

8.2 *Ammodiscus roessleri* (Schmid); [approximate axial section]; MGUH 23616 from GGU 357316-1

8.3 *Glomospira* sp.; [approximate axial section]; MGUH 23617 from GGU 357316-2

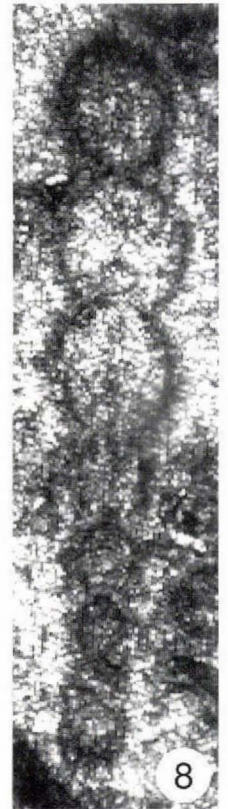
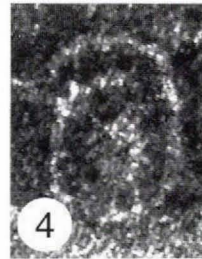
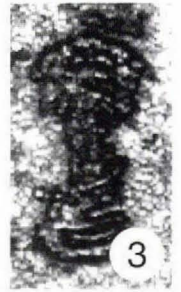
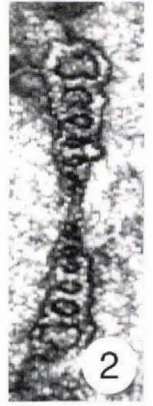
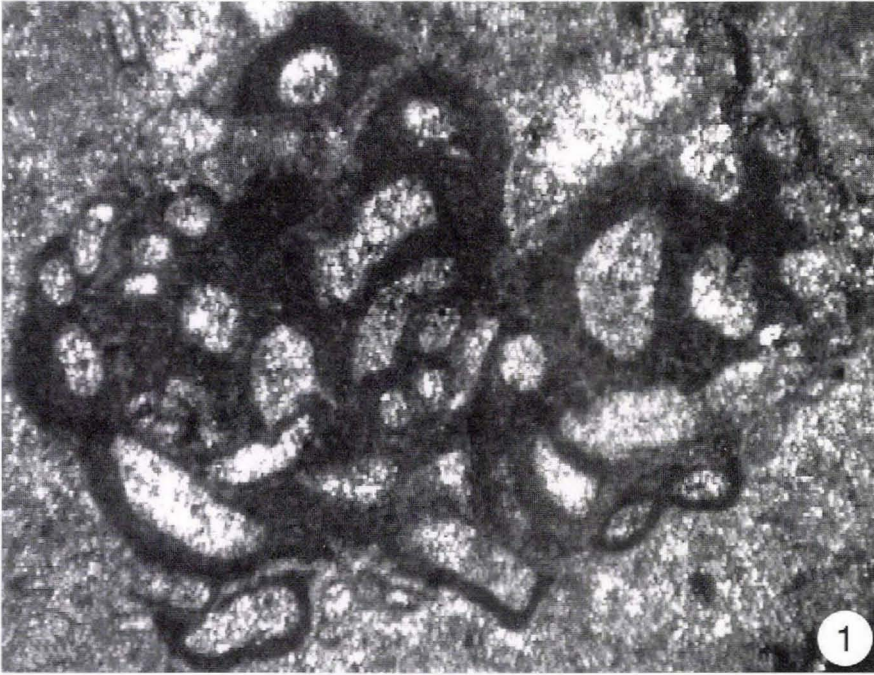
8.4 *Endothyra*?; MGUH 23618 from GGU 298134

8.5 *Calcitornella* sp.; MGUH 23619 from GGU 303113-91

8.6 *Dentalina permiana* Jones; MGUH 23620 from GGU 303129-14

8.7 *Dentalina* cf. *siliquaeformis* Sossipatrova; MGUH 23621 from GGU 393129-21

8.8 *D.* cf. *siliquaeformis*; MGUH 23622 from GGU 303129-9



distorted, originally discoid, *A. roessleri* sensu stricto, but was recognised as a distinct subspecies by Spandel.

Glomospira sp.

Fig. 8.3

Remarks. The test (seen only in thin-section) consists of a proloculus and a tubular second chamber. The latter is streptospirally coiled initially but possibly becomes more evolute. The transverse section of the tube is a compressed semi-circle. The tube increases slowly in width.

Hyperammia recta Scherp

Fig. 5.1, 5.2 = *Hyperammia clavacoidea recta* Scherp, 1962.

Remarks. The test is an elongate, compressed, simple tube with a bulbous early part which could be regarded as a proloculus. The aperture is slit-like. The test wall is fine-grained and probably siliceous.

Rephax ?

Remarks. The test is multilocular, uniserial and rectilinear with a coarse-grained agglutinated wall comparable with that of *Ammobaculites*. Only doubtful, possibly fragmentary, specimens have been seen, both as solid tests and in thin-section.

Suborder Fusulinina

Endothyra ?

Fig. 8.4

Remarks. Seen in thin-section as a planispirally coiled test with short intercameral septa. The test wall is indistinct, but appears to be transparent and single-layered. Reference to the genus *Endothyra* is dubious, merely serving to indicate a possible familial assignment.

Suborder Miliolina

(Seen only in thin-section)

Agathammina pusilla (Geinitz)

Fig. 7.1–7.4 = *Serpula pusilla* Geinitz, 1848 [part]

Remarks. The test is elongate and fusiform, consisting of a globular proloculus followed by a tubular second chamber coiled in a quinqueloculine manner. The transverse

section of the second chamber is hemispherical. The test wall is calcareous and mostly appears homogeneous and grey, but is commonly recrystallised to clear calcite.

Calcitornella spp.

Fig. 8.2, 8.5

Remarks. The test consists of a proloculus followed by a tubular second chamber. The latter increases slowly in diameter; it is irregularly coiled, sometimes in an involute streptospiral, sometimes in an evolute body of variable shape. The transverse section of the tube in the involute tests is hemispherical; in the evolute forms, it can be circular. The test wall is like that of *Agathammina pusilla*. Most of these foraminifera in the East Greenland material appear to be attached to other organic debris: bryozoa etc. However, it is possible that they include free forms which, although similar in every other respect, should properly be assigned to *Orthovertella*.

Suborder Lagenina

The uniserial, rectilinear, calcareous, multilocular foraminifera comprising a large part of these faunas are all described here under the heading of the Lagenina. They were all seen only in thin-sections.

Fig. 9

Magnification $\times 77$

9.1 *Fronidina* sp. A; MGUH 23623 from GGU 346190

9.2 *Fronidina* sp. A; MGUH 23624 from GGU 303130–30

9.3 *Fronidina* sp. B; MGUH 23625 from GGU 303129–48

9.4 *Fronidina thuringica* (Paalzow); MGUH 23626 from GGU 360652

9.5 *Geinitzina postcarbonica* Spandel; MGUH 23627 from GGU 303129–35

9.6 *Nodosaria permiana* (Spandel); MGUH 23628 from GGU 303117–116

9.7 *Pachyphloia*?; MGUH 23629 from GGU 303117–132

9.8 *Geinitzina acuta* (Spandel); MGUH 23630 from GGU 303113–59

9.9 *G. acuta*; MGUH 23631 from GGU 303130–37

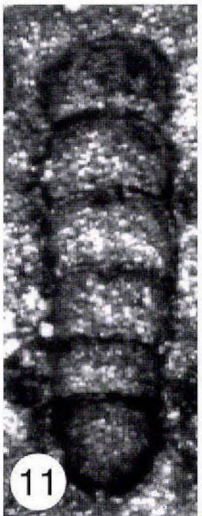
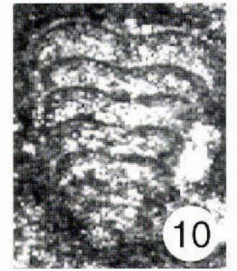
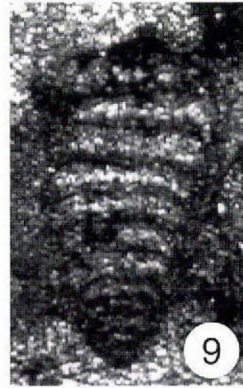
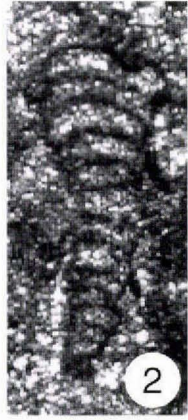
9.10 *G. acuta*; MGUH 23632 from GGU 298134

9.11 *Nodosaria permiana*; MGUH 23633 from GGU 357539

9.12 *Pachyphloia*?; MGUH 23634 from GGU 303129–28

9.13 *chyolaria* cf. *permotaurica* Civrieux & Dessauvagie; MGUH 23635 from GGU 303117–103

9.14 *Globivalvulina*?; MGUH 23636 from GGU 360653



Dentalina permiana Jones

Fig. 8.6 = *Dentalina permiana* Jones, 1850.

Remarks. The test is multilocular and uniserial. It typically has 6 to 9 chambers, each a slender barrel shape, mostly longer than wide, increasing in size although the proloculus may be about the same size as the second chamber. The chambers are arranged in a gentle arc. The test wall is commonly thin and clear, rarely with a very thin, dark, inner layer.

Dentalina cf. *D. siligaeformis* Sosipatrova

Fig. 8.7, 8.8

Remarks. As *D. permiana* but with narrower chambers. The curvature of the test is less regular, and may comprise two arcs facing in opposite directions. Comparable forms, from the Polish Zechstein, were assigned to *D. siligaeformis* Sosipatrova, 1969, by Peryt & Peryt (1977).

Fronidina thuringica (Paalzow)

Fig. 9.4 = *Spandelina thuringica* Paalzow, 1936.

Remarks. The test is multilocular and uniserial with a slightly arcuate line of up to 10 chambers. The latter are irregularly shaped but are all wider than long, and mostly slightly arched over the previous chamber. The test wall is very thin, simple and appears dark in thin-section under ordinary light.

Fronidina sp. A

Fig. 9.1, 9.2

Remarks. As *F. thuringica* but the chambers are wider and more irregularly shaped.

Fronidina sp. B

Fig. 9.3

Remarks. As previous two species but the test is less arcuate and has distinctly arched chambers.

Geinitzina acuta (Spandel)

Fig. 9.8–9.10 = *Geinitzella acuta* Spandel, 1898.

Remarks. The test is multilocular, rectilinear and uniserial but simulating biserial by having a longitudinal central

compression. A spherical proloculus is followed by compressed chambers which initially increase quickly in width. The last part of the test may be parallel-sided. The test wall is double, with a dark inner layer and a generally thicker, paler outer layer.

Geinitzina postcarbonica Spandel

Fig. 9.5 = *Geinitzina postcarbonica* Spandel, 1901.

Remarks. As *G. acuta* but longer and narrower, with a greater proportion of the test parallel-sided.

Nodosaria permiana (Spandel)

Fig. 9.6, 9.11 = *Orthocerina permiana* Spandel, 1898.

Remarks. The test is multilocular, rectilinear and uniserial. A spherical proloculus is followed by generally barrel-shaped chambers which are mostly longer than wide. The test wall commonly appears double, with a thin dark inner layer and a thicker, pale outer layer. This species, both here and in the European Zechstein, might be referable to the genus *Nodosinelloides* Mamet & Pinard but see discussion earlier on nodosariids.

Ichtyolaria cf. *I. permotaurica* Civrieux & Dessauvague

Fig. 9.13

Remarks. The test is multilocular, rectilinear and uniserial. A spherical proloculus is followed by chambers which increase rapidly in width. They are much wider than long and have a chevron shape in thin-section, each embracing the previous chamber. The test wall is thin, simple and clear. The species *I. permotaurica* was erected for externally striate forms from Upper Permian strata in Anatolia, Turkey by Civrieux & Dessauvague (1965).

Pachyphloia ?

Fig. 9.7, 9.12

Remarks. Several specimens with thick, clear, but possibly lamellar test walls have been tentatively assigned to this genus although none of them show the pronounced median wall thickening visible in longitudinal axial sections of typical forms of the genus. They are comparable with the specimens from the Polish Zechstein assigned to *Pachyphloia exilis* Luperto by Peryt & Peryt (1977).

Other form, of doubtful taxonomic assignment

Fig. 9.14

One thin-section of material (sample GGU 360653) from the Wegener Halvø Formation of Clavering Ø shows a coiled, multilocular foraminifer with a clear calcareous test wall. It may be referable to *Globivalvulina* although one non-axial section constitutes insufficient evidence for anything other than a tentative suggestion.

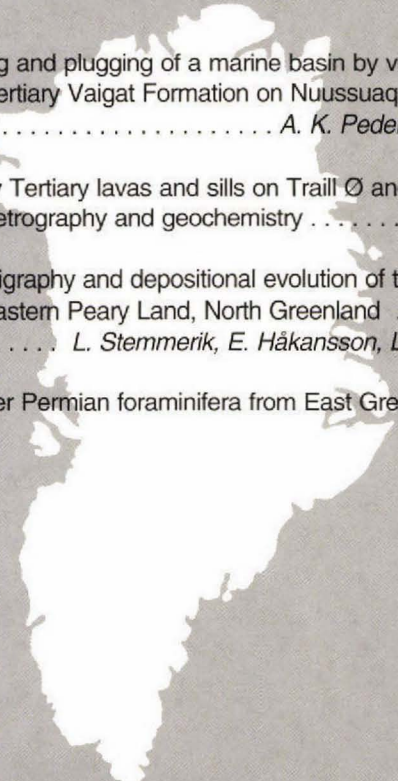
Acknowledgements. The authors wish to thank Dr. S. Piasecki for invaluable help with the photography and Dr. I. P. Wilkinson for his constructive comments on the text.

References

- Christiansen, F. G., Piasecki, S., Stemmerik, L. & Telnæs, N. 1993: Depositional environment and organic geochemistry of the Upper Permian Ravnefjeld Formation source rock in East Greenland. *Amer. Assoc. Petrol. Geol. Bull.* **77**, 1519–1537.
- Civrieux, J. M. S. & Dessauvagie, T. F. J. 1965: Reclassification de quelques Nodosariidae, particulièrement du Permien au Lias. *Maden Tetkik Arama Enstit. Yayinl.* **124**, 178 pp.
- Dunbar, C. O. 1955: Permian brachiopod faunas of central East Greenland. *Meddr Grønland* **110**(3), 172 pp.
- Geinitz, H. B. 1848: *Die Versteinerungen des deutschen Zechsteingebirges*, 26 pp. Dresden & Leipzig.
- Gobbett, D. J. 1973: Permian Fusulinacea. In Hallam, A. (ed.) *Atlas of palaeobiogeography*. Amsterdam: Elsevier.
- Jones, T. R. 1850: In King, W. (ed.) *A monograph of the Permian fossils of England*. *Palaeontogr. Soc. [Monogr.]*, 258 pp.
- Mamet, B. & Pinard, S. 1990: Notes sur la taxonomie des petites foraminifères des Palaeozoic Supérieure. *Bull. Soc. Belg. Geologie*, **99** (3/4), 373–398.
- Maync, W. 1961: The Permian of Greenland. In Raasch, G. O. (ed.) *Geology of the Arctic* **1**, 214–223. Univ. Toronto Press.
- Newell, N. D. 1955: Permian pelecypods of East Greenland. *Meddr Grønland* **110** (4), 36 pp.
- Paalzow, R. 1936: Die Foraminiferen im Zechstein des östlichen Thüringen. *Jb. preuss. geol. Landesanst.* **56**, 26–45.
- Pattison, J. 1989: Permian. In Jenkins, D. G. & Murray, J. W. (ed.) *Stratigraphical atlas of fossil foraminifera*, 87–96. Chichester: Ellis Horwood.
- Peryt, T. M. & Peryt, D. 1977: Otwormice cechszty skie monokliny Przedsudeckiej i ich paleoekologia. *Rocznik. Pol. Towarzystwa geol.* **47**, 301–326.
- Piasecki, S. 1984: Preliminary palynostratigraphy of the Permian – Lower Triassic sediments in Jameson Land and Scoresby Land, East Greenland. *Bull. Geol. Soc. Denmark* **32**, 139–144.
- Rasmussen, J. A., Piasecki, S., Stemmerik, L. & Stouge, S. 1990: Late Permian conodonts from central East Greenland. *Neues Jb. Geol. Palaont. Abh.* **178** (3), 309–324.
- Scherp, H. 1962: Foraminiferen aus dem Unteren und Mittleren Zechstein Nordwestdeutschlands. *Fortschr. Geol. Rheinld West.* **6**, 265–330.
- Schmid, E. E. 1867: Über die kleineren organischen Formen des Zechsteinkalks von Selters in der Wetterau. *Neues Jb. Geol. Petrefacten-Kunde* **1867**, 576–588.
- Scholle, P. A., Stemmerik, L. & Ulmer, D. S. 1991: Diagenetic history and hydrocarbon potential of Upper Permian carbonate buildups, Wegener Halvø area, Jameson Land Basin, East Greenland. *Amer. Assoc. Petrol. Geol. Bull.* **75** (4), 701–725.
- Scholle, P. A., Stemmerik, L., Ulmer-Scholle, D., di Liegro, G. & Henk, F. H. 1993: Palaeokarst-influenced depositional and diagenetic patterns in Upper Permian carbonates and evaporites, Karstryggen area, central East Greenland. *Sedimentology* **40**, 895–918.
- Sosipatrova, G. P. 1972: [Upper Palaeozoic foraminifera of Spitzbergen]. In Sokalov, V. N. & Vasilevskaja, N. D. (ed.) [*Stratigraphy of Spitzbergen*], 126–163. Leningrad: NIIGA. (in Russian).
- Spandel, E. 1898: *Die Foraminiferen des deutschen Zechsteines*. Nürnberg, 15 pp.
- Spandel, E. 1901: Die Foraminiferen des Permo-Carbon von Hooser, Kansas, Nord Amerika. *Festschrift Nat. Ges. Nürnberg* **1901**, 175–194.
- Stehli, F. G. 1973: Permian brachiopods. In Hallam, A. (ed.) *Atlas of palaeobiogeography*, 143–149. Amsterdam: Elsevier.
- Stemmerik, L. 1987: Cyclic carbonate and sulphate from the Upper Permian Karstryggen Formation, East Greenland. In Peryt, T. M. (ed.) *The Zechstein Facies in Europe*, 5–22, *Lecture notes in Earth Sciences*, 10. Berlin, Heidelberg: Springer-Verlag.
- Stemmerik, L. 1991: Reservoir evaluation of Upper Permian buildups in the Jameson Land basin, East Greenland. *Rapp. Grønlands geol. Unders.* **149**, 23 pp.
- Stemmerik, L. 1995: Permian history of the Norwegian–Greenland Sea area. In Scholle, P. A., Peryt, T. M. & Ulmer-Scholle, D. S. (ed.) *The Permian of northern Pangea, 2: Sedimentary basins and economic resources*, 98–118. Berlin: Springer Verlag.
- Stemmerik, L. & Piasecki, S. 1991: The Upper Permian of East Greenland – a review. *Zbl. Geol. Palaont.* **1991**, **1**(4), 825–837.
- Stemmerik, L., Rouse, J. E. & Spiro, B. 1988: S-isotope studies of shallow water, laminated gypsum and associated evaporites, Upper Permian, East Greenland. *Sedimentary Geology* **58**, 37–46.
- Stemmerik, L., Christiansen, F. G., Piasecki, S., Jordt, B., Marcussen, C. & Nøhr-Hansen, H. 1993: Depositional history and petroleum geology of the Carboniferous to Cretaceous sediments in the northern part of East Greenland. In Vorren, T.O. et al. (ed.) *Arctic Geology and Petroleum Potential. Norwegian Petroleum Society Special Publ.* **2**, 67–87.
- Surlyk, F., Hurst, J. M., Piasecki, S., Rolle, F., Scholle, P. A., Stemmerik, L. & Thomsen, E. 1986: In Halbouty, M. T. (ed.) *Future petroleum provinces of the world*. *Mem. Amer. Assoc. Petrol. Geol.* **40**, 629–659.
- Utting, J. & Piasecki, S. 1995: The palynology of the Permian of the northern continents: a review. In Scholle, P. A., Peryt, T. M. & Ulmer-Scholle, D. S. (eds) *The Permian of northern Pangea*, **1**, 236–261. Berlin: Springer Verlag.
- Vangerow, E. F. 1962: Über *Ammodiscus* aus dem Zechstein. *Paläont. Z.* **36** (1/2), 125–133.
- Woszczyńska, S. 1968: Wstępne wyniki badań mikrofauny osadów cechsztynu. *Kwart. Geol.* **12**(1), 92–104.

Woszczyńska, S. 1981: Foraminifera and Ostracoda of the Zechstein carbonate rocks in the Polish lowlands. *In* Depowski, S., Peryt, T. M. & Piatkowski, T. S. (ed.) *Proceedings of International Symposium on Central European Permian*, 502–515. Warszawa: Wydawnictwa Geologiczne.

Contents



Filling and plugging of a marine basin by volcanic rocks: the Tunoqqu Member of the Lower Tertiary Vaigat Formation on Nuussuaq, central West Greenland	<i>A. K. Pedersen, L. M. Larsen, G. K. Pedersen & K. S. Dueholm</i>	5
Early Tertiary lavas and sills on Traill Ø and Geographical Society Ø, northern East Greenland: petrography and geochemistry	<i>N. Hald</i>	29
Stratigraphy and depositional evolution of the Upper Palaeozoic sedimentary succession in eastern Peary Land, North Greenland	<i>L. Stemmerik, E. Håkansson, L. Madsen, I. Nilsson, S. Piasecki & J. A. Rasmussen</i>	45
Upper Permian foraminifera from East Greenland	<i>J. Pattison & L. Stemmerik</i>	73

GEOLOGICAL SURVEY OF DENMARK AND GREENLAND

Thoravej 8
DK-2400 Copenhagen NV

ISSN 0105 3507
Produced in Denmark